AD NUMBER: AD0835774

LIMITATION CHANGES

TO:

Approved for public release; distribution is unlimited.

FROM:

Distribution authorized to US Government Agencies only; Export Control; 1 Jul 1968. Other requests shall be referred to Air Force Wright Aeronautical Laboratory, Wright-Patterson AFB, OH 45433.

AUTHORITY

AFWAL ltr dtd 14 Apr 1987

AD 835 774

AUTHORITY:
AFWAL etc.,
14 Apr 87

AFFDL-TR-68-84
VOLUME I

FLIGHT TEST INVESTIGATION OF TRANSONIC SHOCK-BOUNDARY LAYER PHENOMENA

Jones F. Cahill
Bill L. Cooper
LOCKHEED-GEORGIA COMPANY

TECHNICAL REPORT AFFDL-TR-68-84
VOLUME I

JULY 1968

AIR FORCE FLIGHT DYNAMICS LABORATORY
AIR FORCE SYSTEMS COMMAND
WRIGHT-PATTERSON AIR FORCE BASE, OHIO

75

NOTICES

When Government drawings, specifications, or other data are used for any purpose other than in connection with a definitely related Government procurement operation, the United States Government thereby incurs no responsibility nor any obligation whatsoever; and the fact that the Government may have formulated, furnished, or in any way supplied the said drawings, specifications, or other data, is not to be regarded by implication or otherwise as in any manner licensing the holder or any other person or corporation, or conveying any rights or permission to manufacture, use, or sell any patented invention that may in any way be related thereto.

The distribution of this document is limited because disclosure of its contents would diminish the technology lead of the United States.

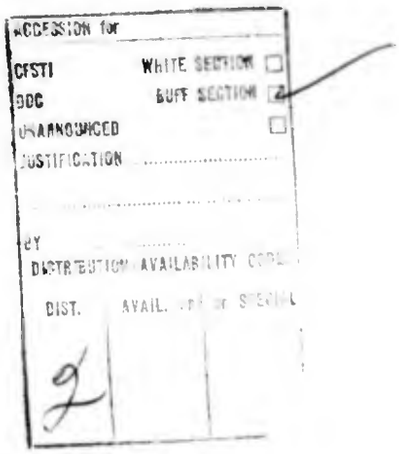

Copies of this report should not be returned unless return is required by security considerations, contractual obligations, or notice on a specific document.

BLANK PAGE

FLIGHT TEST INVESTIGATION OF TRANSONIC SHOCK-BOUNDARY LAYER PHENOMENA

Jones F. Cahill
Bill L. Cooper

FOREWORD

This report describes a flight investigation of the phenomenon of scaling effects on shock-boundary layer interaction in transonic flow. It was prepared by the Flight Sciences Division of the Lockheed-Georgia Company, Marietta, Georgia, under Air Force Contract F33615-67-C-1777. The work was administered under the direction of the Air Force Flight Dynamics Laboratory, with Mr. A. J. Murn, FDMM, as Project Monitor.

The work reported here was performed during the period from 5 October 1967 to 15 July 1968. This report was submitted by the authors in July 1968.

The authors acknowledge the contributions of the following members of the Lockheed-Georgia Company to the project: Mr. H. J. Coley who supervised the Design, Construction and Installation of the Test Equipment; Mr. A. J. Youngs who directed the Flight Operations; Mr. B. M. Coleman who directed the Data Reduction; and Messrs. W. J. Campbell, P. E. Cole, T. T. Eckert, and Mrs. C. H. Sullins who assisted in the test program and data analysis.

This technical report has been reviewed and is approved.

Philip P Antonatos

PHILIP P. ANTONATOS
Chief, Flight Mechanics Division
Air Force Flight Dynamics Laboratory

ABSTRACT

A flight test investigation was made using a Lockheed C-141 airplane to obtain data related to scale effects on transonic shock-boundary layer interactions. The primary measurements consisted of wing surface chordwise pressure distributions at three spanwise stations, and boundary layer profiles for three chordwise positions at one spanwise station. Tests were made at nominal altitudes of 20,000 feet and 40,000 feet, resulting in Reynolds number values of approximately 70×10^6 and 40×10^6, respectively. At each altitude data were collected at a number of combinations of Mach number (from 0.7 to 0.85) and lift coefficient (from 0 to approximately 0.4). Variations in lift coefficient were obtained by varying load factor.

Volume I contains the data analysis and discussions of the test results. Volume II contains a detailed discussion of the data acquisition and reduction procedures plus a complete presentation of the basic data.

Results obtained, when compared with previously available wind tunnel data, showed that large scale effects on chordwise pressure distribution can occur with turbulent boundary layers on a wing having small Mach number gradients forward of the shock. A shock-induced separation, followed by flow reattachment, was shown to occur when the shock pressure rise reached a value approximately equal to that indicated in NACA Report 1356. Increasing Mach number or angle-of-attack sufficiently beyond the initial separation point caused the separation bubble to spread to the trailing-edge, resulting in an abrupt forward movement of the shock. While the flight shock locations were within the spread of those shown by low Reynolds number wing tunnel results, no single wind tunnel configuration (transition strip, Reynolds number, vortex generator) provided a good indication of the flight result over the whole range of conditions tested. For wing sections of the type used on the C-141, scale effects on buffet phenomena should be anticipated also.

Distribution of this abstract is unlimited.

BLANK PAGE

TABLE OF CONTENTS

LIST OF ILLUSTRATIONS

LIST OF ILLUSTRATIONS (CONTINUED)

LIST OF ABBREVIATIONS

c	chord
c_l	section lift coefficient
C_L	airplane lift coefficient ($\sim N_z W/qS$)
N_z	load factor
q	dynamic pressure
S	wing area
W	airplane weight
C_m	section moment coefficient
C_p, $\Delta P/Q$	pressure coefficient
C_{p_1}	crest pressure coefficient
$C_{P_{T.E.}}$	pressure coefficient at the trailing edge
H	shape factor, δ^*/θ
M	mach number
M_1	shock upstream mach number
M_∞	freestream mach number
M_L	local mach number
MAC	mean aerodynamic chord
$\Delta P/P_{o\infty}$	pressure rise parameter. See page 49.
$\Delta P/\Delta P_{SEP}$	pressure rise parameter. See page 39.
Re	Reynolds number
V_{BL}	velocity in the boundary layer
V_L	velocity outside the boundary layer

x/c	streamwise coordinates in terms of airfoil chord
Y	vertical coordinate as measured from wing surface
boom alpha	angle-of-attack as recorded by nose test boom
corrected alpha	boom alpha corrected for position error
equivalent angle-of-attack (α)	corrected alpha minus aeroelastic twist
δ^*	boundary layer displacement thickness
θ	boundary layer momentum thickness
$\Lambda_{L.E.}$	leading edge sweep angle
$\Lambda_{T.E.}$	trailing edge sweep angle

BLANK PAGE

SECTION I

INTRODUCTION

The subject of scale effects on aerodynamic characteristics of airfoils at transonic speeds is currently being studied with renewed interest. In the past, a rather considerable number of wind tunnel, flight, and analytical studies had indicated that scale effects should be minor with turbulent boundary layers, Reference 1. Recent experience on a number of aircraft, however, has shown that severe scale effects can exist for conditions where shock strength is great. The Lockheed C-141 airplane is a case in point. Results obtained during flight test, Reference 2, revealed that shock location changes of as much as 20% chord existed between wind tunnel and flight test results. The shock location differences, in some cases, resulted in doubling the section pitching moment.

Following the disclosure of this problem by flight test several additional C-141 wind tunnel tests were performed. Test in the AEDC 16 Foot Wind Tunnel, Reference 3, showed scale effects for both natural and fixed transition conditions at Reynolds number between 2.8×10^6 and 8.5×10^6. Natural transition tests at low Reynolds number generally showed reasonable agreement with flight data. However, as the Reynolds number was increased the shock moved forward. With the transition fixed near the leading edge, the shock was much farther forward than with natural transition at low Reynolds number and moved aft only slightly as the Reynolds number was increased. High Reynolds number tests for both natural and fixed transition conditions tended to give the same shock locations. Tests in the Langley 8 Foot Tunnel showed that variations in transition strip location (Re 4.2×10^6) moved the shock over the entire range of locations indicated by the AEDC results, Reference 4.

Studies by B. H. Little, Reference 5, confirmed Pearcy's conclusions that the existence of a supersonic tongue, just downstream of the shock, can result in more severe separation. Knowledge of the flow in this region is limited but the scaling effects are thought to be quite pronounced. E. Stanewsky's results, Reference 6, show that shock location is little affected by changes in Reynolds number or transition strips for a circular arc half-body on the tunnel floor. Airfoil shape would appear to influence the scale effect, especially when considering airfoils that have steep Mach gradients as compared to flat-top type distributions.

The previously mentioned C-141 flight test program was made with the pressure orifices rather widely spaced. Since a considerable amount of both flight and wind tunnel data has been accumulated using the C-141 configuration, it was apparent that a more precise definition of shock location and flow conditions should be made. It would then be possible to conduct a better assessment of the differences between flight and wind tunnel conditions and also to evaluate various wind tunnel attempts to simulate the flight conditions. The present investigation was therefore initiated with the following objectives:

a) To obtain a more precise definition of the wing section pressure distributions in flight.
b) To determine the magnitude of the scale effects on aerodynamic characteristics over the widest possible flight Reynolds number range.
c) To obtain some experimental boundary layer data for correlation with wind tunnel data.

SECTION II

TEST PROGRAM

General

The data for this program were measured on a standard production C-141 airplane. The primary measurements consisted of wing surface chordwise pressure distributions at three spanwise stations, and boundary layer profiles for three chordwise positions at one spanwise station. Information on flight condition (Mach number, dynamic pressure, ambient pressure and temperature, and airplane load factor) was obtained from the standard airplane instrumentation and a nose boom.

Tests were made at nominal altitudes of 20,000 feet and 40,000 feet to obtain the widest practicable spread in Reynolds number, resulting in values of approximately 70×10^6 and 40×10^6, respectively. At each altitude data were collected at a number of combinations of Mach number (from 0.7 to 0.85) and lift coefficient (from 0 to approximately 0.4). Variations in lift coefficient were obtained by varying load factor since the range available from gross weight changes alone was not wide enough for the purposes of this investigation.

A complete description of instrumentation and data acquisition and reduction, and plots of all the basic data measured are contained in Volume II of this report.

Data Acquisition And Reduction

Surface pressures were measured on the right wing at the three spanwise locations shown in Figure 1. STRIP-A-TUBE of approximately one-eighth inch height and three inch width was bonded to the wing surface and holes drilled at the desired chordwise positions. Each of these pressure orifices was connected through the STRIP-A-TUBE to SCANIVALVES which were located in the flap cove area. Wiring from the SCANIVALVES was routed to an oscillograph located in the cargo compartment. Three boundary layer rakes were located on the left wing at one spanwise station. This location corresponded to the middle station used in wing surface pressure measurements. Figure 2 presents photographs of the rakes used in the investigation. Boundary layer profile data were also recorded using an oscillograph. Wing static pressures were referenced to boom static pressure and boundary layer rake pressures were referenced to boom total pressure.

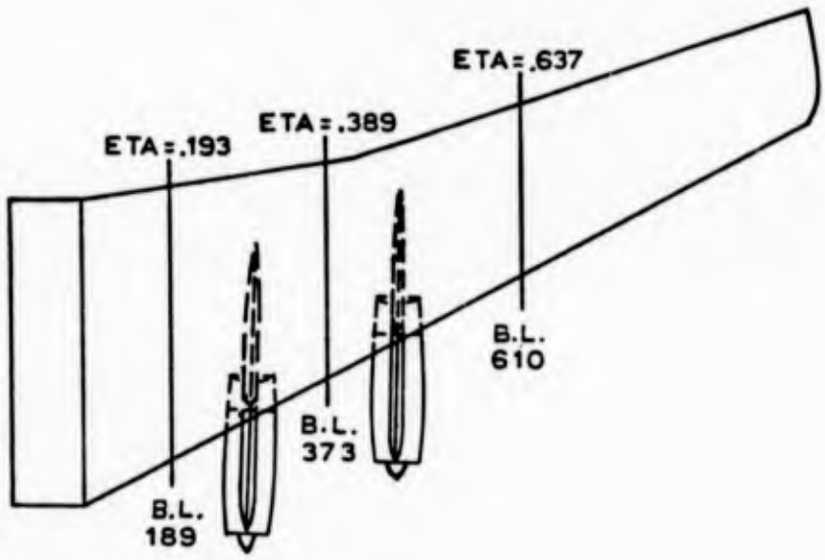

WING DIMENSIONS

Span	159.67 ft
Area total including aileron flaps and 450.0 sq ft of fuselage	3228.1 sq ft
Aspect ratio	7.90
Airfoil Chord:	
At root	398.00 in.
At construction tip	132.62 in.
Mean (MAC)	266.51 in.
Airfoil Section Designation and Thickness (Percent Chord):	
At root NACA 0013.00 (Mod)	13.00
At construction tip NACA 0010.00 (Mod)	10.00
At construction joint (B.L. 415) NACA 0011.00 (Mod)	11.00
Incidence:	
At root	4.89 deg
At construction break	2.25 deg
At construction tip	-0.69 deg
Sweep at 25 Percent Chord:	
Outboard of construction joint	25.02 deg
Inboard of construction joint	23.73 deg
Dihedral at 25 Percent Chord:	
Outboard of construction joint	-1.195 deg
Inboard of construction joint	-0.941 deg

FIGURE 1 WING PLANFORM AND DIMENSIONS

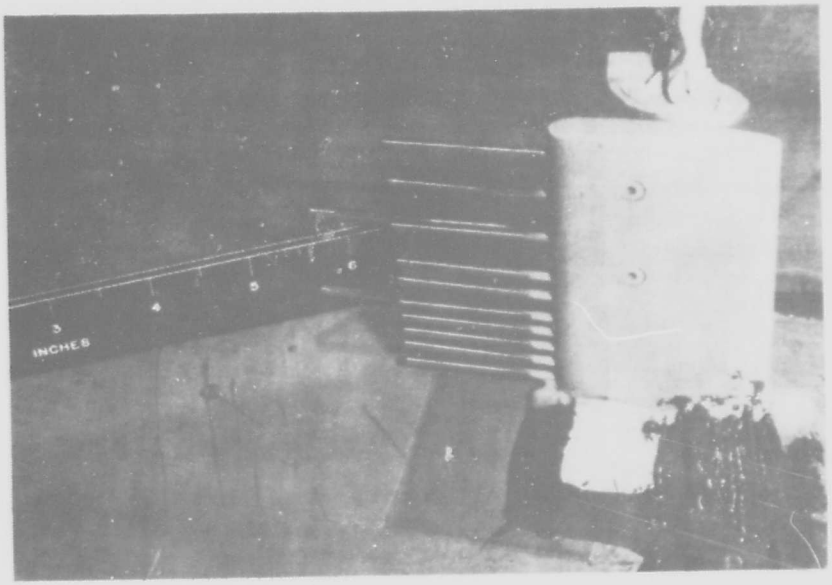

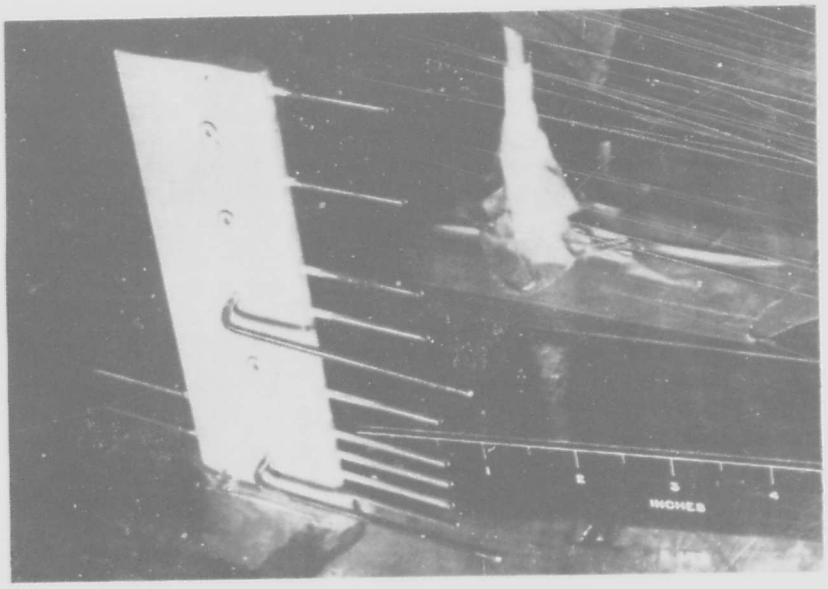

FIGURE 2 BOUNDARY LAYER RAKES

The nose boom, which is illustrated in Figure 3, provided measurements of total and static pressure and angles-of-attack and sideslip. The boom-measured pressures were supplemented by similar data measured by the standard airplane instrumentation. When appropriate position error corrections were applied to these data excellent correlation was demonstrated. The standard airplane airspeed probe is shown in Figure 4.

Surface pressure measurements were reduced to pressure coefficients and boundary layer profile measurements to velocity ratios using the conventional equations presented in Volume II. These computations were performed by a UNIVAC 1108 computer and the data plotted by a cathode ray tube plotter.

Effect Of Maneuvering Flight On Pressure Data

Since it is not possible to maintain constant values of all primary flight conditions (Mach number, altitude, lift coefficient) during tests of this type, it was considered desirable to demonstrate the absence of extraneous effects in the data measured. In this test series, the most practicable procedure was to hold Mach number and load factor constant, and to accept the altitude changes which were necessary to attain the desired test point.

Figures 5 and 6 present the results of tests designed to measure the lag effects on total and static pressures due to altitude changes. Conditions 547/4B1 and 547/4B2 were made in stable flight at an altitude of approximately 20,000 feet. The pressure data were recorded holding the aircraft at constant altitude, Mach number, and load factor. The effects of lag were tested and are shown as conditions 547/4A1 and 547/4A2. The aircraft was placed in a dive at an altitude of approximately 30,000 feet and a constant rate-of-sink established at 8,000 feet per minute. As the aircraft passed through 20,000 feet, the data as shown for conditions 547/4A1 and 547/4A2 were recorded. The Mach numbers and load factors were the same as recorded during the constant altitude test. The results indicate that the measurable lag in the pressure system is zero. Therefore, any altitude changes that might exist in the remainder of the test data should be of no consequence.

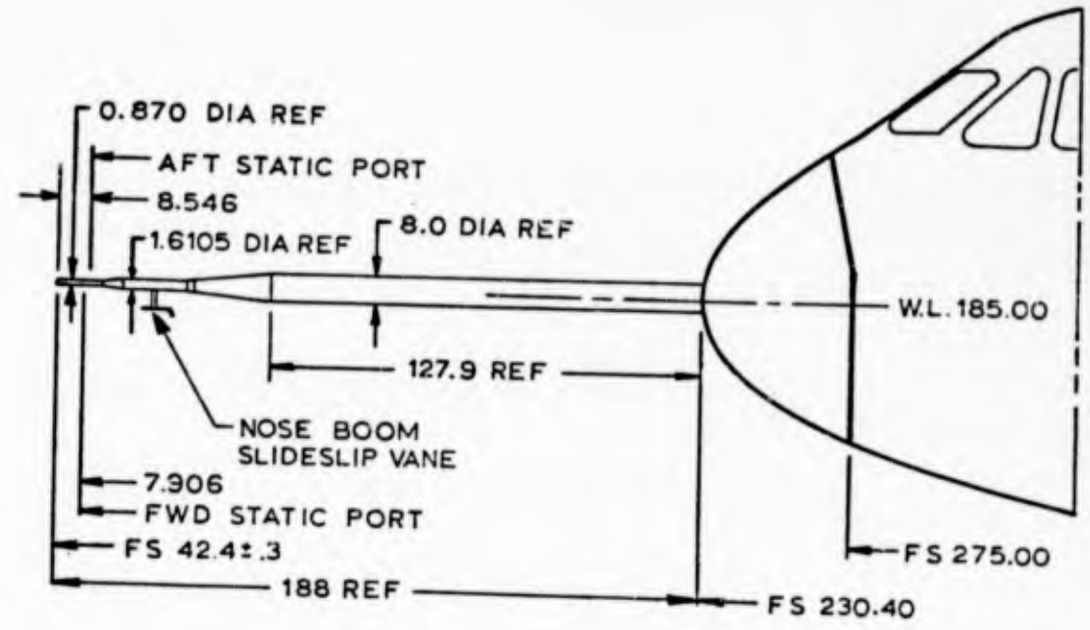

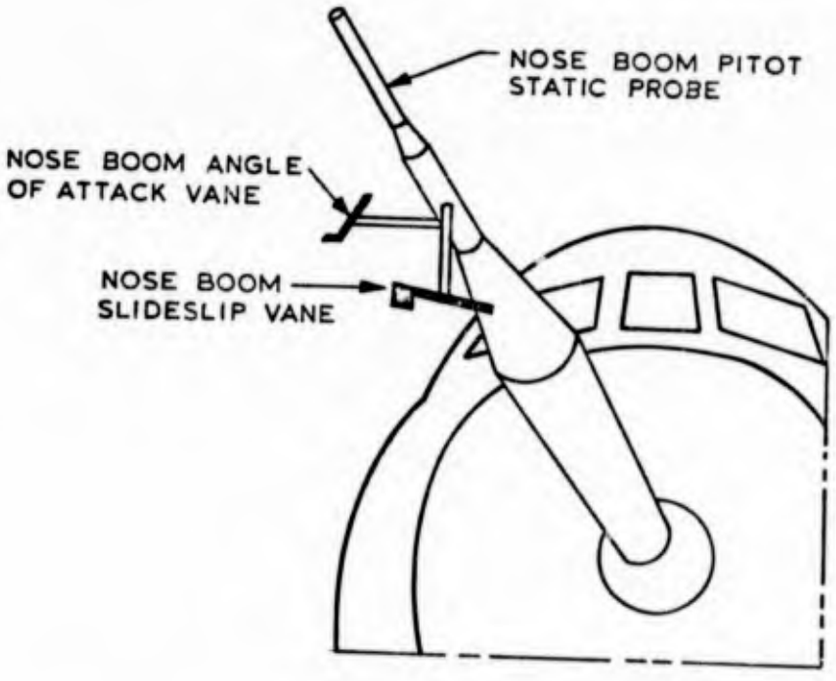

FIGURE 3 NOSE BOOM INSTALLATION

FIGURE 4 SHIP SYSTEM PITOT-STATIC PROBE INSTALLATION (RIGHT SIDE)

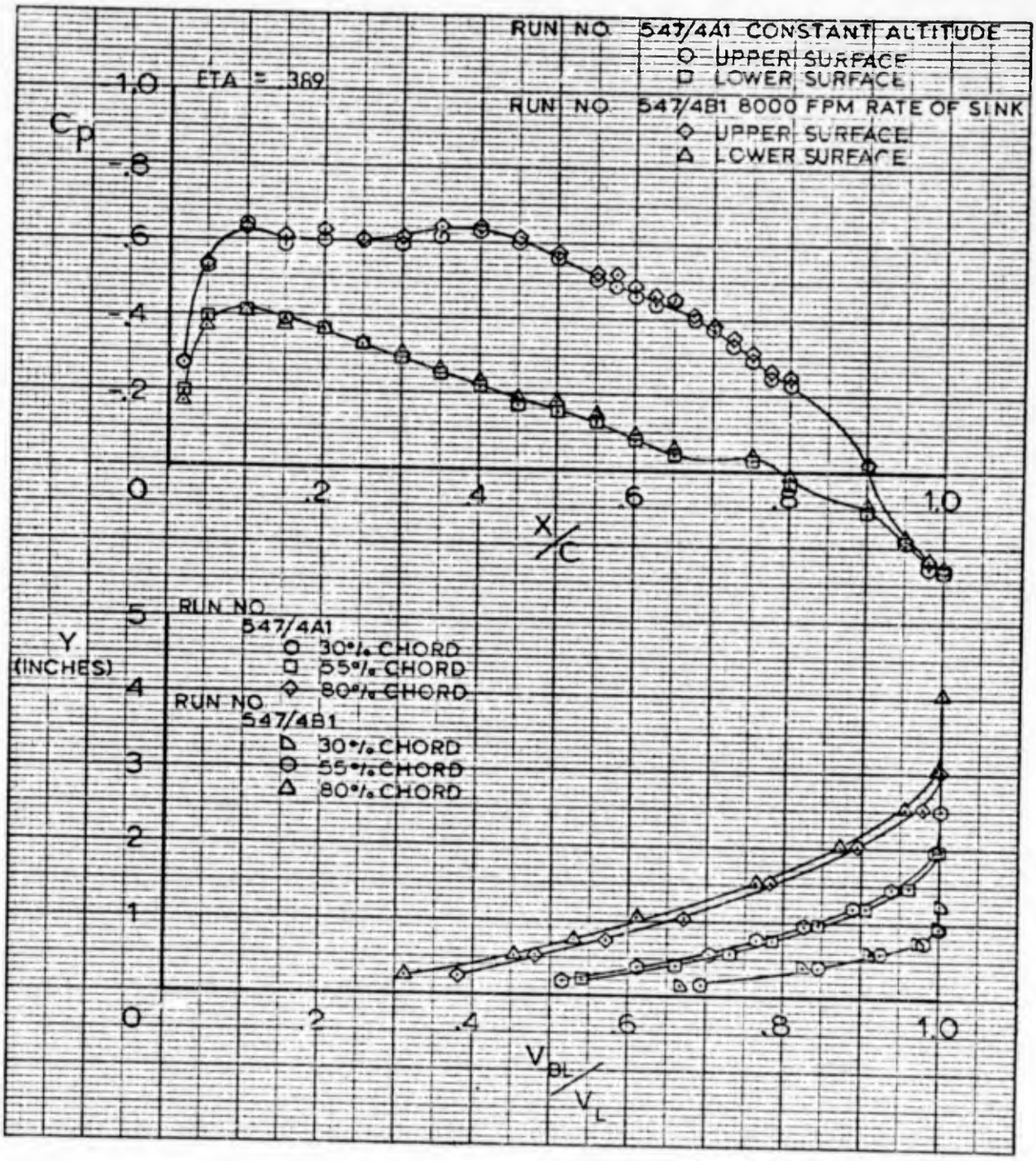

FIGURE 5 PRESSURE DISTRIBUTION COMPARISON
LAG CHECK MACH = .742

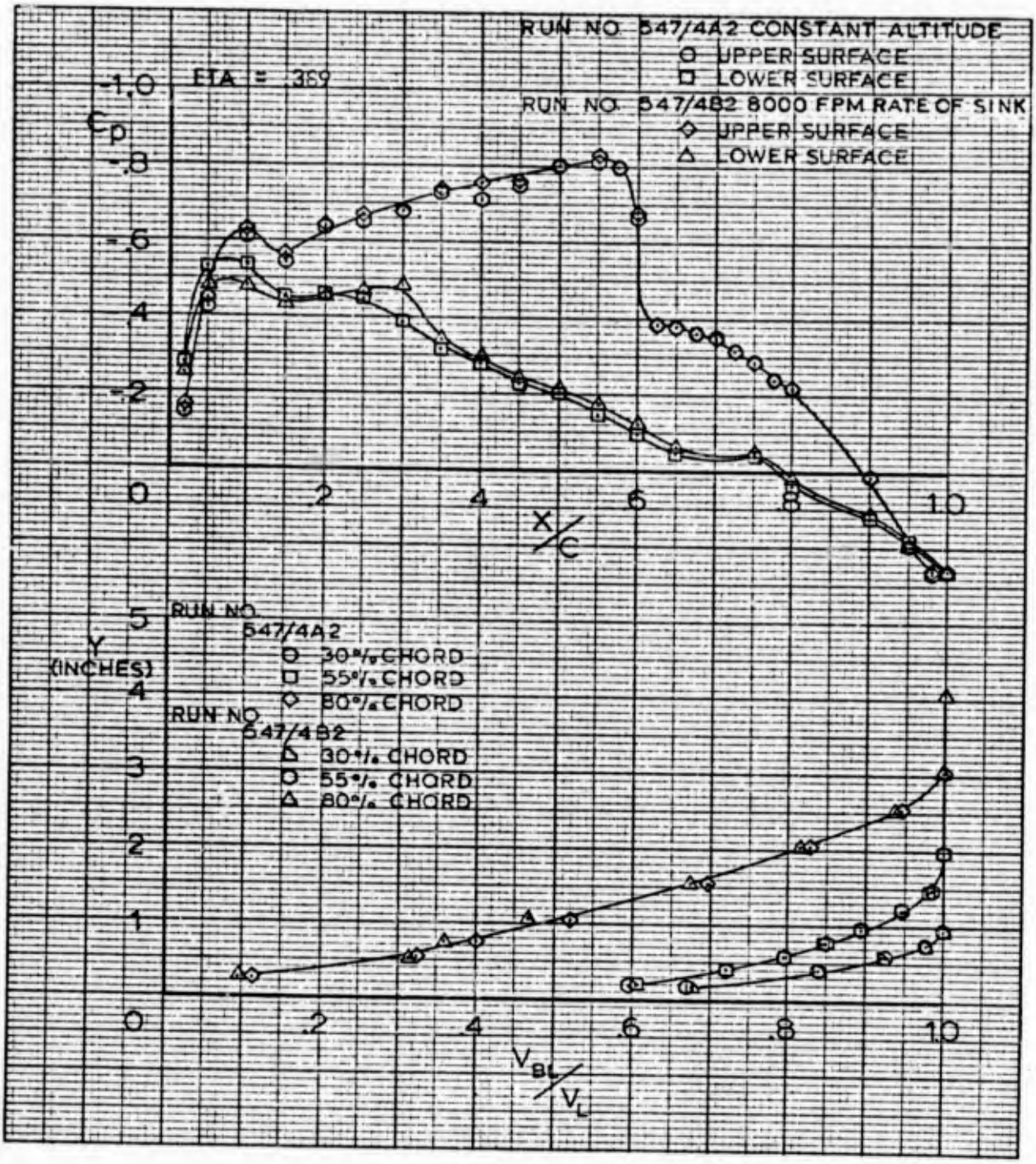

FIGURE 6 PRESSURE DISTRIBUTION COMPARISON
LAG CHECK MACH = .800

SECTION III

RESULTS AND DISCUSSION

Wing Section Characteristics

Figure 7 presents the wing section lift characteristics obtained from integration of the measured pressure distributions for a series of Mach numbers. Section lift coefficient is plotted against an equivalent angle-of-attack, defined as the fuselage reference line angle required on a rigid airplane to produce the geometric angle-of-attack at a given spanwise station. This requires a consideration of the aeroelastic twist and enables comparisons with data from rigid wind tunnel models. Some scatter is evident and is believed to occur from inaccuracies in the determination of the equivalent section angle-of-attack. The scatter is very slight at the lowest Mach number and increases as Mach number is increased. Angle-of-attack is one of the most difficult parameters to measure accurately in flight. There does not appear to be any Reynolds number effect in the range of values tested.

The section lift-pitch characteristics are shown in Figure 8 for a series of Mach numbers. The data are very smooth and only at the highest Mach number is any scatter present. The data shown at the highest Mach number cover a Mach range of 0.84 to 0.86. The airspeed differences will explain most of the data scatter. Again, the data do not tend to indicate any scale effect.

Figure 9 presents a comparison between flight and wind tunnel data from Reference 3 at one Mach number and three spanwise stations. The comparisons show the complexity of trying to ascertain a single wind tunnel testing technique that will duplicate flight results. For each Mach number, it would appear that at each test angle-of-attack (or C_L) a different test condition would be required at each spanwise station. At the inboard station, it is evident that the use of vortex generators delays the separation effects and over-fixes the problem. At the two outboard stations, the generators would help match flight conditions at some angles-of-attack but not at others. The variation of Reynolds number with natural model transition would also accomplish similar results. Wind tunnel data were also obtained with transition fixed during the tests reported in Reference 3. The data obtained at 2.8×10^6 Reynolds number with fixed transition are presented and show good agreement with flight test for the most inboard section but very poor agreement at ETA = .389 and ETA = .637.

Reynolds numbers effects are presented in Figure 10 for one spanwise station at one Mach number at one angle-of-attack. At the lowest Reynolds number, the difference between natural and fixed transition testing shows section pitch differences on the order of 2 to 1. For this particular case, the fixed transition testing, combined with vortex generators at 55 percent chord, would give a good correlation with flight results. It cannot be concluded that using fixed transition and vortex generators would produce the same good correlation at other conditions.

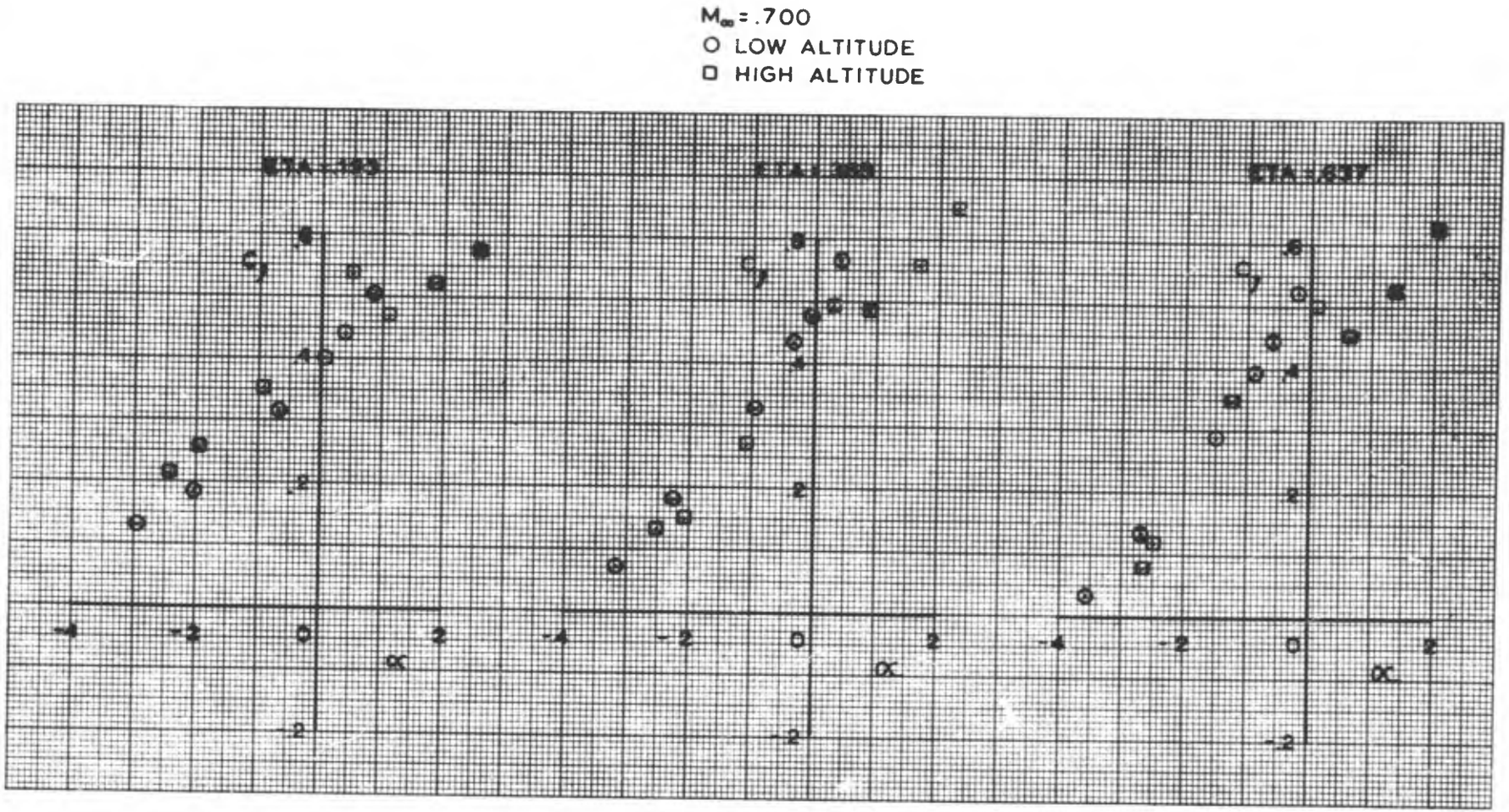

FIGURE 7 (a) WING SECTION LIFT CHARACTERISTICS
MACH = .700

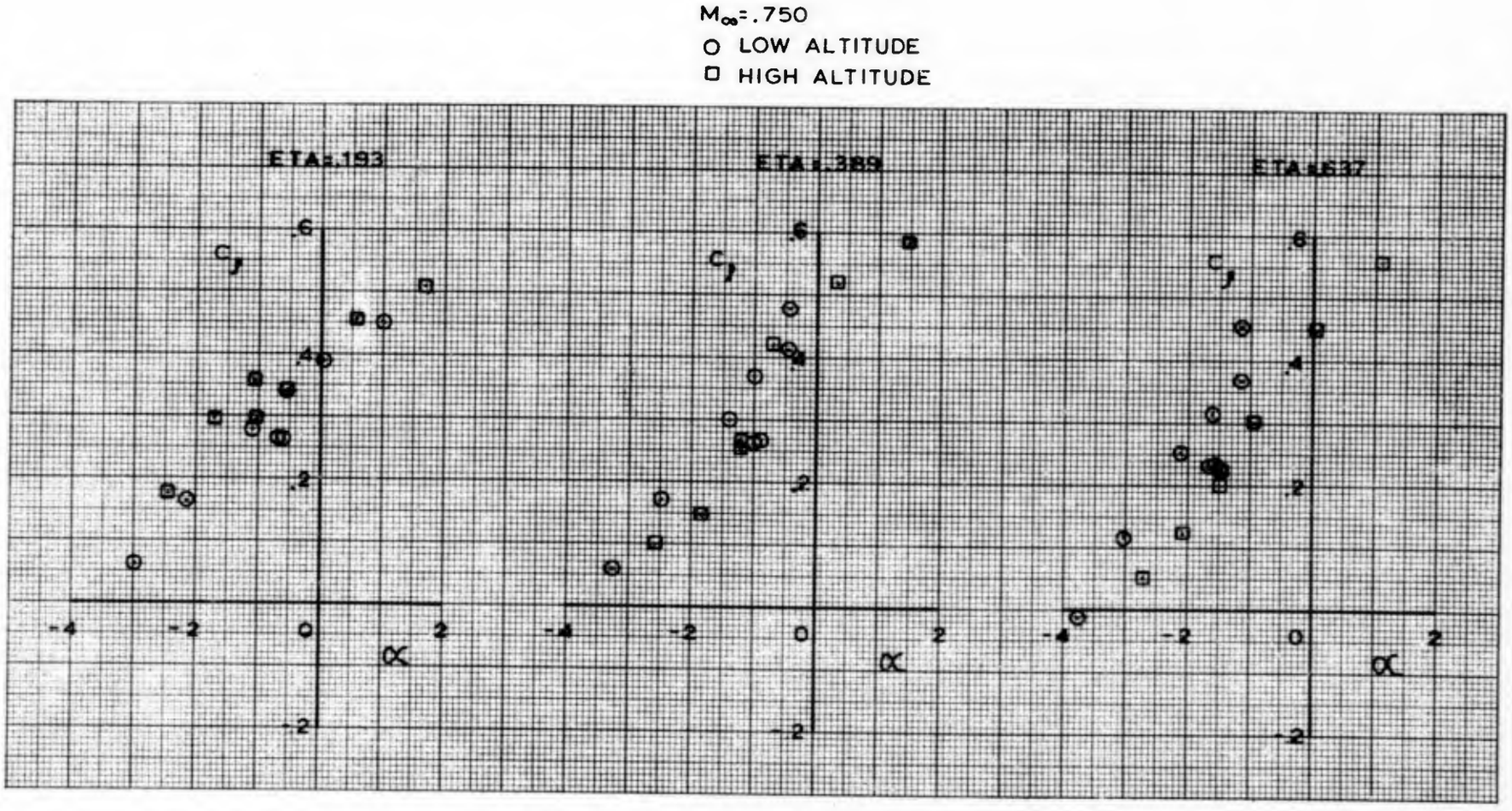

FIGURE 7 (CONTINUED)
(b) MACH = .750

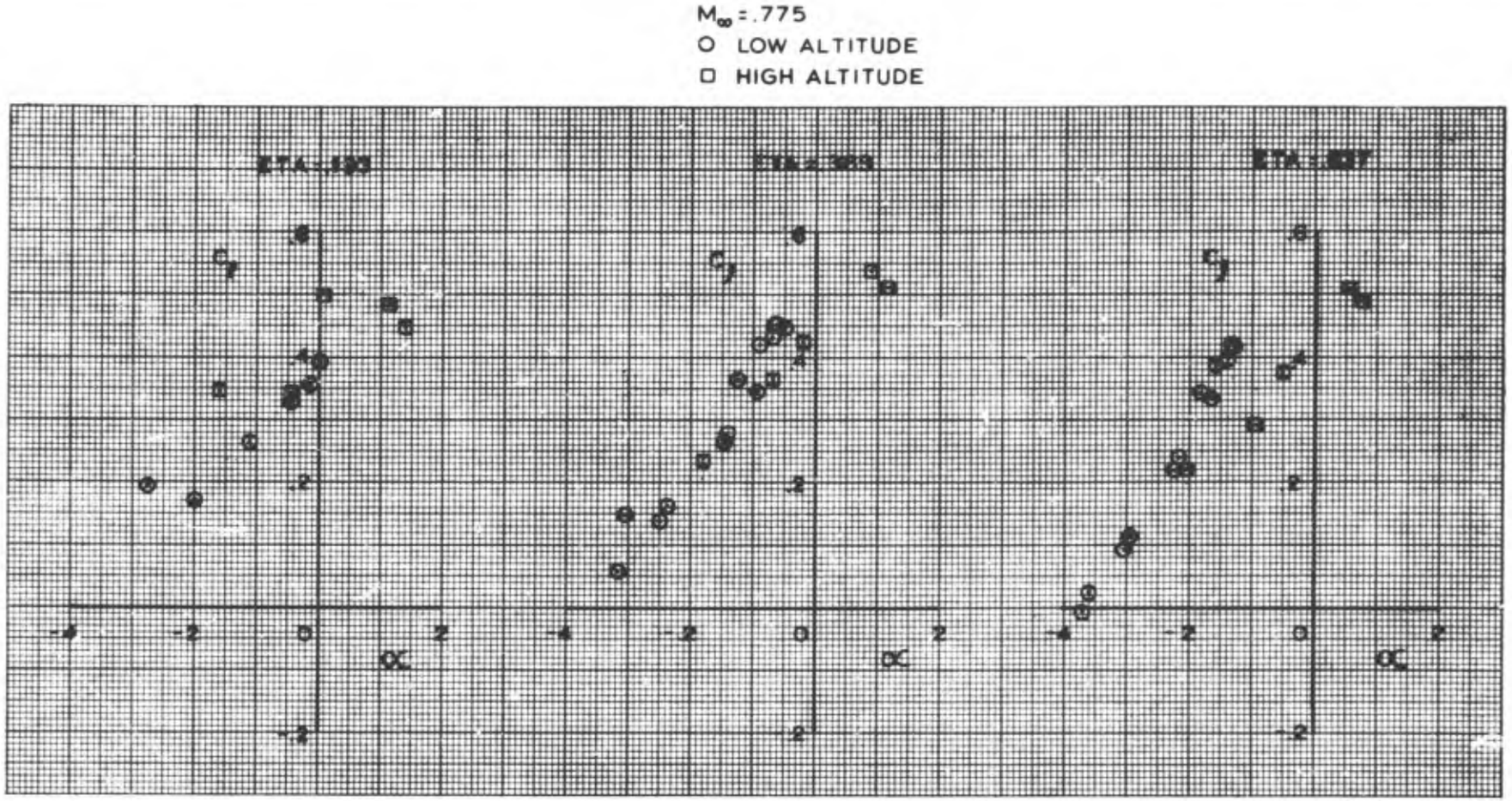

FIGURE 7 (CONTINUED)
(c) MACH = .775

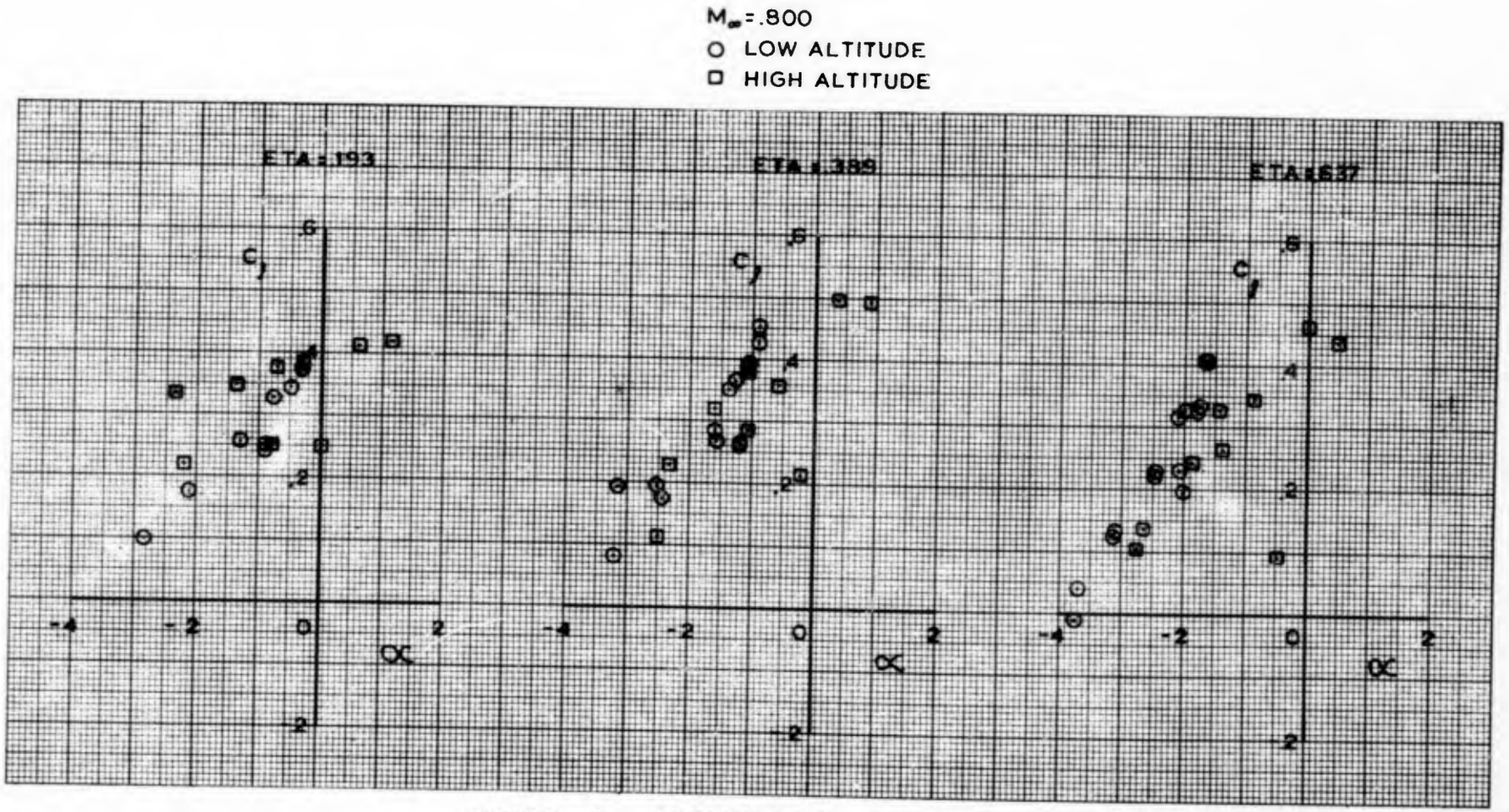

FIGURE 7 (CONTINUED)
(d) MACH = .800

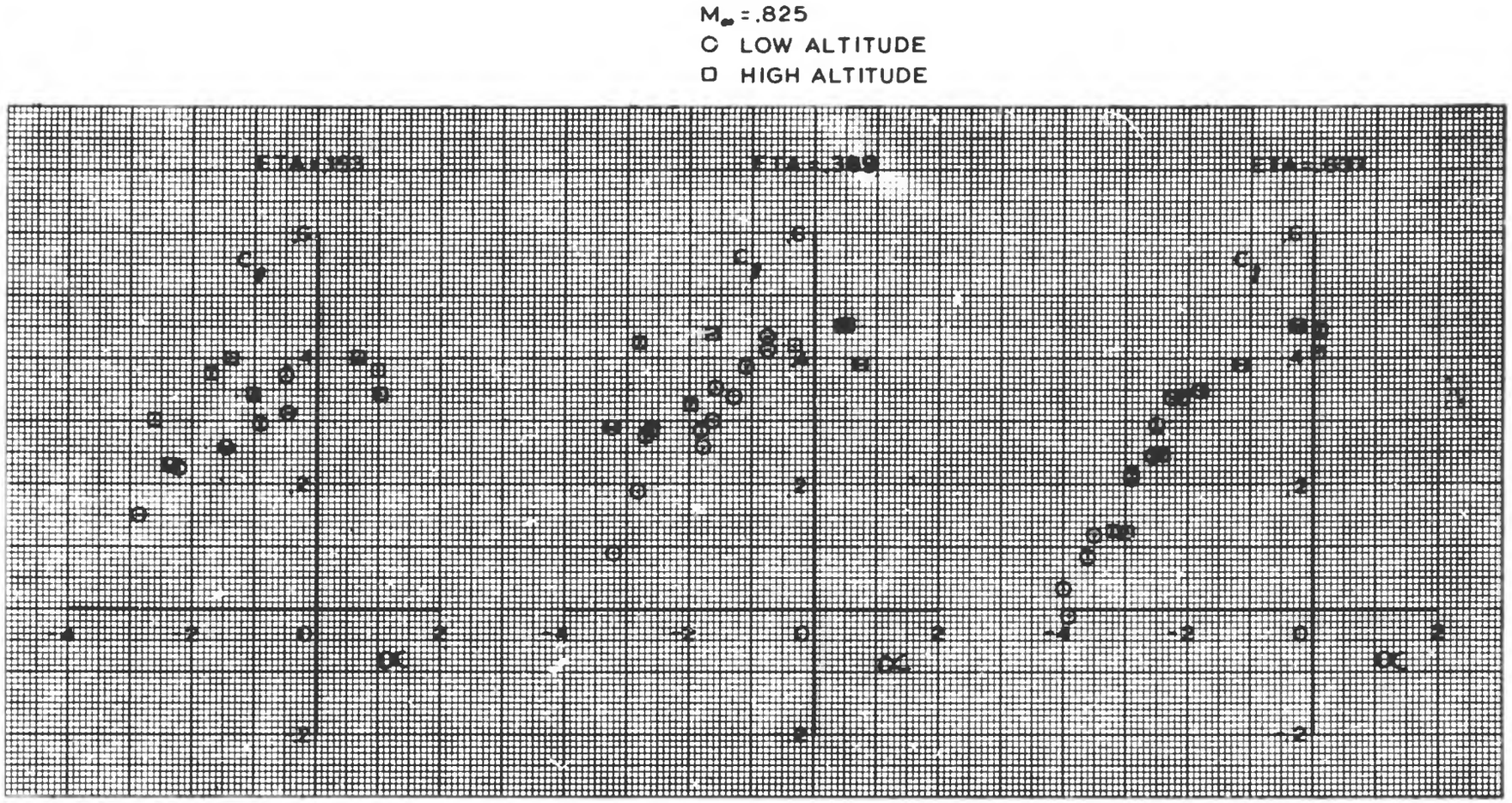

FIGURE 7 (CONTINUED)
(e) MACH = .825

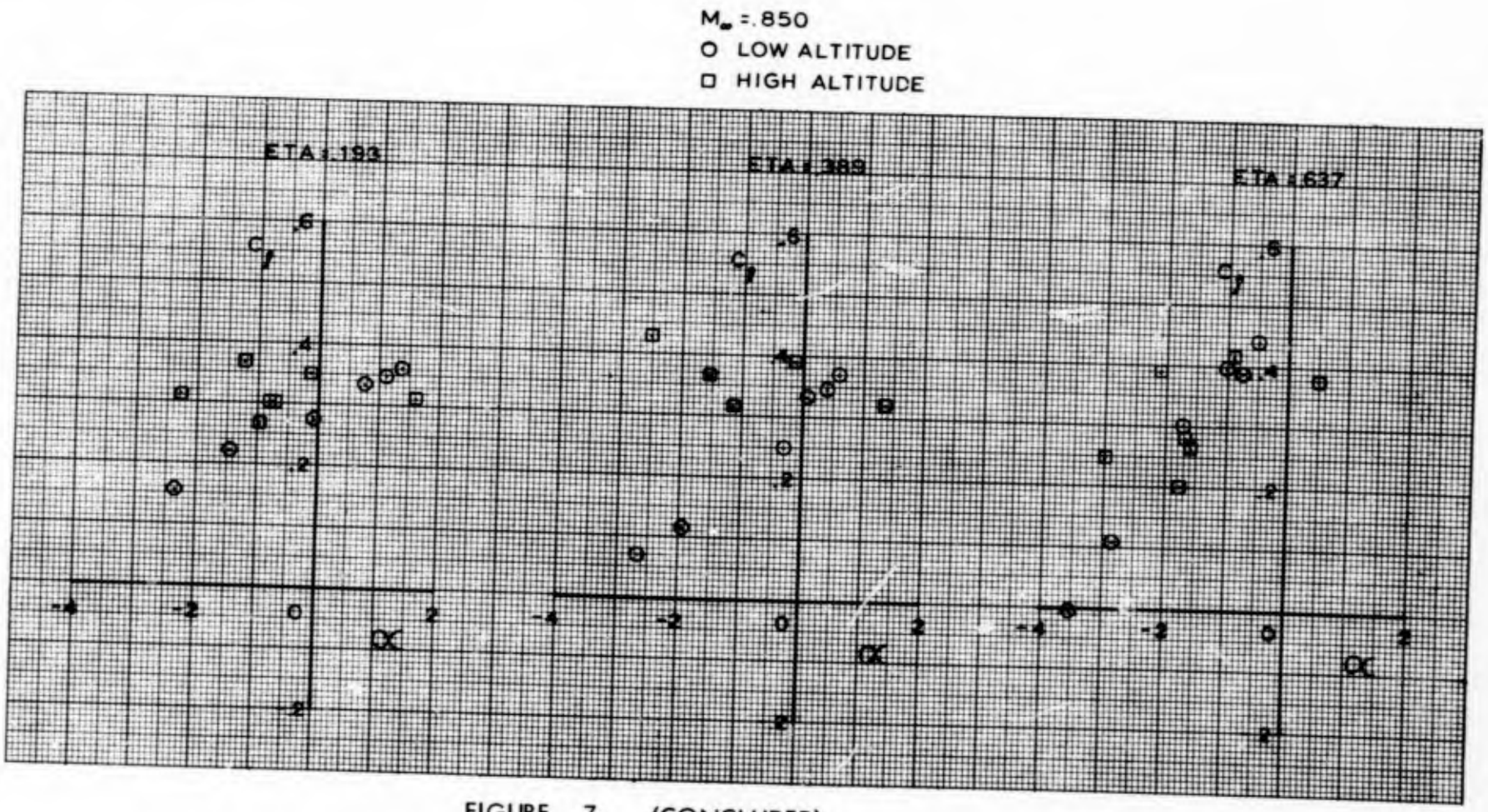

FIGURE 7 (CONCLUDED)
(f) MACH = .850

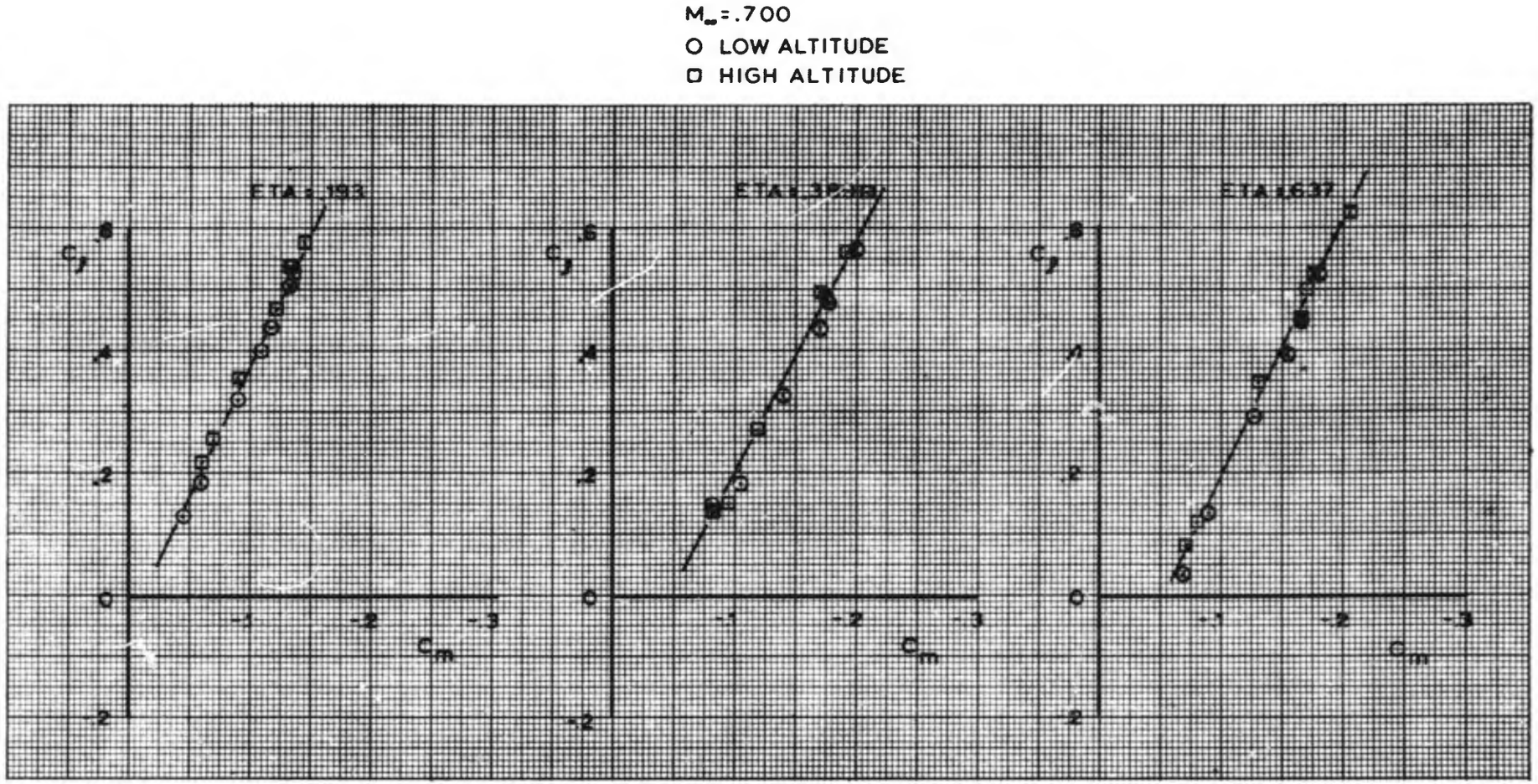

FIGURE 8 WING SECTION LIFT & PITCH CHARACTERISTICS
(a) MACH - .700

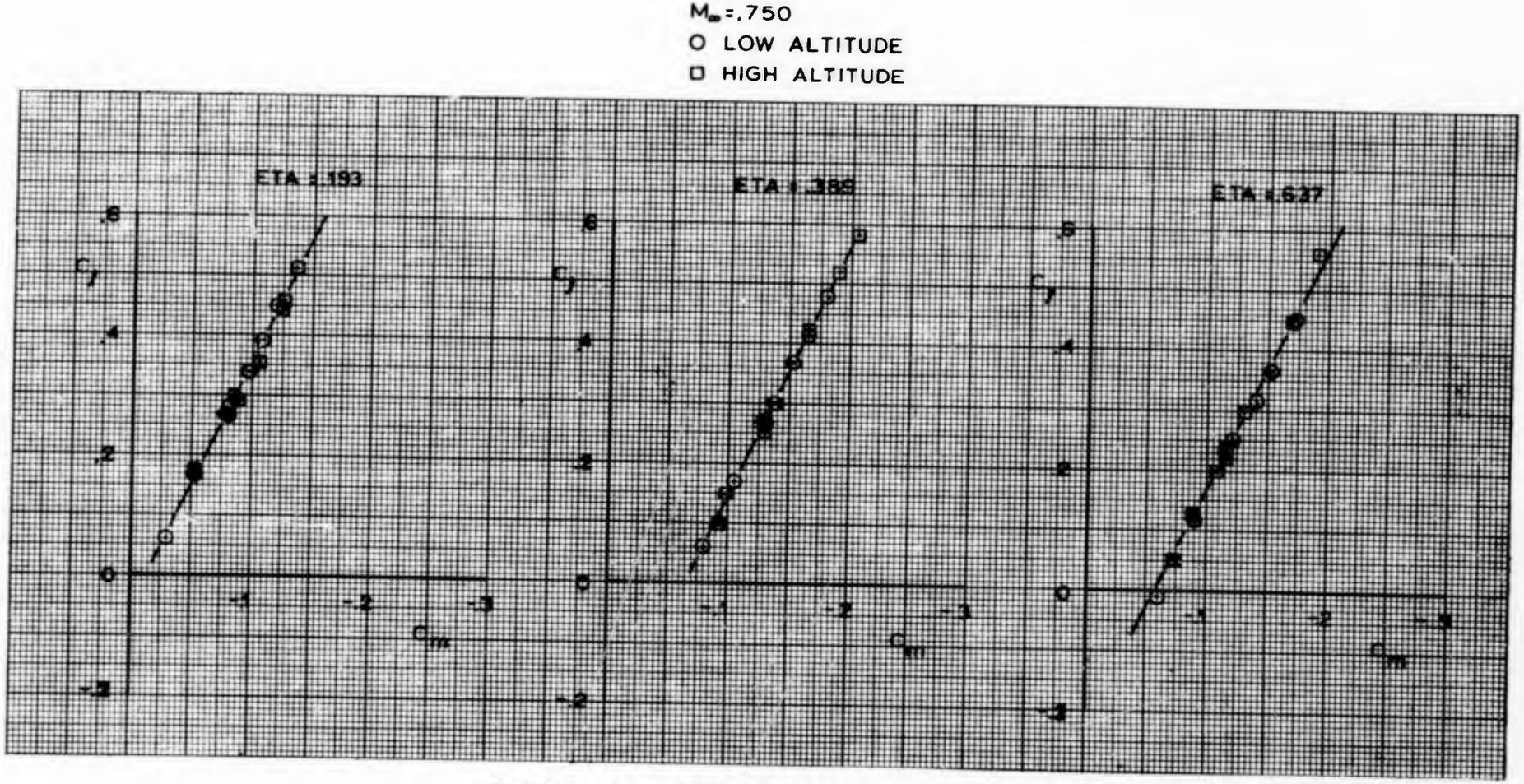

FIGURE 8 (CONTINUED)
(b) MACH = .750

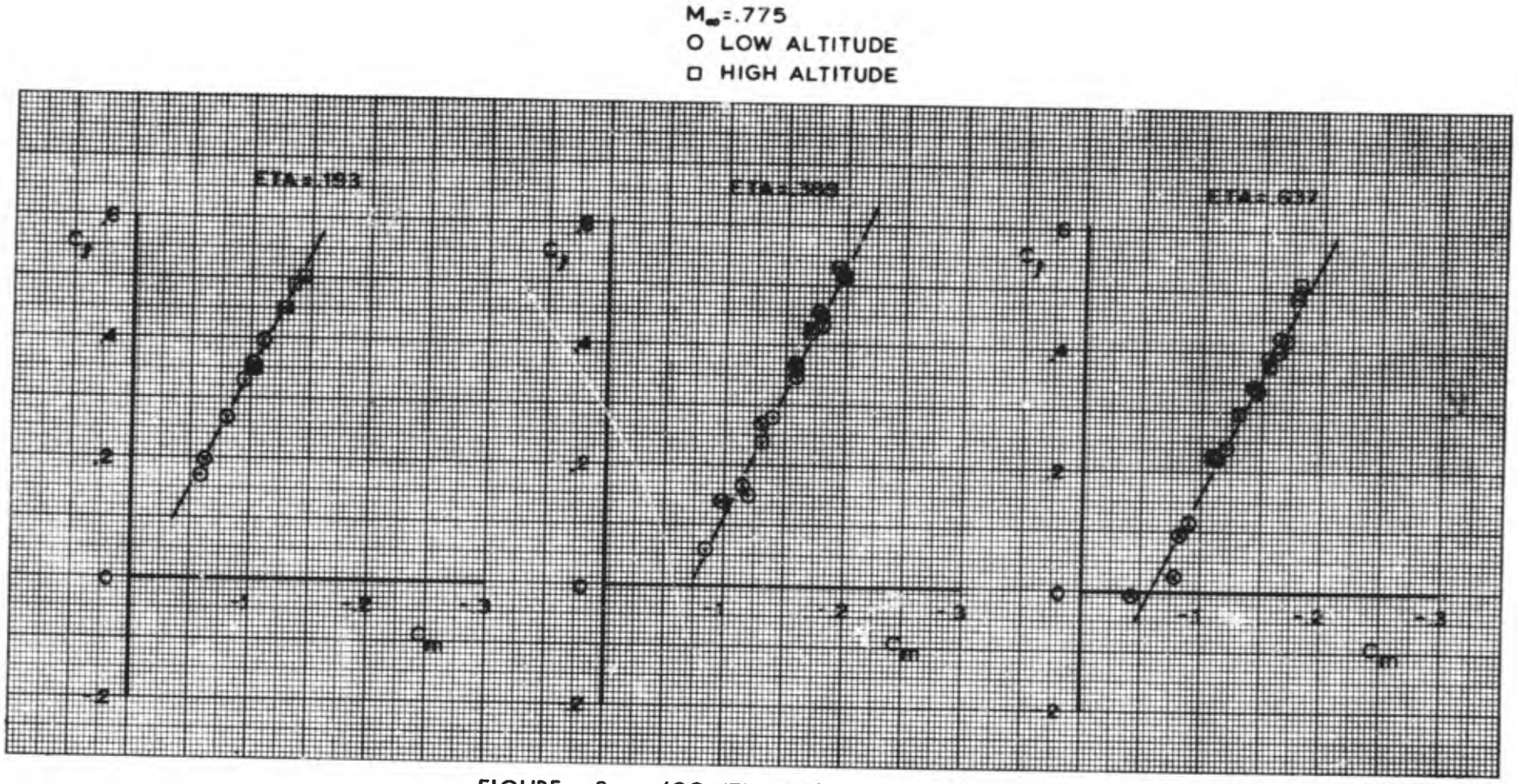

FIGURE 8 (CONTINUED)
(c) MACH = .775

$M_\infty = .800$
O LOW ALTITUDE
□ HIGH ALTITUDE

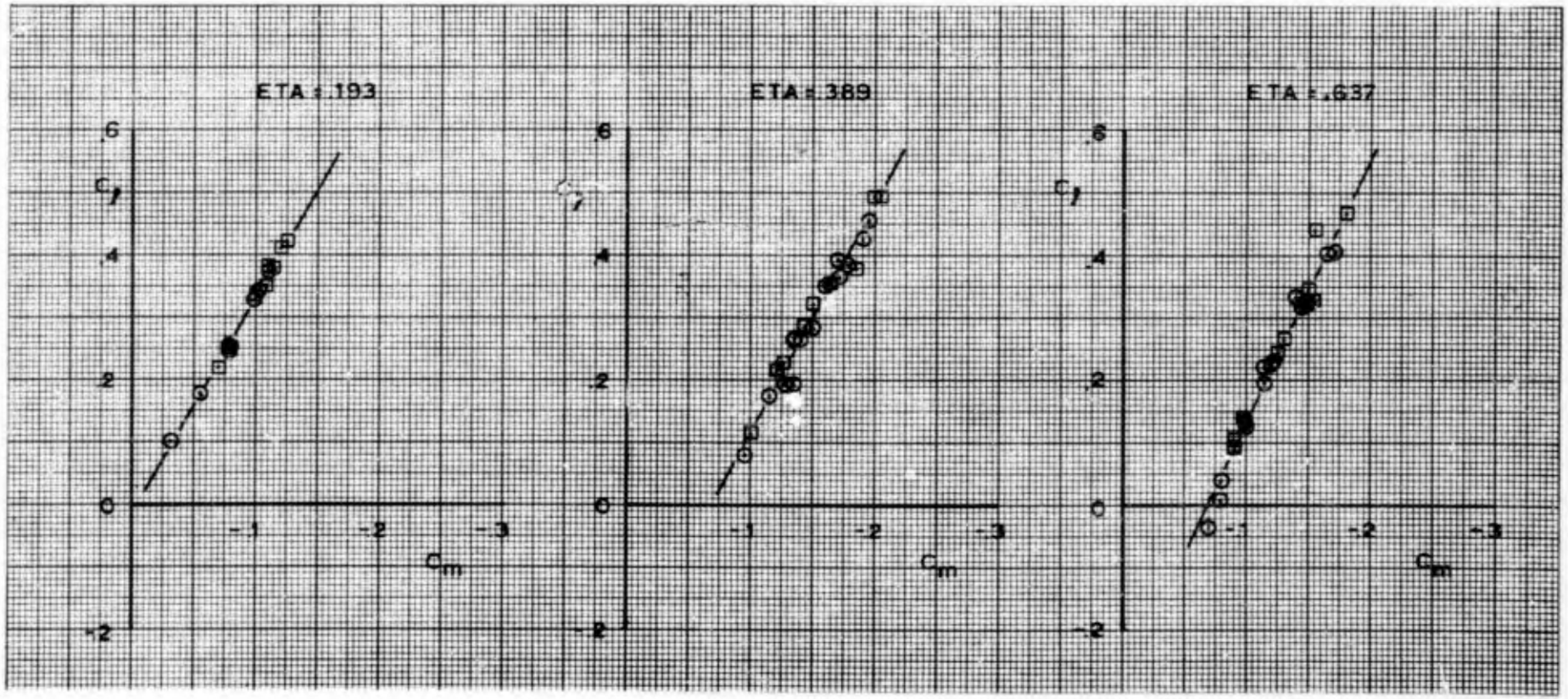

FIGURE 8 (CONTINUED)
(d) MACH = .800

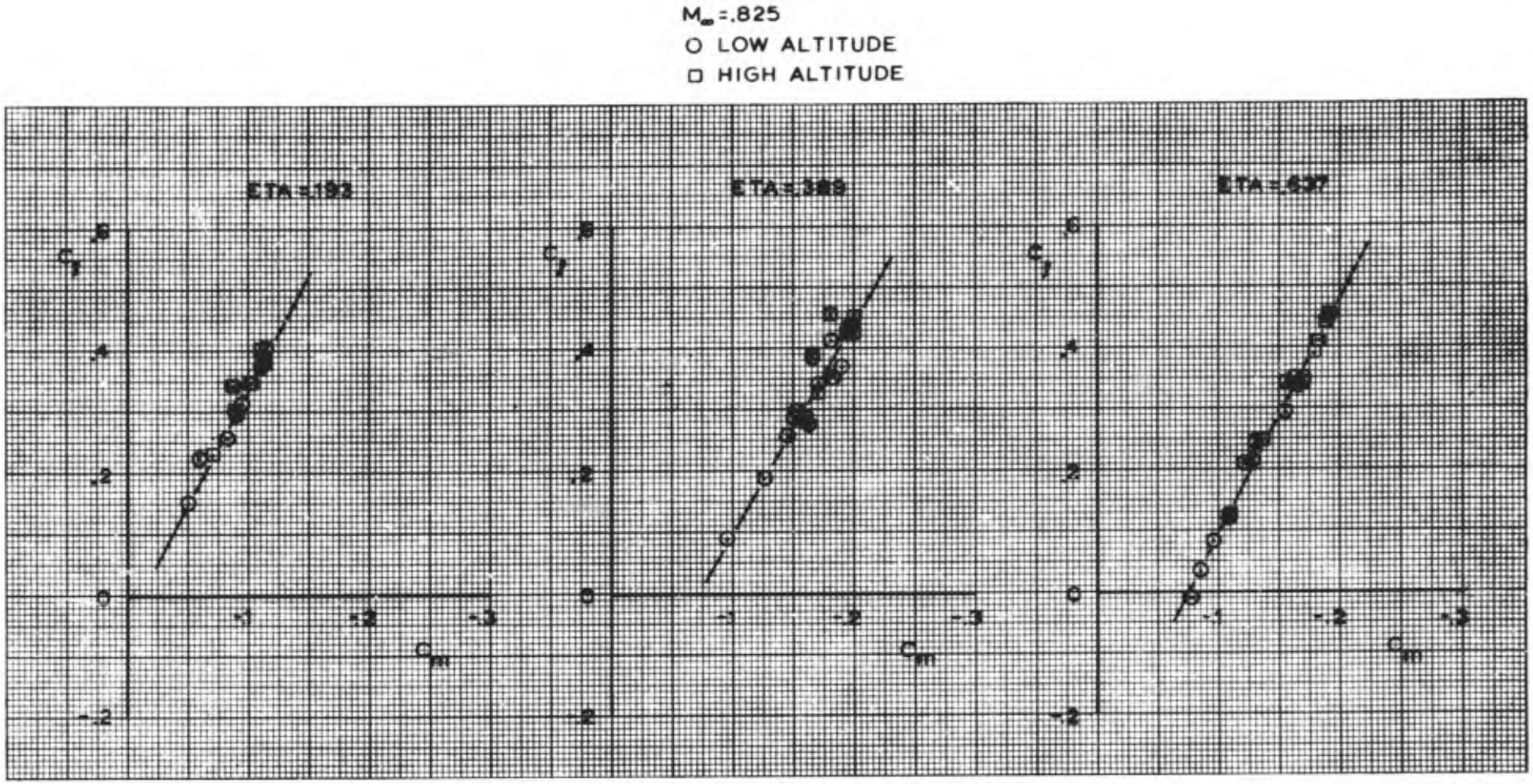

FIGURE 8 (CONTINUED)
(e) MACH = .825

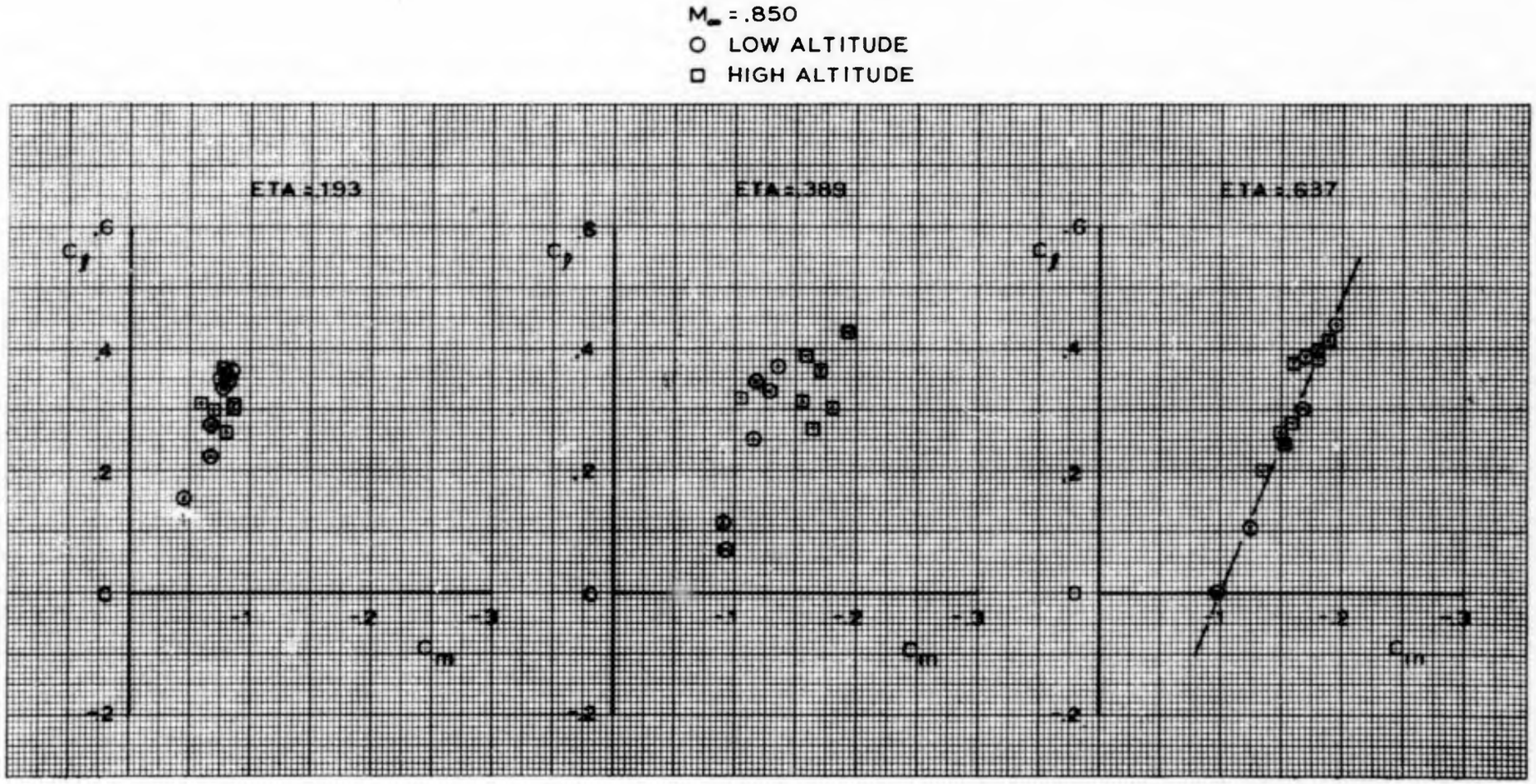

FIGURE 8 (CONCLUDED)
(f) MACH = .850

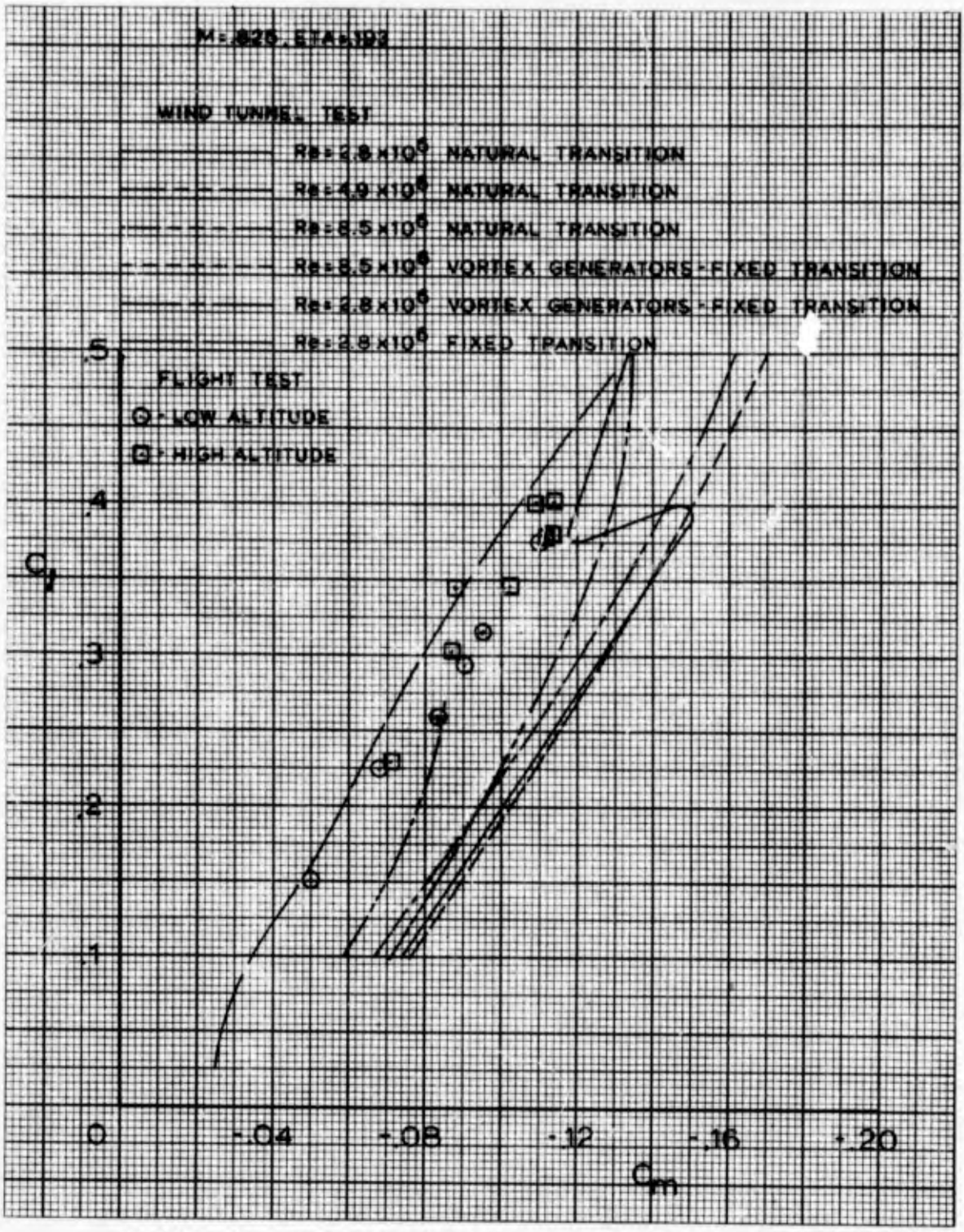

FIGURE 9 WING SECTION LIFT AND PITCH COMPARISONS
(a) ETA = .193

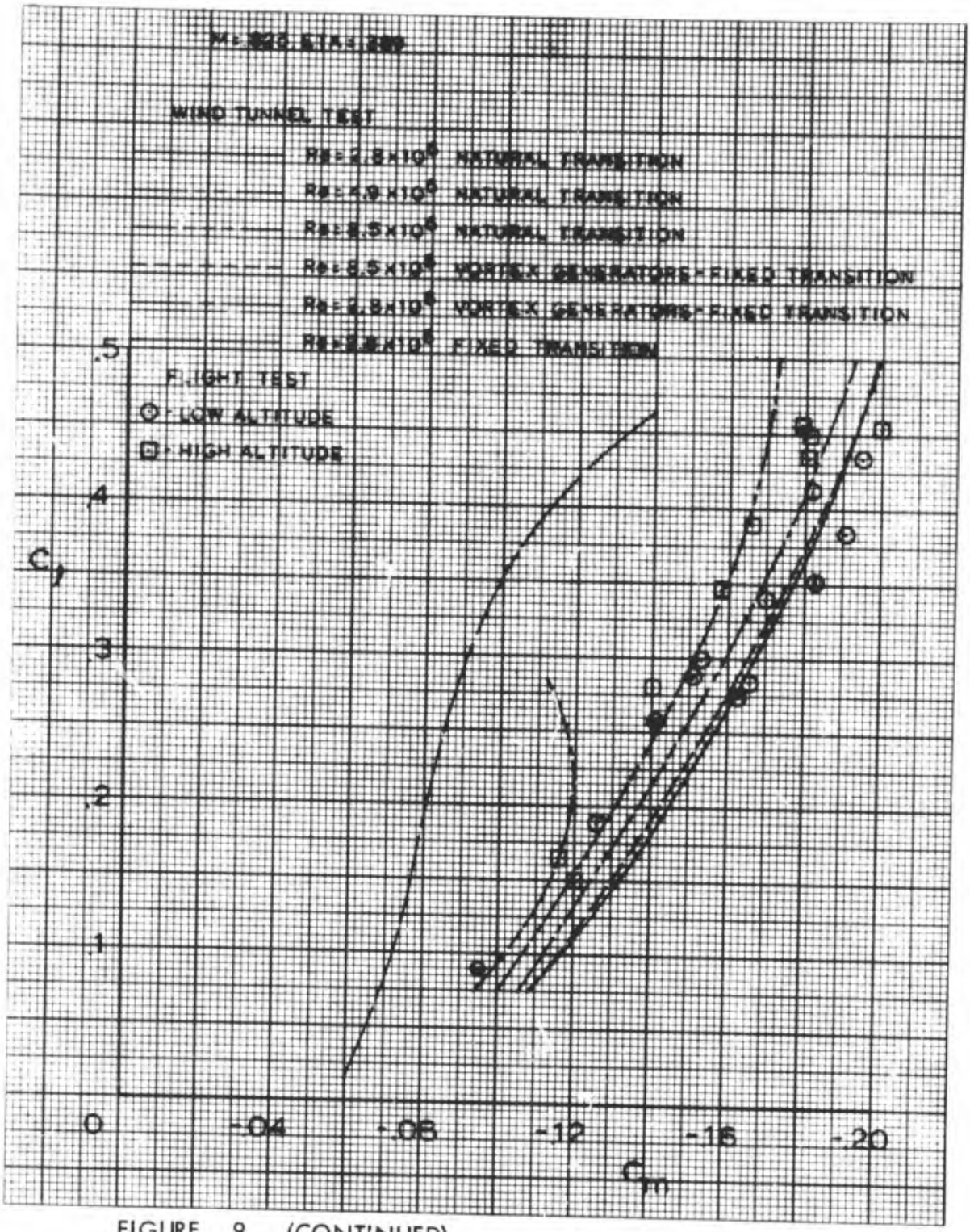

FIGURE 9 (CONTINUED)
(b) ETA = .339

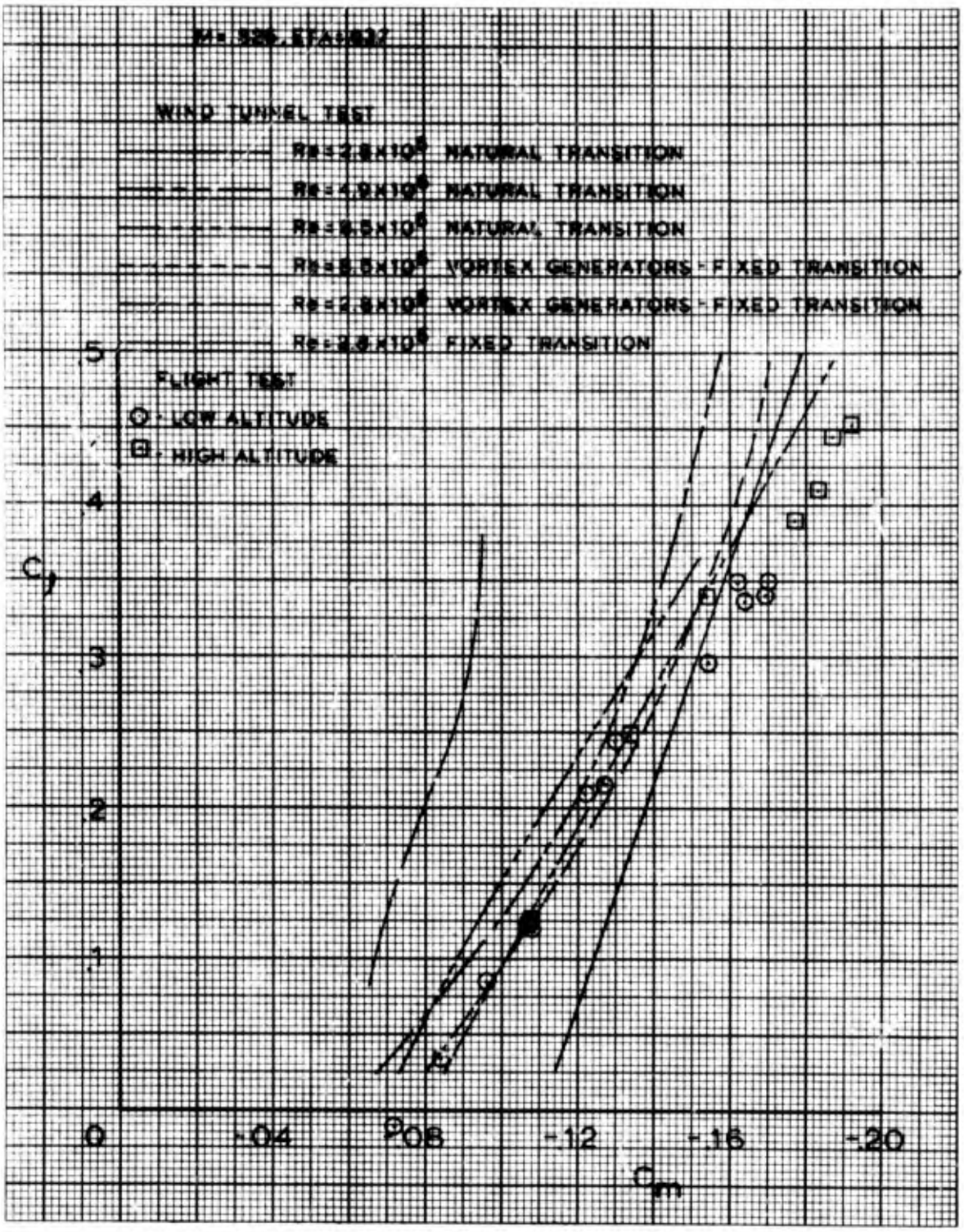

FIGURE 9 (CONCLUDED)
(c) ETA = .637

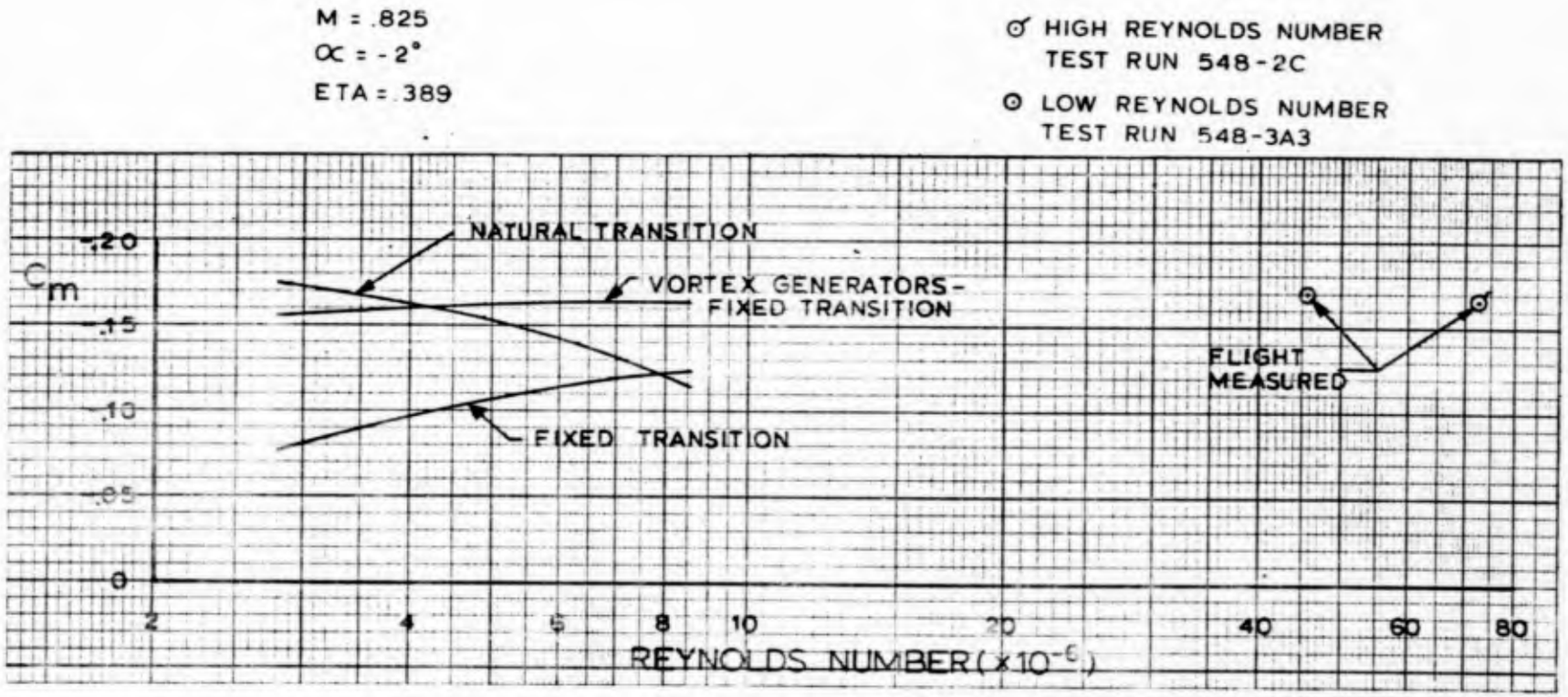

FIGURE 10 SECTION PITCH VARIATIONS WITH REYNOLDS NUMBER

Surface Pressure Distributions

All of the pressure distributions measured in this program are presented in Volume II. Several cases for which wind tunnel data are also available are shown in this section to illustrate similarities and differences in the data. Pressure distribution comparisons between wind tunnel test and flight test are shown in Figures 11 through 14. Figures 11, 12, and 13 are comparisons with wind tunnel data from Reference 3 measured at a Reynolds number of 2.8×10^6 with natural transition. Figure 14 is a comparison using low Reynolds number data from Reference 7.

The comparison at an ETA of 0.193, Figure 11, shows good agreement between the wind tunnel and flight cases except in the lower surface mid-chord region. This good agreement does not conflict with the indication shown by Figure 9a since, in the present comparison, the flow is only slightly supercritical and the shock strength is not great enough to cause a significant interaction. The differences in pressure distribution in the lower surface mid-chord region are due to differences in fuselage and wheel pod shapes between the model and the airplane. Figures 12 and 13 show some differences in shock location and in the shape of the pressure distribution just upstream of the shock. The gradual recompression just forward of the strong shock shown by the wind tunnel data is attributed to weak oblique shocks, resulting either from relatively thick boundary layers or from laminar boundary layers at the shock. Figure 13 shows a difference in trailing edge pressure and would indicate that trailing edge separation has occurred on the model. Figure 14 shows good agreement in the comparison even at a very large negative angle-of-attack.

Shock Location Analysis

Pearcey has discussed in Reference 10 (Page 1208) the flow changes which take place when shock-induced separation becomes significant. A brief review of some points of that discussion is useful as an aid in understanding the shock location changes observed in this investigation. Considering data for an airfoil at a constant angle-of-attack, in an inviscid flow the shock moves aft continuously as the stream Mach number is increased. Local Mach number forward of the shock and shock strength increase as the shock moves aft. In a real flow, the pressure rise through the shock will reach, at some Mach number, a value large enough to cause separation. Reattachment can occur aft of this separation, enclosing a bubble of separated flow. Increasing the Mach number beyond this initial separation condition causes the bubble to grow in chordwise extent. The presence of the bubble causes only a minor distortion of the pressure distribution when reattachment occurs. If the Mach number is increased sufficiently, however, the bubble grows to the trailing edge, producing the condition Pearcey has termed "significant separation". The normal rearward movement of the shock with increase in Mach number is then arrested. The condition for which this significant separation occurs is readily identified as the Mach number above which the trailing-edge pressure recovery departs from its low speed value. For airfoils considered at the time Reference 2 was prepared, little effect of changes in boundary layer properties was observed so long as the boundary layer was definitely turbulent.

Flight Test
- ♂ Upper Surface
- ♂ Lower Surface
- $\alpha = 0°$
- $M_\infty = .775$
- Run No. 548/2A3

Wind Tunnel Test
- ● Upper Surface
- ■ Lower Surface
- $\alpha = 0°$
- $M_\infty = .775$
- $R_e = 2.8 \times 10^6$
- Natural Transition
- Reference 3

ETA = .193

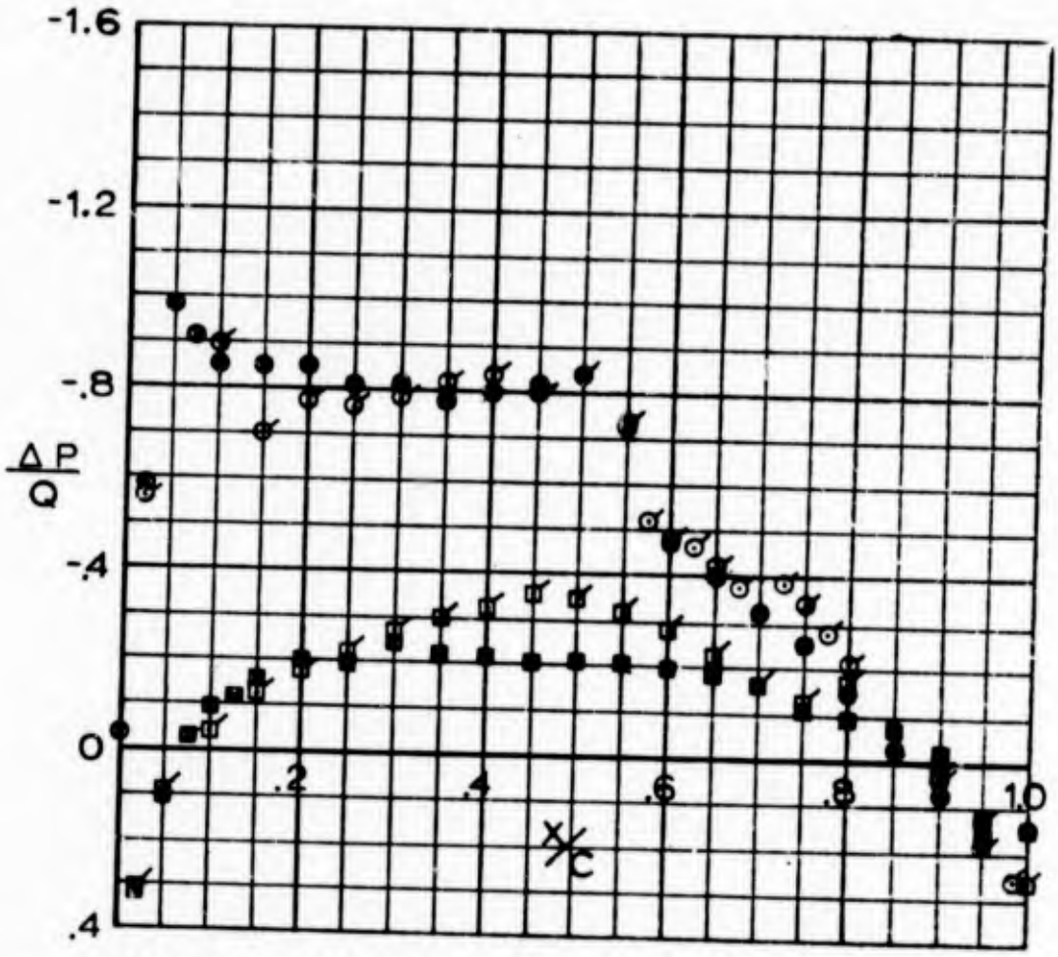

FIGURE 11 PRESSURE DISTRIBUTION COMPARISON
ETA = 0.193 MACH = .775

Flight Test

- ♂ Upper Surface
- ♂ Lower Surface
- $\alpha = -1.98°$
- $M_\infty = .820$
- Run No. 548/3A3

Wind Tunnel Test

- ⊗ Upper Surface
- ⊠ Lower Surface
- $\alpha = -2°$
- $M_\infty = .825$
- $R_e = 2.8 \times 10^6$
- Natural Transition
- Reference 3

ETA = 0.389

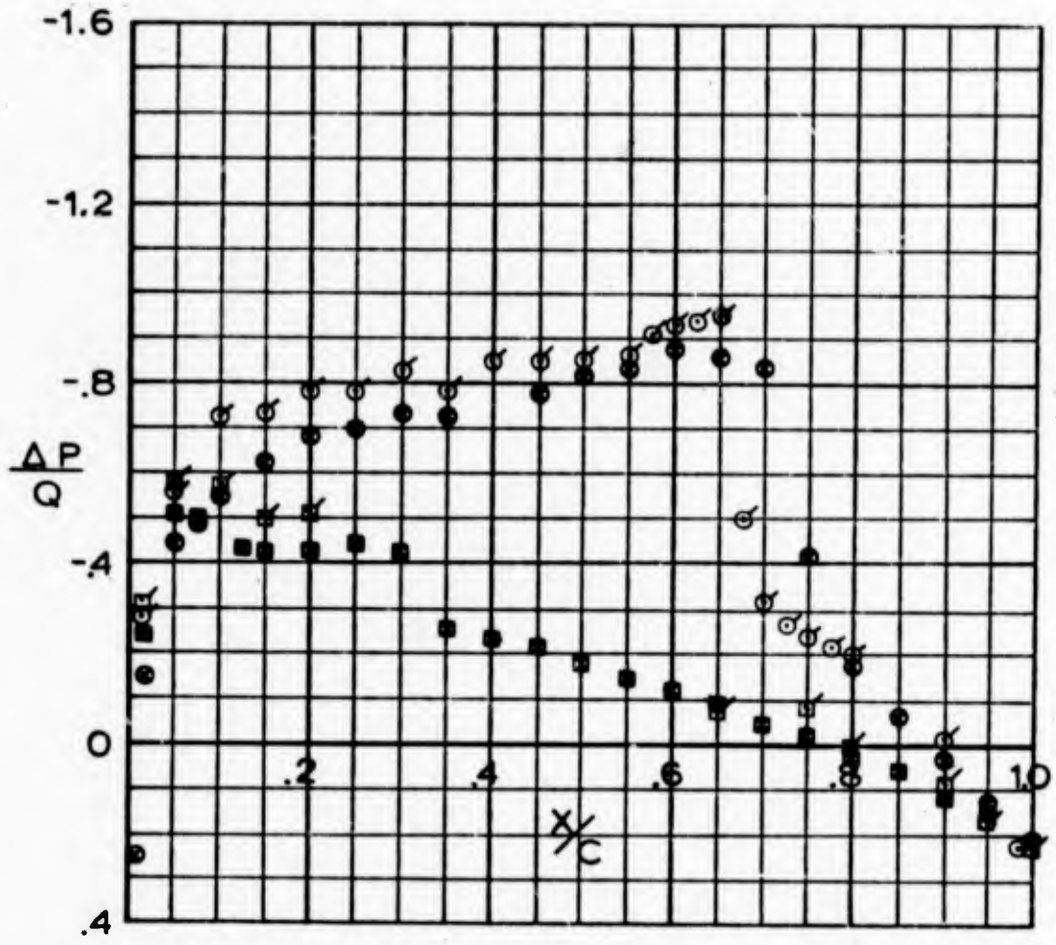

FIGURE 12 PRESSURE DISTRIBUTION COMPARISON
ETA = 0.389 MACH = .825

Flight Test

- Upper Surface
- Lower Surface
- α = -1.02°
- M_∞ = .840
- Run No. 547/2A1

Wind Tunnel Test

- Upper Surface
- Lower Surface
- α = -1.00°
- M_∞ = .850
- $R_e = 2.8 \times 10^6$
- Natural Transition
- Reference 3

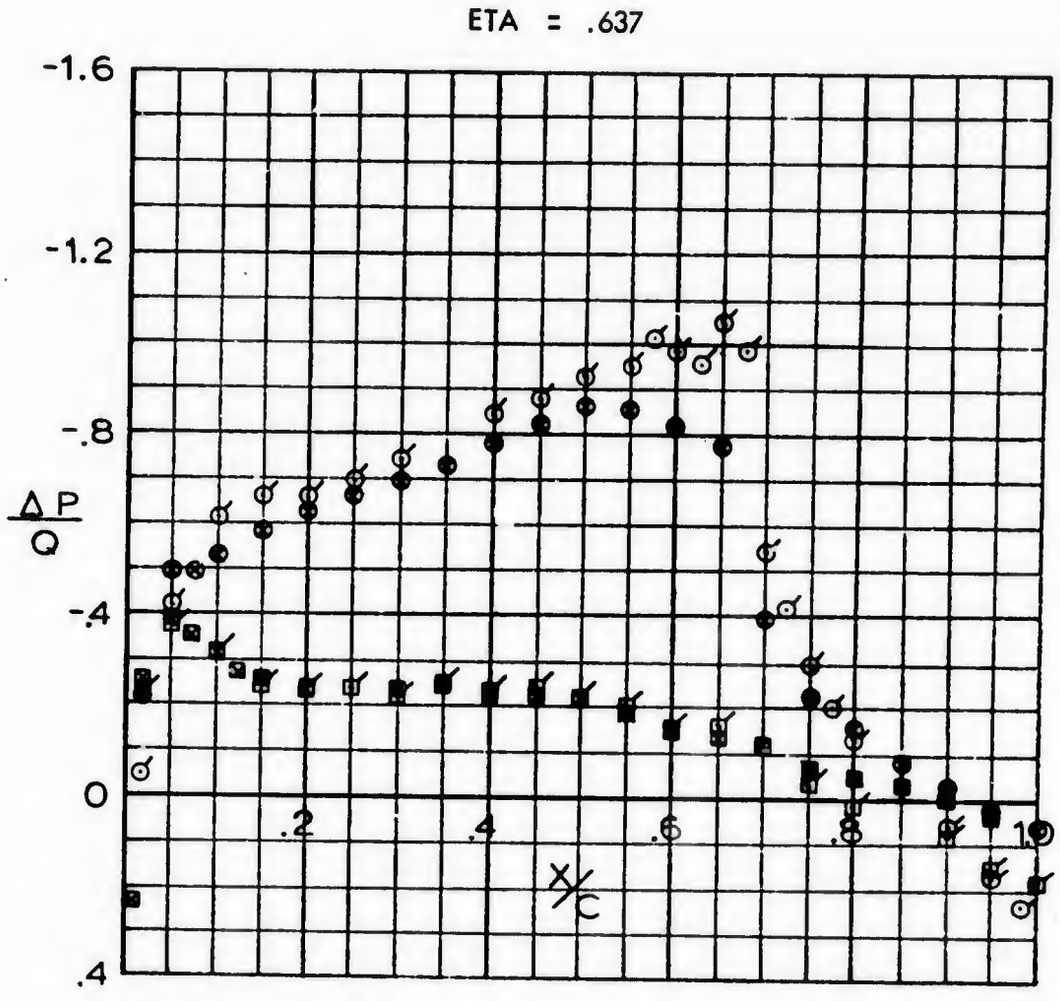

FIGURE 13 PRESSURE DISTRIBUTION COMPARISON
ETA = 0.637 MACH = .850

Flight Test

- Upper Surface
- Lower Surface

$\alpha = -4.00°$

$M_\infty = .820$

Run No. 548/2C5

Wind Tunnel Test

- Upper Surface
- Lower Surface

$\alpha = -4.00°$

$M_\infty = .825$

$R_e = 1.44 \times 10^6$

Natural Transition

Reference 7

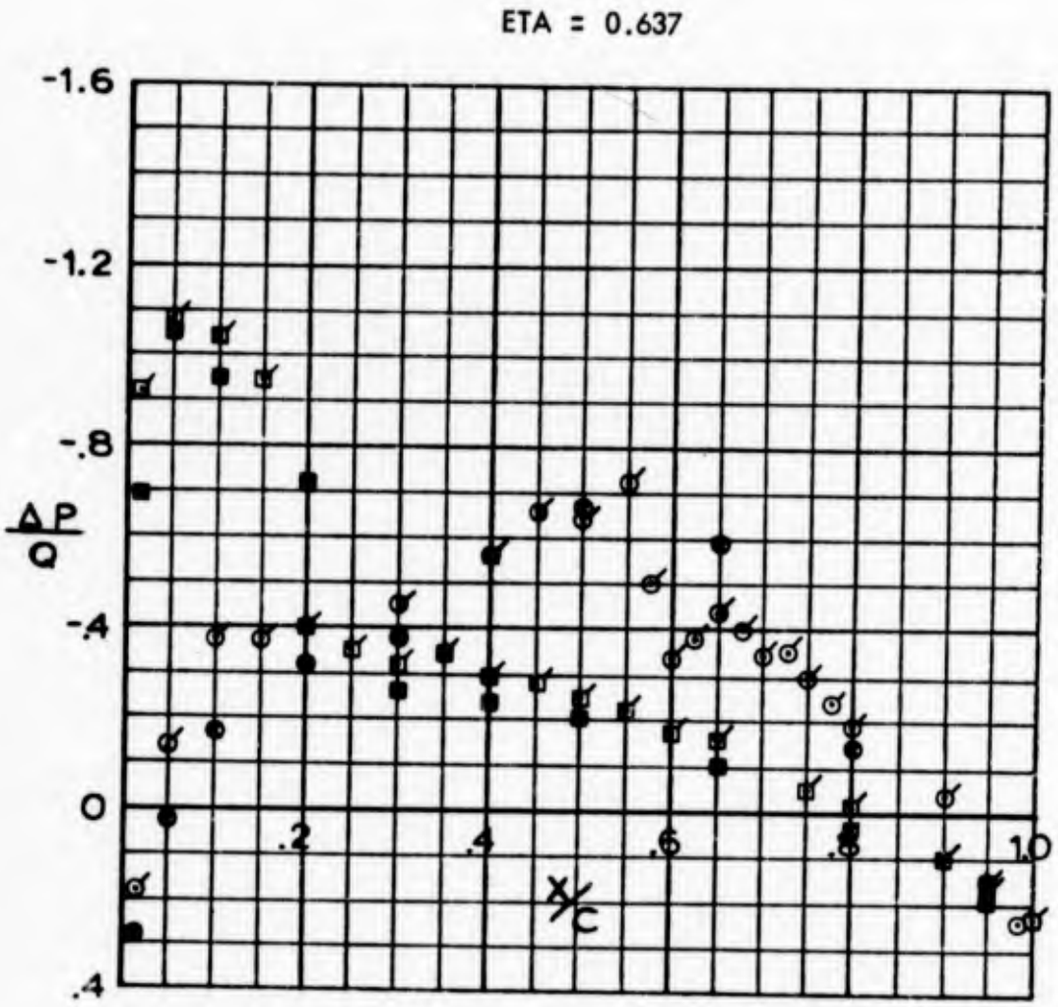

FIGURE 14 PRESSURE DISTRIBUTION COMPARISON
ETA = 0.637 MACH = .825

For airfoils of the type used on the C-141, however, the effect of changes in turbulent boundary layer thickness has been shown to be quite large. Pressure distribution data from the investigation reported in Reference 4 are shown in Figure 15, illustrating the changes resulting from increases in turbulent boundary layer thickness as a transition fixing strip is moved forward on the wing chord. The pressure rise through the shock is large enough to cause separation in all cases shown and the existence of a separation bubble is indicated by the "bumps" in the pressure distributions immediately behind the shock. With no transition strip, the bubble is rather short and the trailing-edge pressure recovery indicates no great separation at the trailing-edge. As the boundary layer is thickened by moving the transition strip forward, the reattachment point is seen to move aft, the trailing-edge pressure recovery decreases, and the shock moves forward. Similar data from Reference 3 are shown in Figure 16 indicating a similar variation of shock location and trailing-edge pressure recovery as the boundary layer thickness increases due to forward movement of the natural transition point with an increase in Reynolds number from 2.8 to 8.5×10^6.

The mechanism responsible for shock movement has also been discussed by Pearcey. At and aft of the wing trailing-edge, a balance must exist among flow conditions resulting from the upper surface boundary layer, the lower surface boundary layer, and the ambient undisturbed flow. There is no hard boundary to support a pressure difference. The required balance is established by the mixing processes taking place in the wake. It is clear, therefore, that the lower surface flow and the mixing phenomena in the wake establish a boundary condition which must be satisfied by the upper surface flow. In a manner similar to that occurring in supersonic diffusers, the shock seeks a location such that its pressure rise, when combined with the subsequent subsonic pressure rise, and their combined effect on the boundary layer will satisfy that downstream boundary condition. Change in shock location accomplishes this change in pressure rise, of course, by changing the local Mach number at which the shock occurs. This phenomenon is the reason that the C-141 airfoil section, with its flat Mach number variation forward of the shock, is subject to large changes in shock location while other airfoils, with steeper Mach number gradients, display smaller shock location changes. The data presented in Reference 6 for circular arc airfoils having relatively large Mach number gradients, for instance, show little or no change in shock location despite wide changes in Reynolds number and boundary layer thickness.

The variation of shock location with Mach number from the current flight investigation is shown in Figure 17 in comparison with various wind tunnel conditions which had previously been investigated. The wind tunnel data are taken from Reference 3. Since it was not possible in these flight tests to maintain precise values of Mach number and angle-of-attack for direct comparison with the wind tunnel data, the flight-measured shock locations shown in Figure 17 were taken from those contours. It can be seen that the data obtained in the present investigation show variations similar to those indicated by Pearcey. The shock location moves aft as the Mach number is increased from its lowest value, reaches a peak, and then moves slightly forward. Examination of the pressure data shows that the trailing-edge pressure recovery is excellent for Mach numbers up to those showing the most aft shock location, and indicate definite trailing-edge separation for Mach numbers above that value.

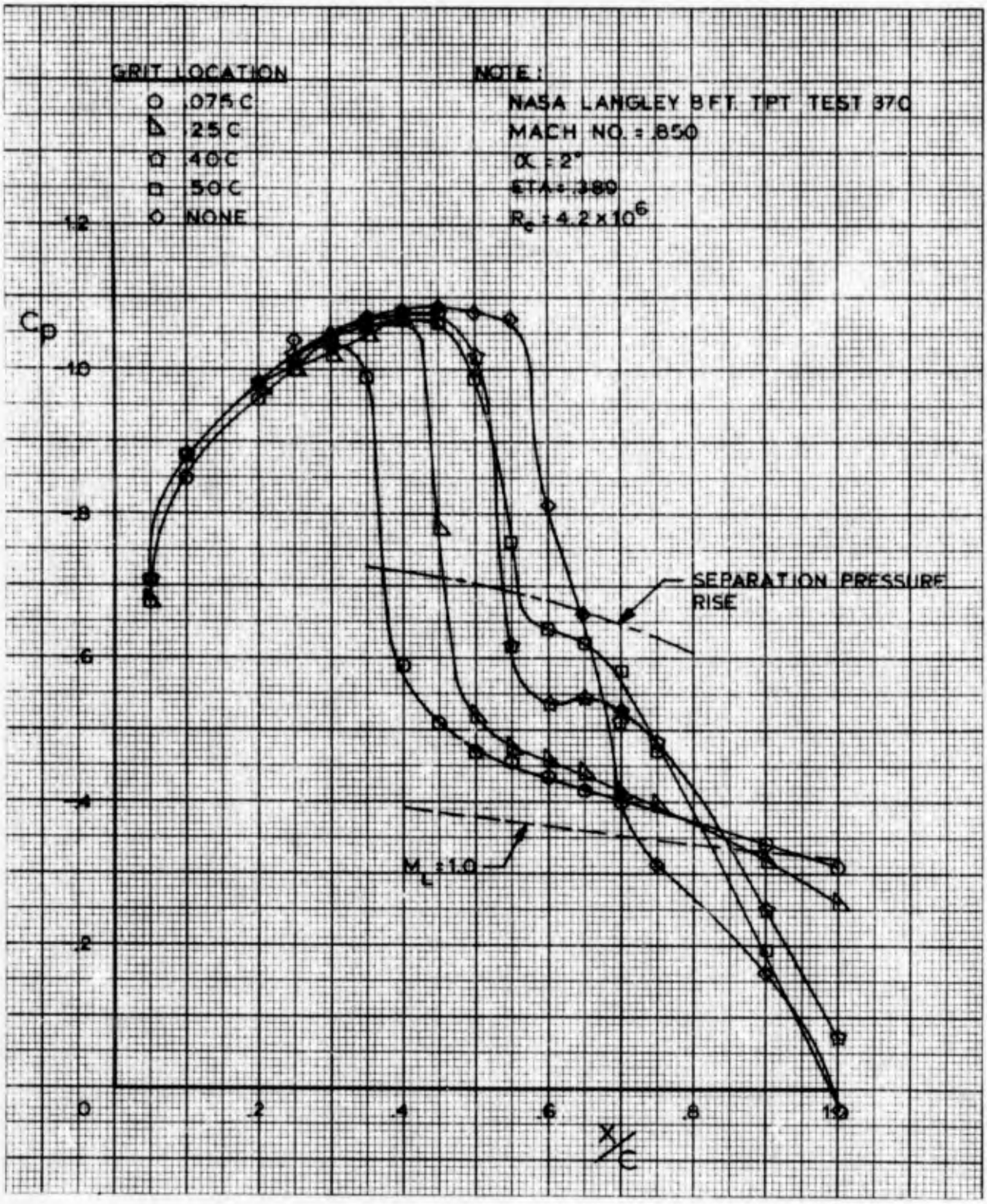

FIGURE 15 EFFECT OF TRANSITION STRIP LOCATION ON WING PRESSURE DISTRIBUTION

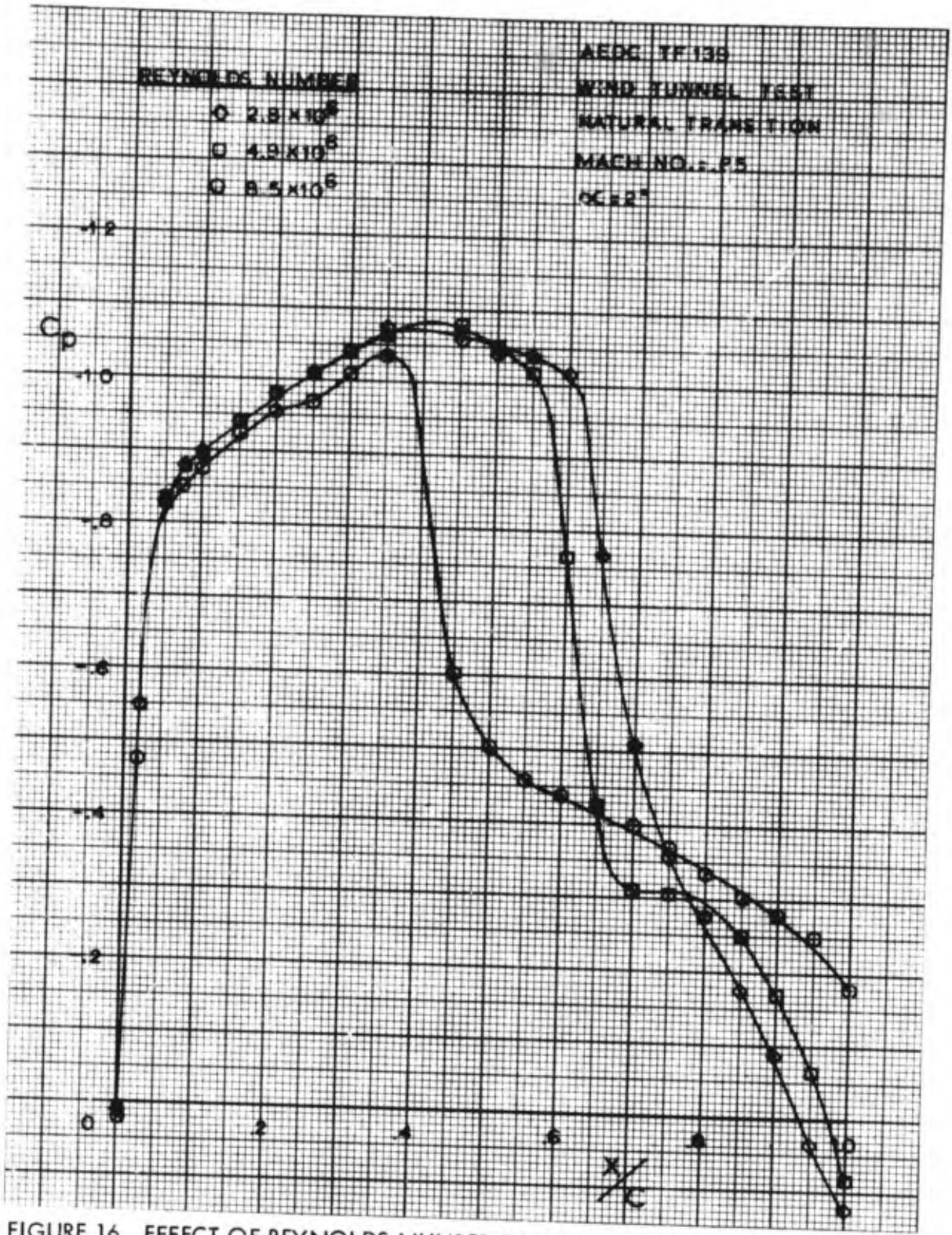

FIGURE 16 EFFECT OF REYNOLDS NUMBER ON WING, PRESSURE DISTRIBUTION - NATURAL TRANSITION

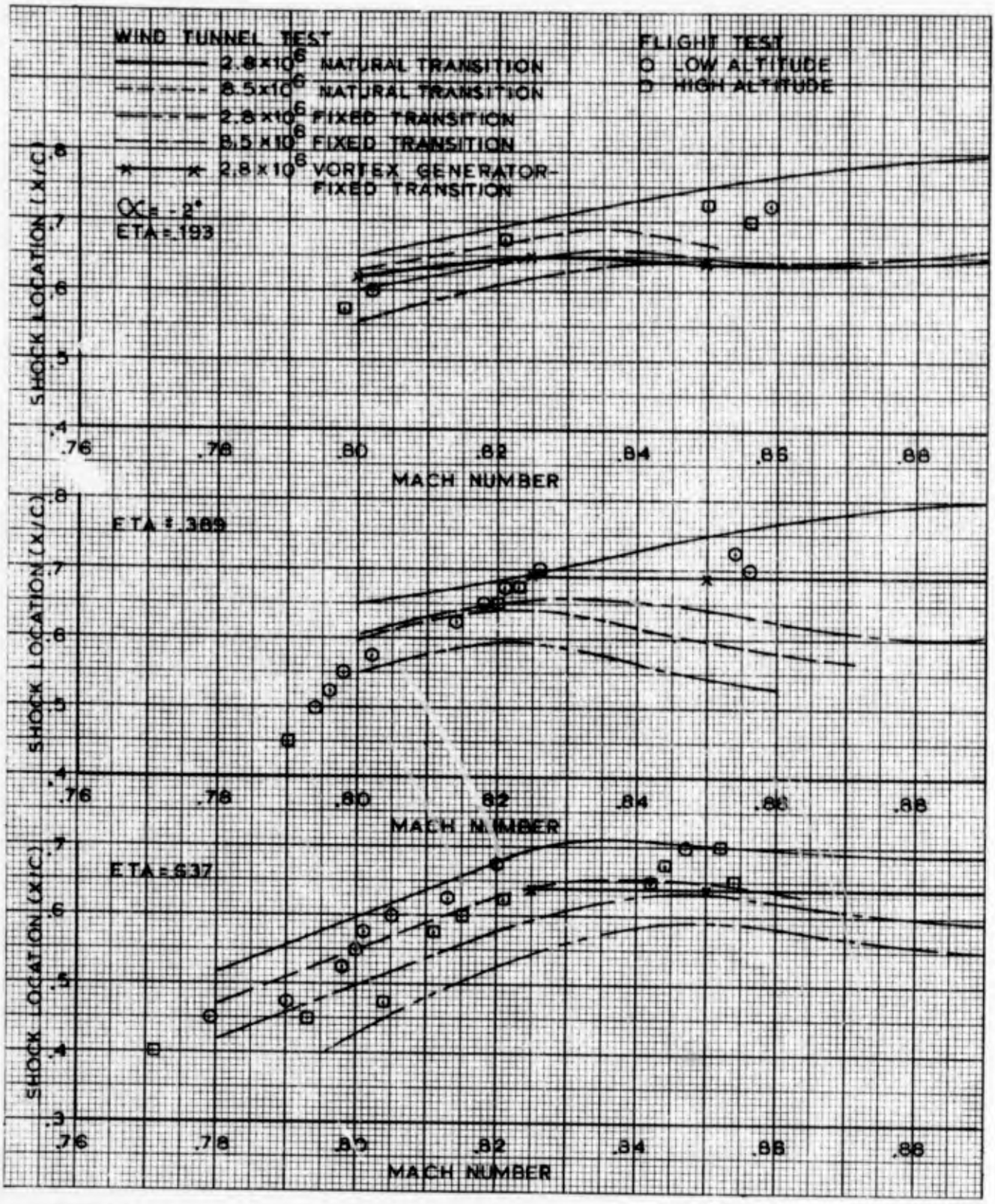

FIGURE 17 VARIATION OF SHOCK LOCATION WITH MACH NUMBER
(a) $\alpha = -2°$

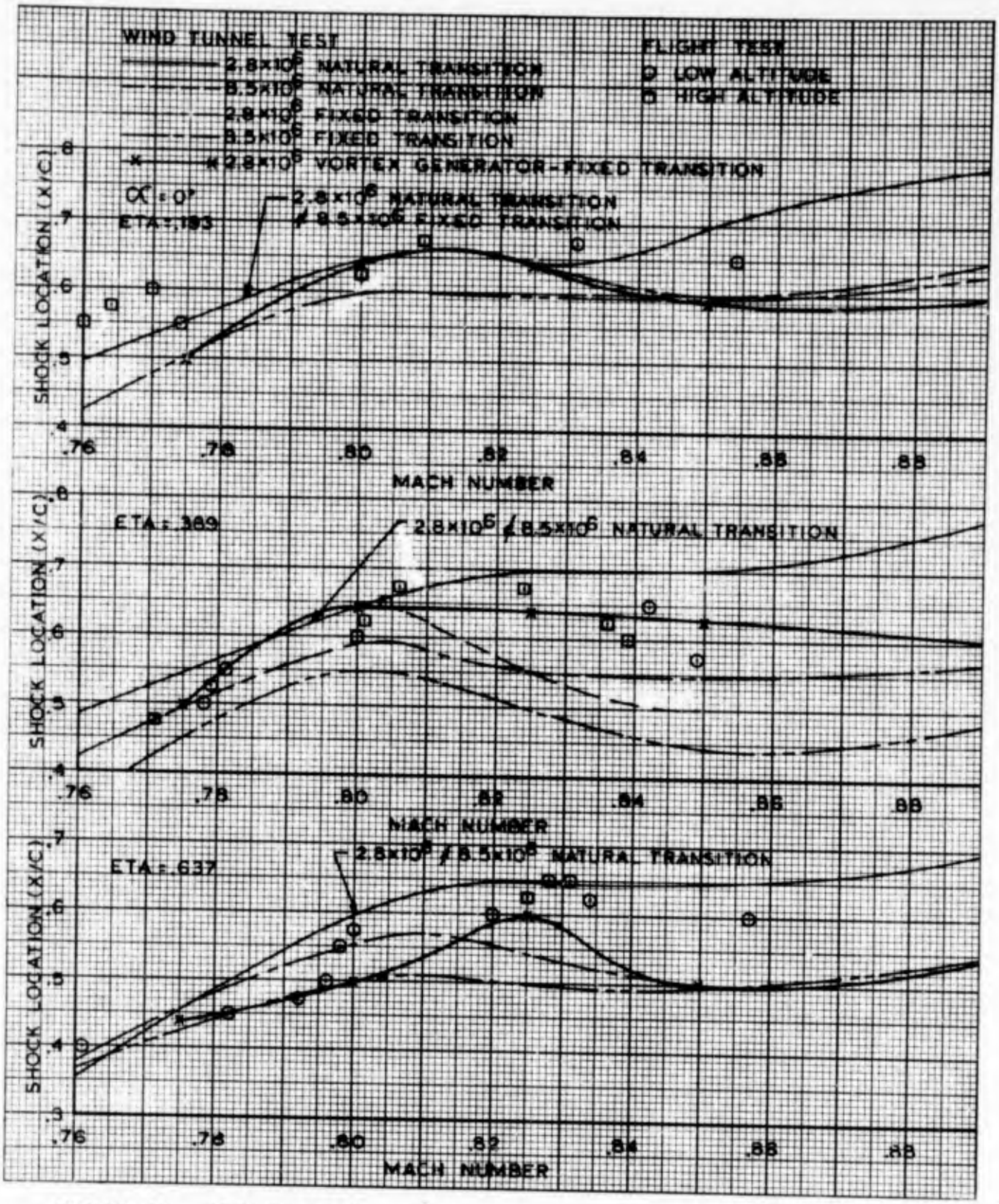

FIGURE 17 (CONTINUED)
(b) $\alpha = 0°$

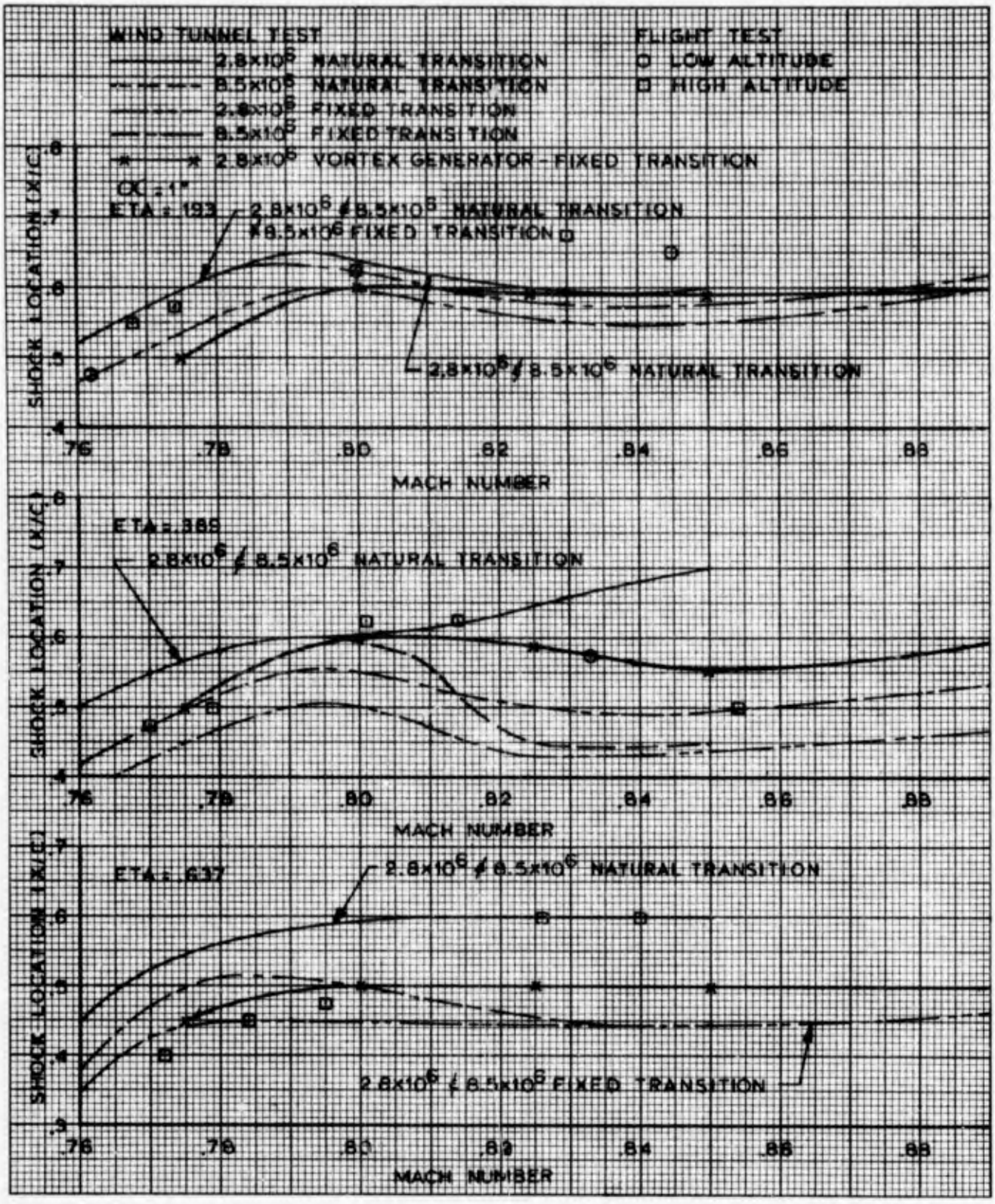

FIGURE 17 (CONCLUDED)
(c) $\alpha = 1°$

Figure 18 is presented to show the range of local flow conditions demonstrated by the data obtained in the current flight program. Data obtained in this investigation provide a graphic demonstration of the separation-reattachment phenomenon discussed by Pearcey. The boundary-layer rake at 80% chord indicated reversed flow for a large number of cases where the trailing-edge pressure recovery showed that the trailing-edge was not separated. Data are presented in Figure 18 to show the conditions under which this phenomenon occurred. The pressure rise from just forward of the shock to 80% chord, and to the trailing-edge, are plotted against local Mach number forward of the shock. The pressure rise is divided, in each case, by the pressure rise required for shock induced separation as defined by the data of Reference 12; and the local Mach number is defined in the direction normal to the local wing element lines. Skin friction values indicated by the boundary layer rake data at 55% chord are used in defining the separation pressure rise. In cases where the rake at 80% chord showed separated flow, the symbols are shown shaded. Questionable separation is indicated by partially shaded symbols. Flags on the symbols are used to denote those test points for which the flow is separated at the trailing-edge. A trailing-edge pressure coefficient less than +0.2 was used to define trailing-edge separation.

Although the data scatter too widely to justify discrete lines through these points, the variation of all the data can be described by rather narrow bands. As the angle-of-attack is increased at constant Mach number, these curves progress upward to the right, reach a peak, and then decrease abruptly as trailing-edge separation occurs. As would be expected, the trailing-edge pressure rise decreases much more abruptly at separation than does the 80% chord value.

Separation as indicated by the 80% rake is shown to be predicted quite well by the shock separation criterion of Reference 12. In the majority of cases tested however, the flow reattaches behind this separation, the total pressure rise to the trailing-edge reaching three times the shock separation value before the trailing-edge itself is separated. Neither the precise origin of the separation, nor the dimensions and growth of the bubble, can be determined from the measurements which were possible during this investigation. However, an examination of the 80% chord rake data shows that the height of the "zero velocity" point generally increases as the pressure rise increases above the separation value. The maximum depth of this separation bubble prior to trailing-edge separation is approximately 1% chord. At trailing-edge separation, the 80% separation depth increases abruptly.

The separation pressure rise criterion used in Figure 18 is, of course, applicable only at the shock. The good correlation between predicted and actual separation shown by the 80% chord data results from the fact that the shocks are rather far aft, and the pressure rise at 80% chord is not greatly different from the pressure rise through the shock. Following reattachment, however, the boundary layer is rather quickly rehabilitated to have velocity profiles approaching those before the shock. Data are presented in Reference 14 which show this rehabilitation quite clearly. Following reattachment therefore, the boundary layer is capable of withstanding additional pressure rise and the shock pressure rise to separation obtained from Reference 12 is not applicable to the total pressure rise to the trailing-edge. The form of presentation used in Figure 18 is useful, however, to show the two sets of pressure rise data on a common basis.

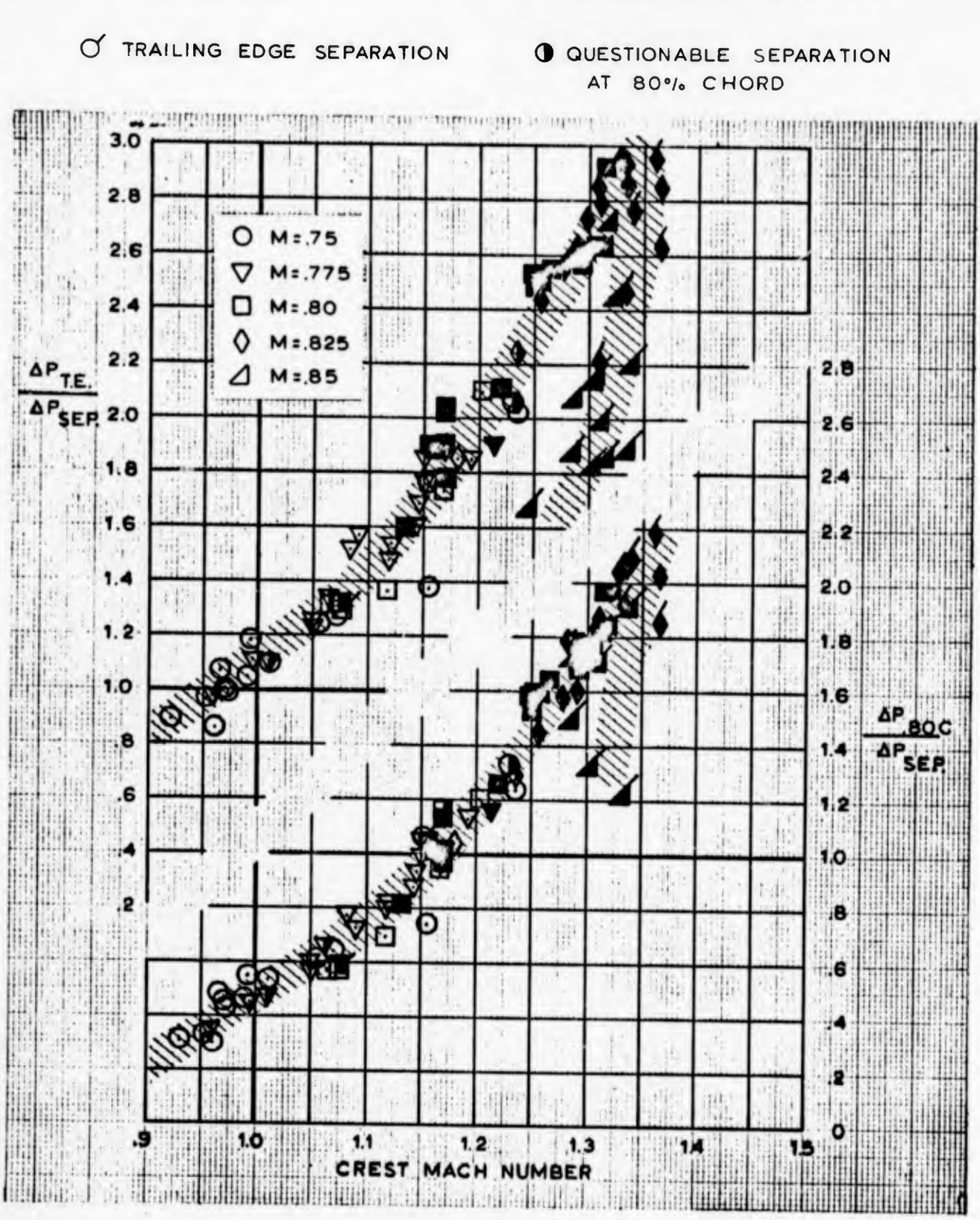

FIGURE 18 SHOCK-INDUCED SEPARATION

The question as to whether the ultimate complete separation results from a trailing-edge separation creeping forward or from the separation bubble growing aft cannot be answered with the data available from the current investigation. Future studies of this point would appear to be desirable however, since the relative growth of these two separations is probably dependent on Reynolds number, and might therefore be a key factor in these scale effects.

Referring again to Figure 17, it can be seen that the variation of shock location with Mach number is similar to that shown by the wind tunnel data, but no wind tunnel condition matches the flight data in all respects. It is interesting to note that the use of vortex generators tends to produce the best match of the techniques considered in these wind tunnel tests. It is not felt, however, that the use of vortex generators can be considered a generally acceptable concept in producing accurate predictions of flight results. While vortex generators are known to suppress separation in a manner similar to increases in Reynolds number, the effectiveness of vortex generators certainly cannot be controlled to cause a match with any arbitrary flight condition. The agreement shown by Figure 17 must therefore be considered fortuitious.

The effect of changes in Reynolds number and surface condition on shock location is shown in a different form in Figure 19. Shock locations for angles-of-attack of -2°, 0°, and 1° are shown plotted against Reynolds number for Mach numbers of .825 and .850. Although some scatter exists in these data, the basic variations are quite clear and are similar for the two Mach numbers shown. With the transition location artificially fixed near the leading-edge, the wind tunnel data show shock locations moving consistently aft as the Reynolds number is increased. Furthermore, it would seem reasonable that the variation at very high Reynolds numbers should be an approximate extension of this variation since at those Reynolds numbers, the natural transition location is at the leading-edge. A single line is shown, therefore, connecting these points through the complete Reynolds number range, and the change in shock location over the range covered is approximately 20% of the wing chord. When the wind tunnel model was tested smooth, the shock location at low Reynolds number was roughly similar to that observed in flight and increases in Reynolds number caused the shock to move forward. In this instance, the shock locations at 8.5×10^{6} Reynolds number were approximately the same with and without the transition strip. This variation of shock location is attributed to the fact that appreciable runs of laminar flow were observed in the wind tunnel tests at low Reynolds number, resulting in very small boundary layer thicknesses at the shock. Increasing Reynolds number moves the transition forward, increases boundary layer thickness, and causes the shock to move forward.

Boundary Layer Parameters

All of the basic boundary layer profiles measured in this program are presented in Volume II. Boundary layer thicknesses and form factors obtained from integration of those profiles are shown in Figure 20. These data were measured on the left wing of the airplane (the surface-pressure-measuring STRIP-A-TUBE was on the right wing) at $x/c = .30$, .55, and .80 at approximately an ETA of .389. The rakes were staggered slightly to avoid interference of the forward rakes on those behind. Both high and low Reynolds number data for the flight conditions tested are shown in Figure 20 but, over the Reynolds number range covered by these tests, the scale effect on boundary layer parameters is scarcely discernible. Data are not shown for the rake at 80% chord for a number of cases because the profiles show that the flow is separated in those cases. The values of the form factor for 80% chord would indicate imminent separation for all except the lowest Mach numbers and lift coefficients. At the higher Mach numbers, the boundary layer thickness on the forward part of the chord shows little variation with lift

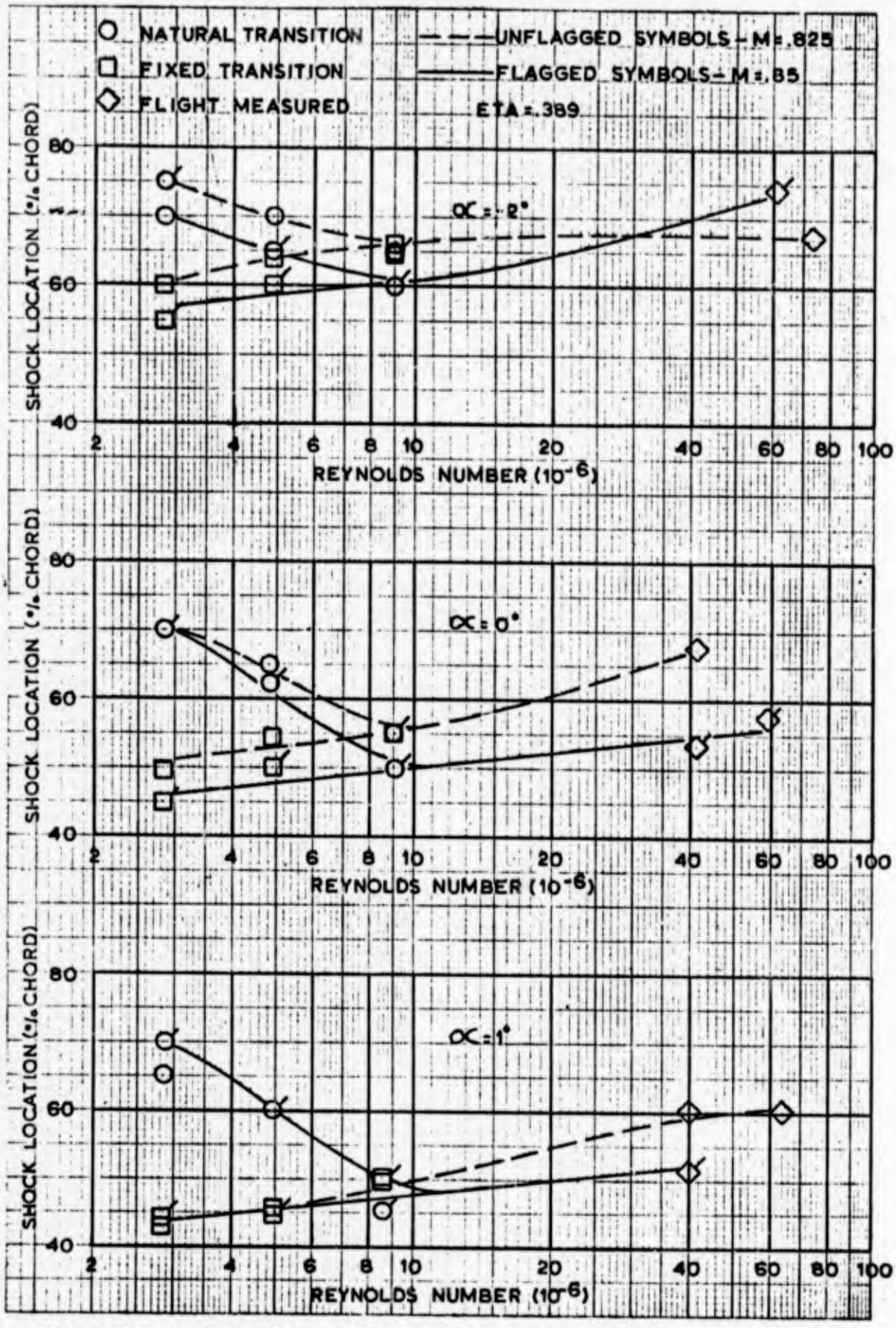

FIGURE 19 VARIATION OF SHOCK LOCATION WITH REYNOLDS NUMBER

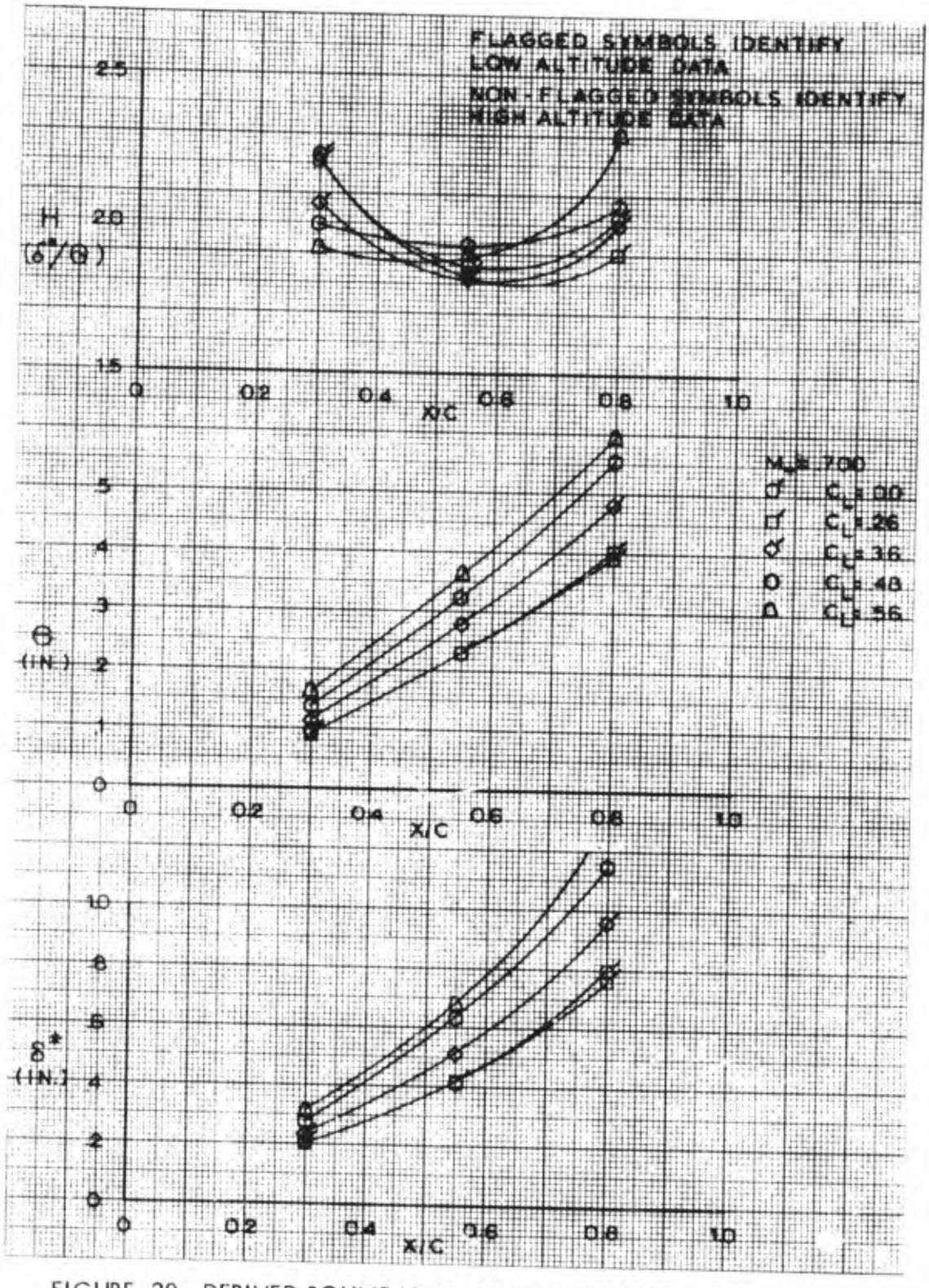

FIGURE 20 DERIVED BOUNDARY LAYER PARAMETERS
(a) $M_\infty \approx .70$

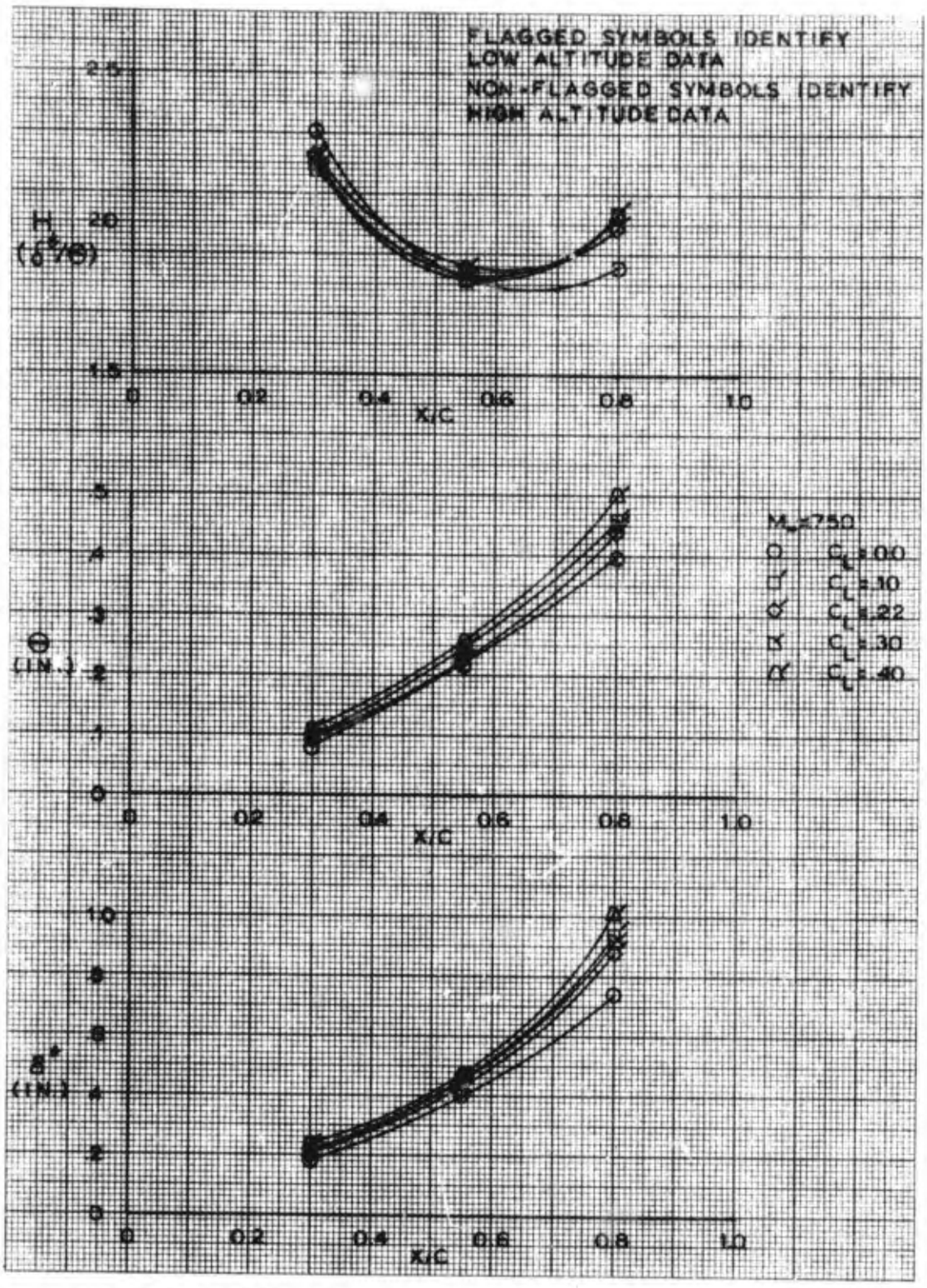

FIGURE 20 DERIVED BOUNDARY LAYER PARAMETERS
(b) M_∞ = .75

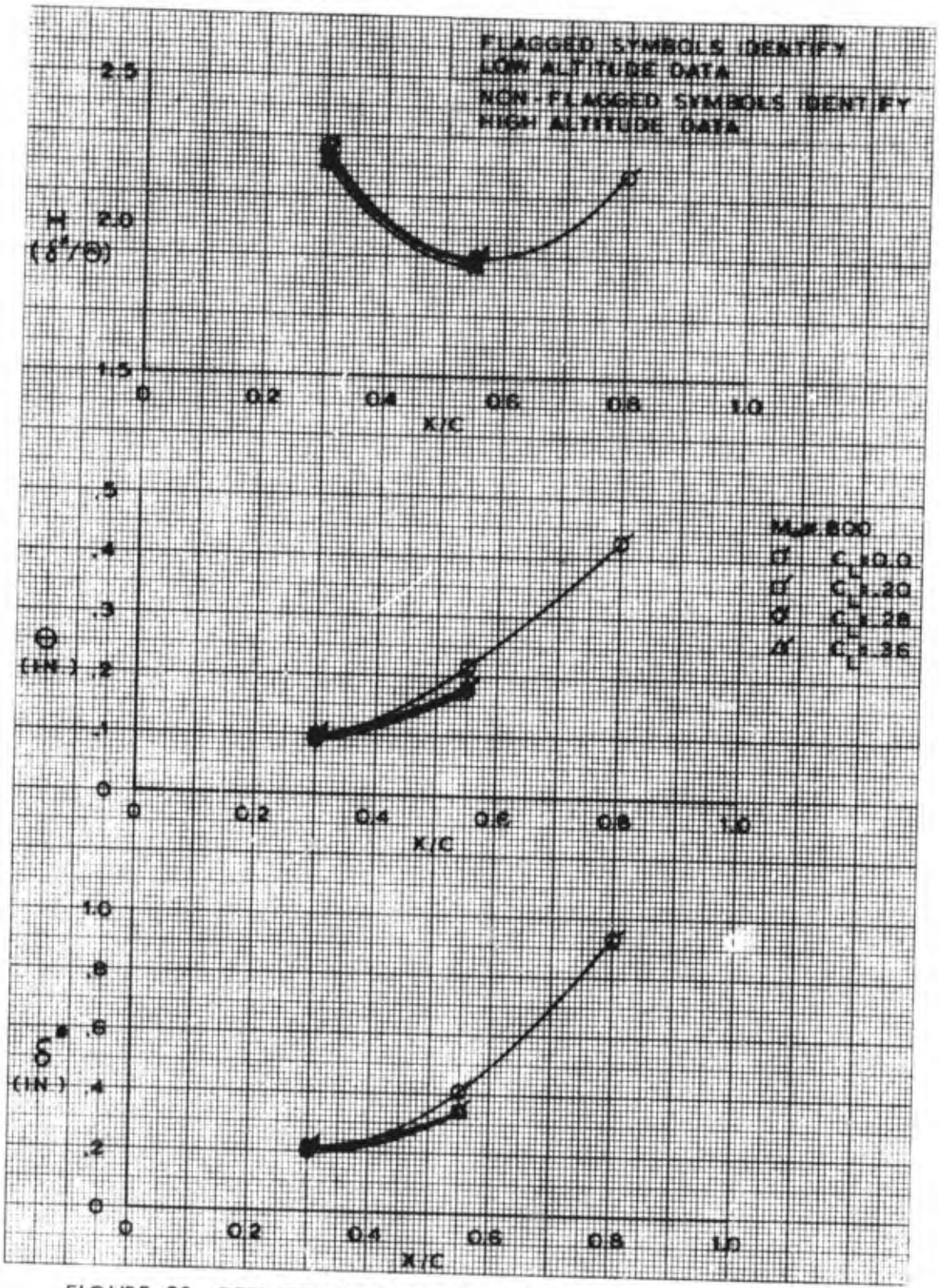

FIGURE 20 DERIVED BOUNDARY LAYER PARAMETERS
(c) M_∞ = .800

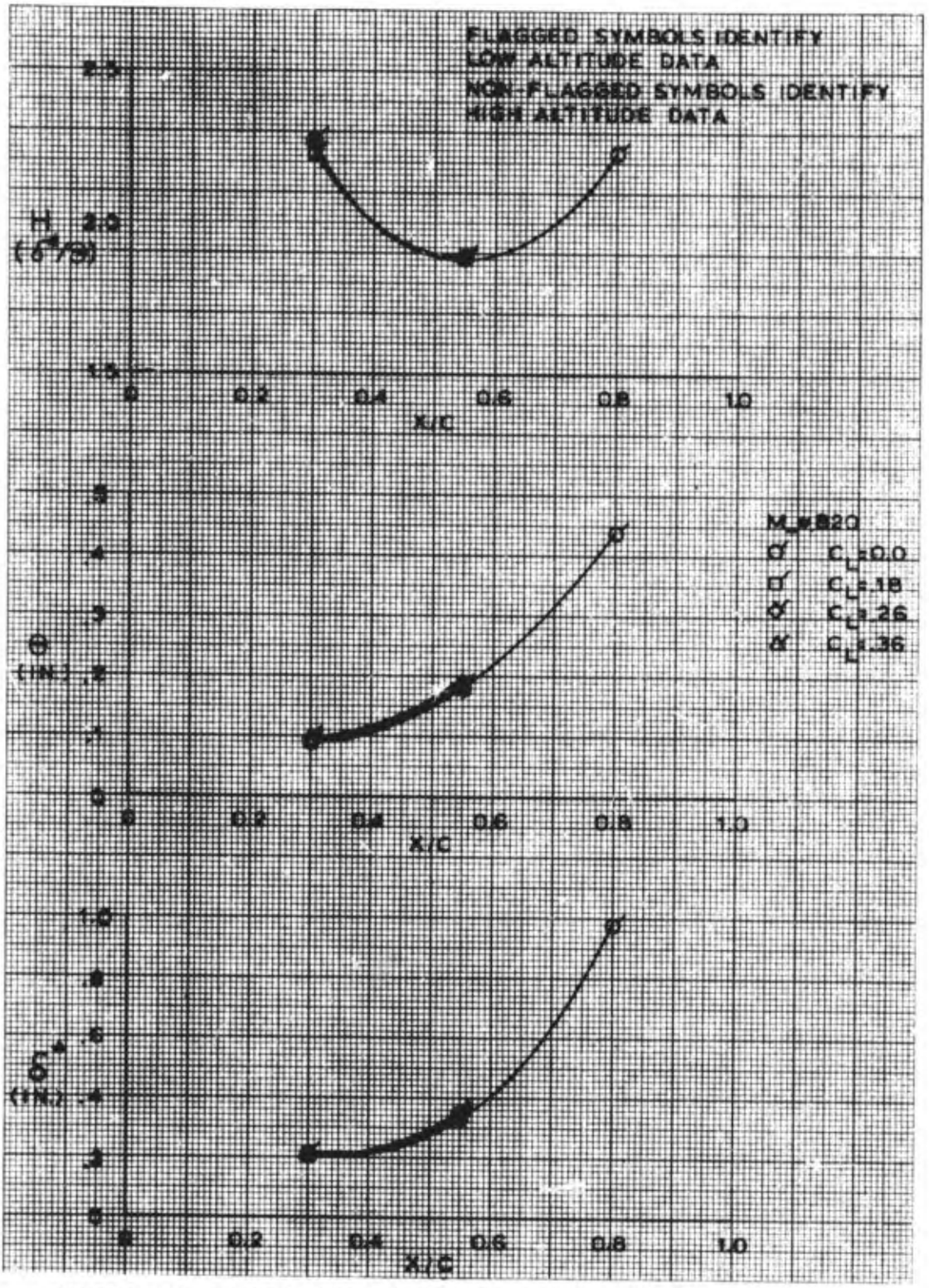

FIGURE 20 DERIVED BOUNDARY LAYER PARAMETERS
(d) M_∞ = .820

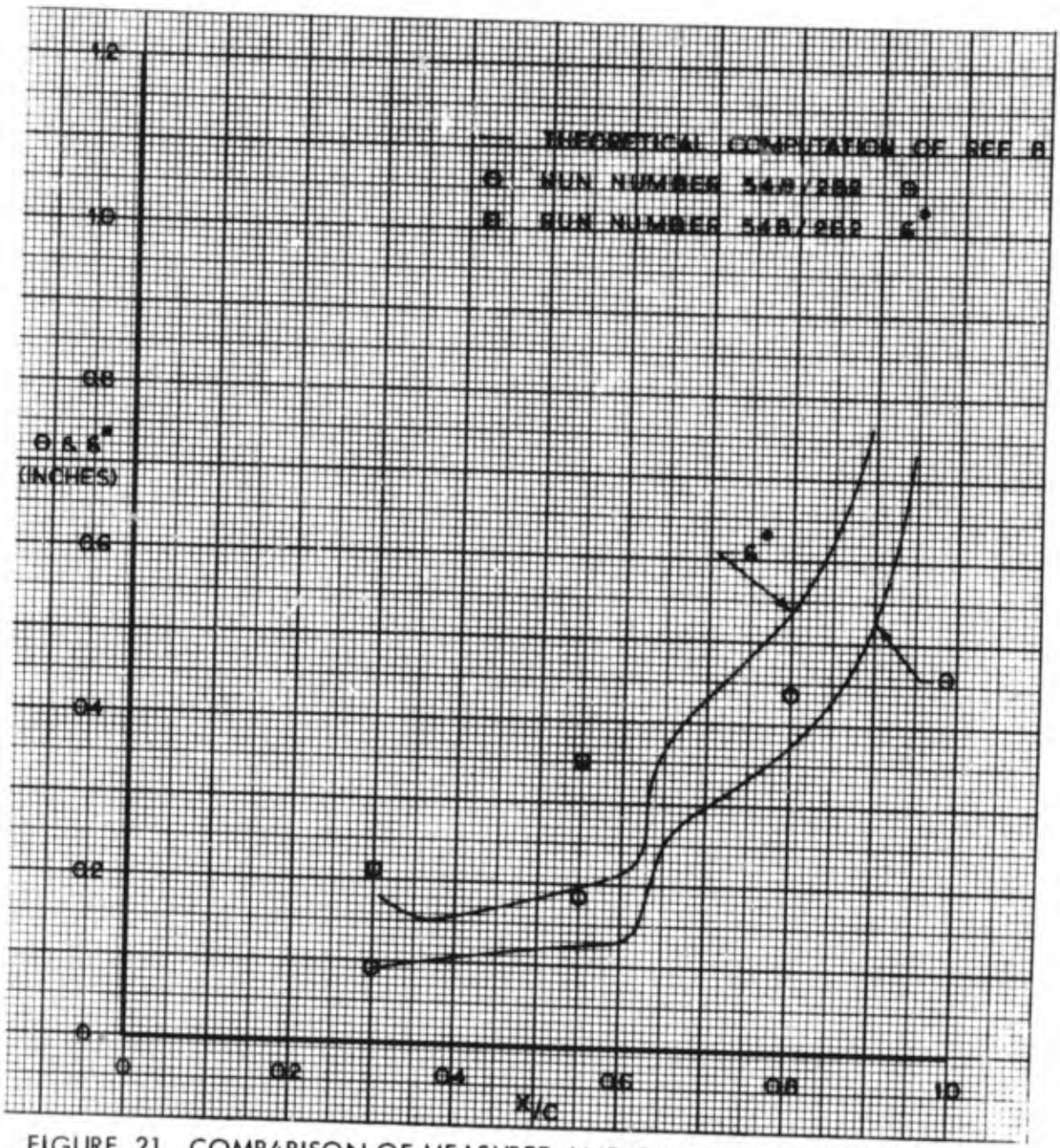

FIGURE 21 COMPARISON OF MEASURED AND CALCULATED BOUNDARY LAYER THICKNESS

coefficient due to the absence of leading-edge pressure peaks at these transonic Mach numbers.

A comparison is shown in Figure 21 between measured boundary layer thicknesses and values computed using the two-dimensional method presented in Reference 8. Initial computations of boundary layer development were made starting from the leading-edge. However, uncertainties with regard to transition phenomena prevented any conclusive comparisons. Computations were therefore made beginning with initial conditions (θ and H) derived from the boundary layer profiles measured at 30% chord. The results of a sample case computed on that basis are shown in Figure 21. The experimental boundary layer thickness is shown to increase at a significantly greater rate than that computed using these two-dimensional assumptions. It is possible that the strong three-dimensional components of the flow field on this swept wing, combined with spanwise drift within the boundary layer, cause this discrepancy. In any case, it would seem that refined methods of accounting for the boundary layer development are required to establish the precise conditions at the shock in the conditions tested.

As a part of the analysis reported in Reference 6, a correlation was shown between total pressure rise (from just forward of the shock to the trailing-edge) and the peak value of the local Mach number ahead of the shock. The shape of this variation was similar for all conditions investigated in Reference 6; small changes in specific values were produced by changes in Reynolds number or boundary layer tripping device, and somewhat larger changes by increasing thickness ratio of the circular arc airfoils from 6% to 10%. Figure 22 defines the parameters considered in this correlation. Curves are presented in Figure 23 correlating the data from the present investigation in a similar manner. In this case, the value of M_1 is taken as the component of local Mach number normal to the local wing element lines using the equation:

$$M_1 = \sqrt{\frac{5.0 + M_\infty^2 \cos^2\beta}{((\gamma C_{p_1} M_\infty^2/2) + 1.0)\frac{x_{cr}}{t}}} - 5.0$$

where $$\beta = \tan^{-1}\left[\tan\Lambda_{LE} - (X/C)(\tan\Lambda_{LE} - \tan\Lambda_{TE})\right]$$

At low Mach numbers, the variation of pressure rise with peak Mach number is similar to that shown in Reference 6, with the value of pressure rise increasing nearly linearly as the lift coefficient is increased. At higher values of local Mach number, however, the sequence of phenomena resulting from shock-induced separation was distinctly different and the pressure rise curves therefore have a different shape. In the wind tunnel tests of circular arc airfoils, the separation initiated somewhat aft of the shock and moved forward to the shock as the Mach number increased. Reattachment was never observed in those tests due to the very short chord length aft of the initial separation. The peak of the pressure-rise curve indicates the test condition for which the separation occurs at the shock. In the current investigation, however, the initial separation point is apparently at the shock; reattachment occurs for the majority of cases, and the pressure rise increases at a nearly constant rate up to its maximum value. After the bubble has spread to the trailing-edge, both the pressure rise and peak local Mach number decrease abruptly. Some additional discussion of this flow development was presented in an earlier section related to shock location.

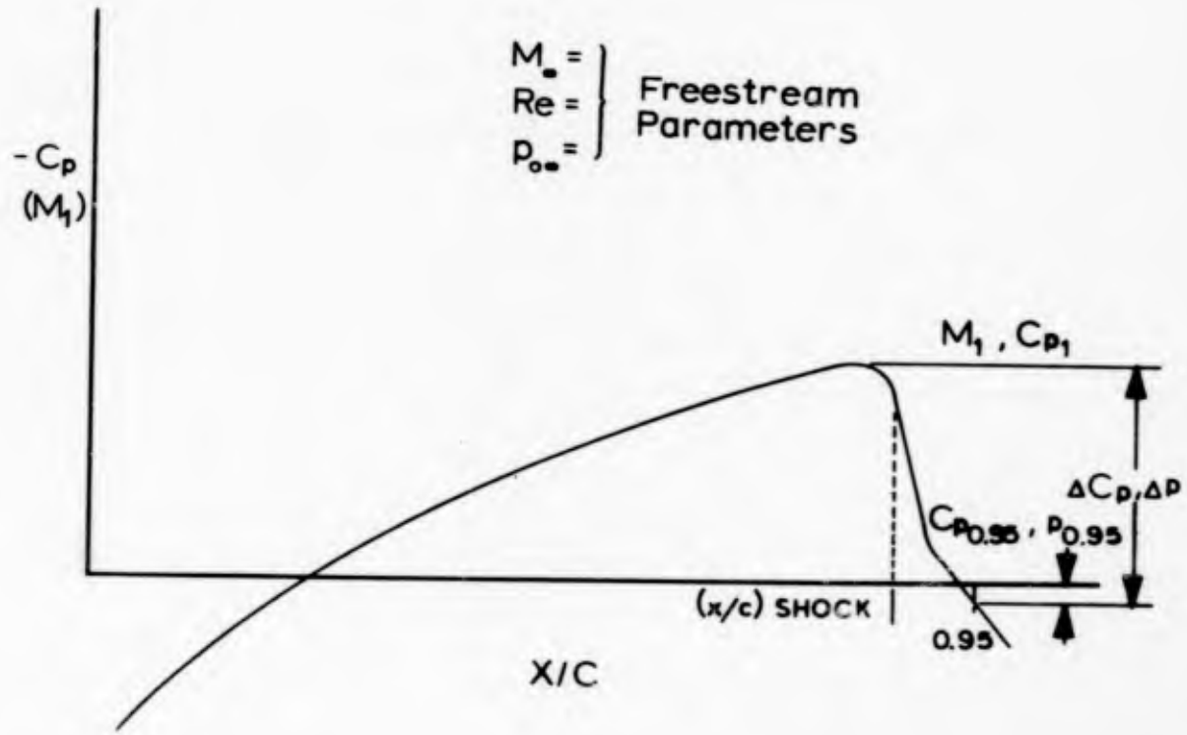

FIGURE 22 DEFINITION OF PARAMETERS USED IN PRESSURE RISE CORRELATION

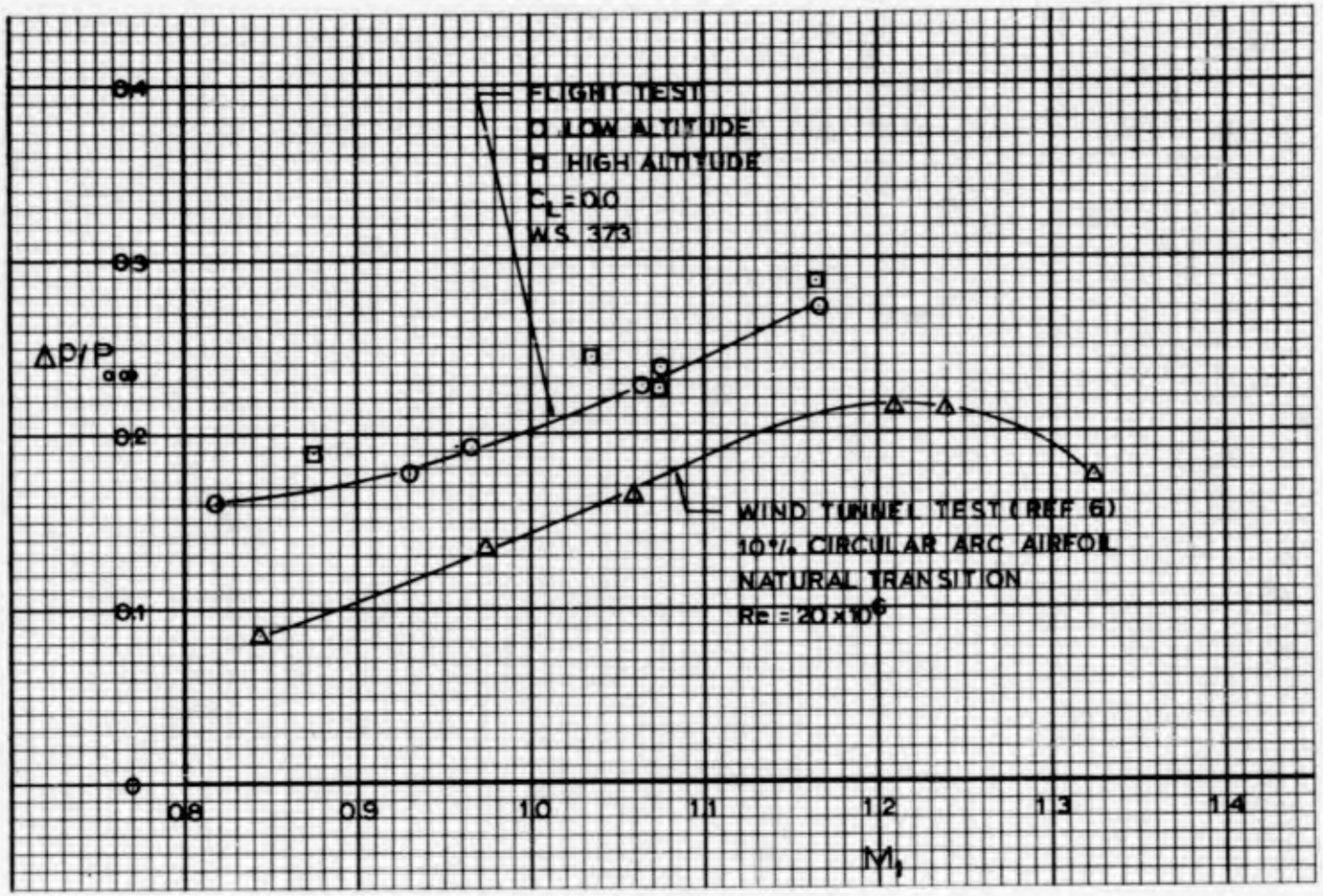

FIGURE 23 TOTAL PRESSURE RECOVERY CORRELATION
(a) $C_L \approx 0$

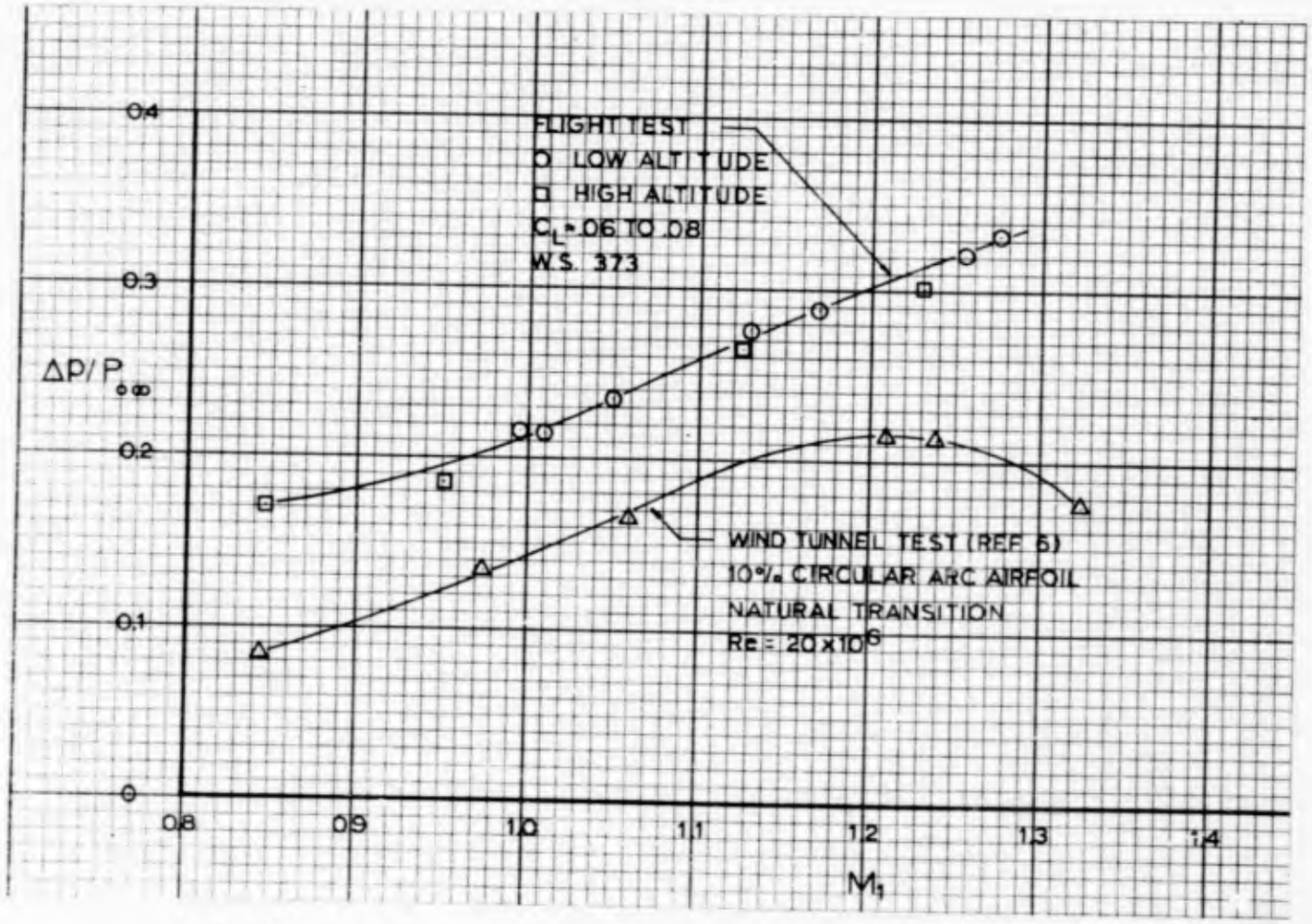

FIGURE 23 TOTAL PRESSURE RECOVERY CORRELATION
(b) C_L ≈ .06 TO .08

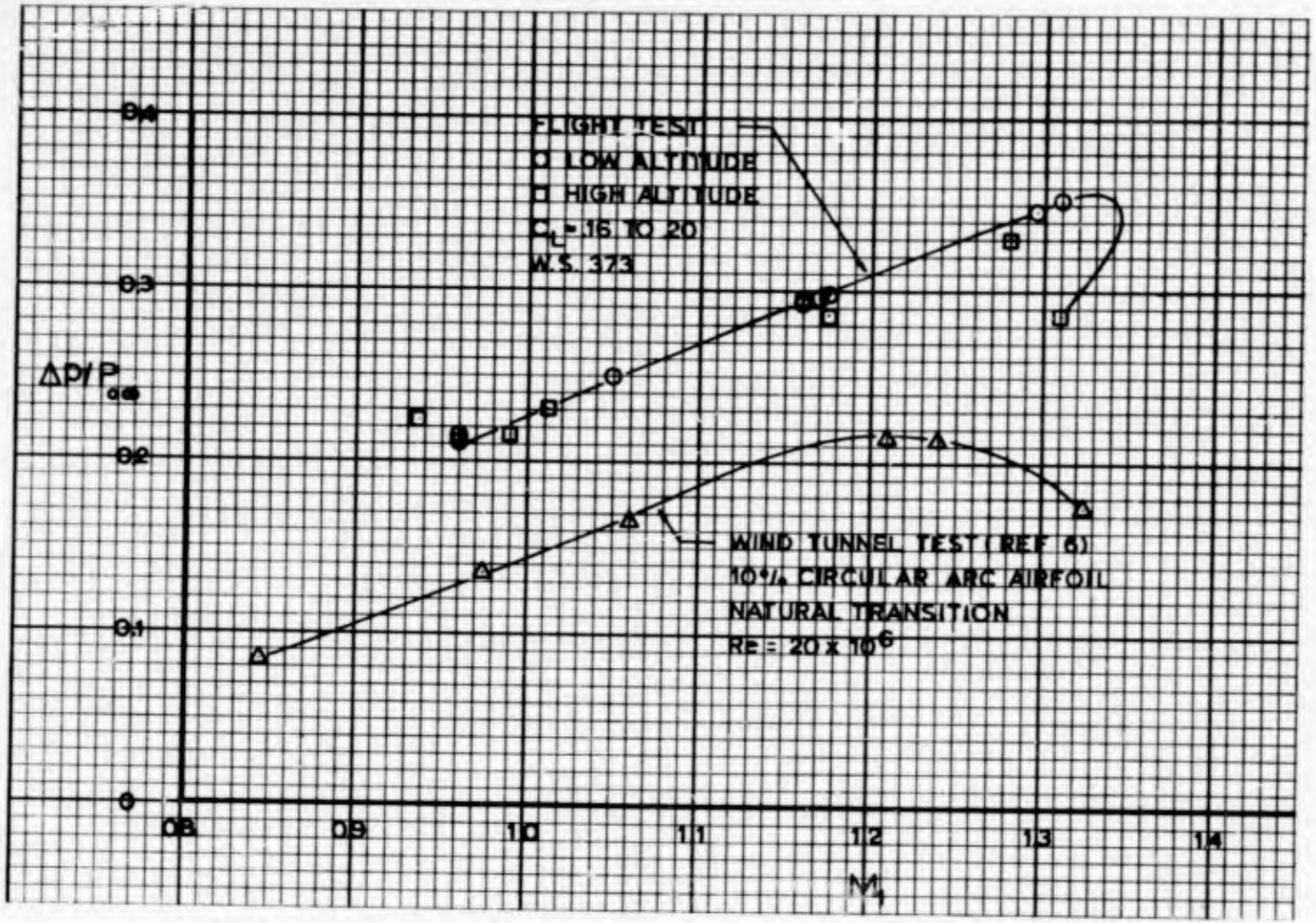

FIGURE 23 TOTAL PRESSURE RECOVERY CORRELATION
(c) C_L ≈ .16 TO .20

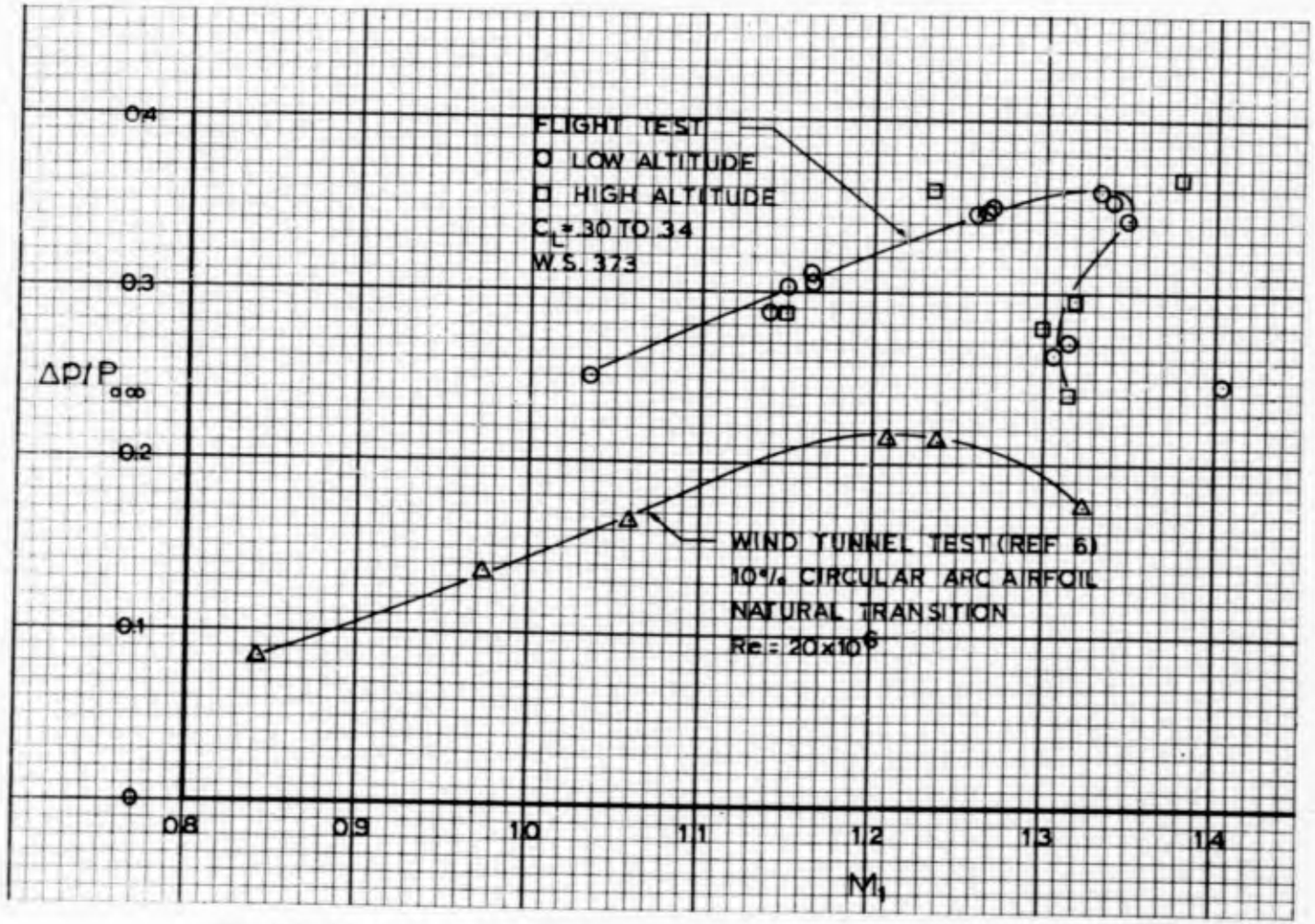

FIGURE 23 TOTAL PRESSURE RECOVERY CORRELATION
(d) C_L = .30 TO .34

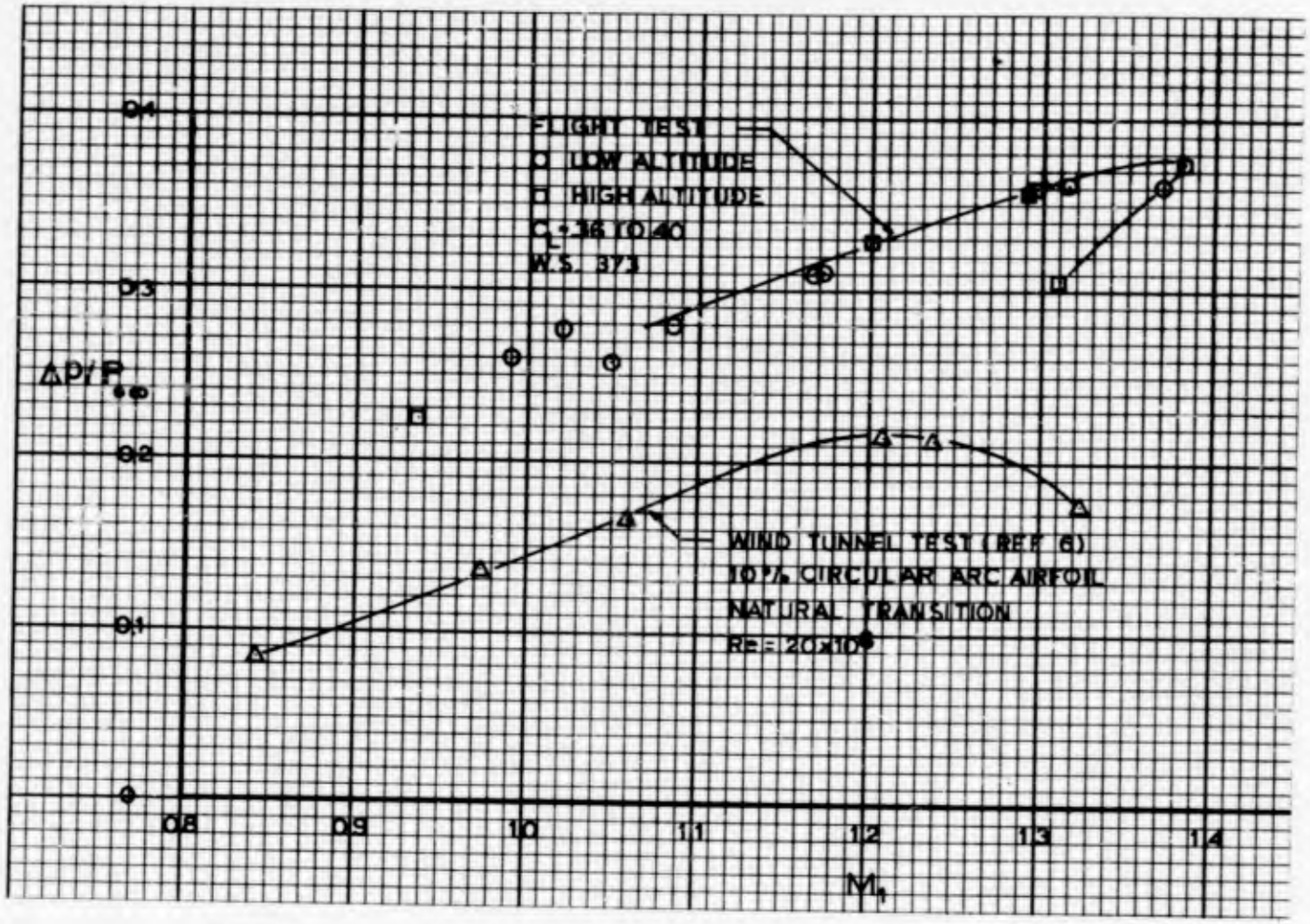

FIGURE 23 TOTAL PRESSURE RECOVERY CORRELATION
(e) C_L = .36 TO .40

Buffet Consideration

A very limited amount of flight test data were recorded during conditions of aircraft buffet. Figure 24 presents the pressure coefficients measured at the wing trailing-edge as a function of airplane lift coefficient and freestream Mach number. Also shown are the buffet boundaries as measured by the Air Force during stability and control tests, Reference 9. Wind tunnel data are presented for comparison purposes. At these specific Mach numbers, the fixed transition testing with vortex generators located at 55 percent chord would offer the best indication of the buffet boundary. Due to lack of sufficient data, it has not been possible to determine good comparisons at other spanwise stations. Again, it cannot be concluded that the use of vortex generators will always produce good results. They may over-fix a problem or be improperly located and contribute nothing to solving the separation problem.

Flow Model

It has been indicated in earlier sections of this report that previous studies by Pearcey and others had disclosed the principal features of the shock-boundary layer interaction phenomenon on wings at transonic speeds. Since the results of the present investigation verify some aspects of those previous studies, a short review of the flow model discussed by Pearcey is useful in showing the relation of the current results with previous work.

Figure 25, adapted from Pearcey's discussion in Reference 10 shows the main features of this flow model. The boundary layer growth on the forward part of the airfoil is dependent on Reynolds number, surface condition, and stream turbulence. Rather large variations can be achieved at low Reynolds numbers by artificially fixing transition forward of its natural location. At higher Reynolds numbers, especially with swept wings, the natural transition occurs quite close to the leading-edge. At the shock a rapid thickening occurs in the boundary layer, and this thickening can project forward into the supersonic flowfield if the boundary layer approaching the shock is sufficiently thick. Data in Reference 13 show that this forward influence can be expected to reach 50 to 100 displacement thicknesses forward of shocks with turbulent boundary layers. With this rapid thickening, oblique shocks can be formed due to the supersonic flow deflection. These oblique shocks are responsible for the gradual recompression forward of the main shock in a number of the pressure distribution diagrams obtained. When the shock strength becomes sufficiently great, a separation will occur at the shock. The flow may subsequently reattach, enclosing a separation bubble. The factors controlling reattachment are probably the least understood aspect of the total interaction phenomenon. Data presented in Figures 15 and 16 show that the growth of the bubble responds to changes in boundary layer thickness caused by transition strip location or by changes in Reynolds number, and purely physical reasoning would indicate that surface curvature should strongly affect reattachment. Pearcey has shown, and the results of Reference 5 confirm, that distinct differences occur in the reattachment process depending on whether the Mach number immediately behind the shock is subsonic or supersonic. Measurements made in the current investigation do not enable a detailed assessment of this "supersonic tongue" concept. In any case, the pressure rise in the separated region is much more gradual

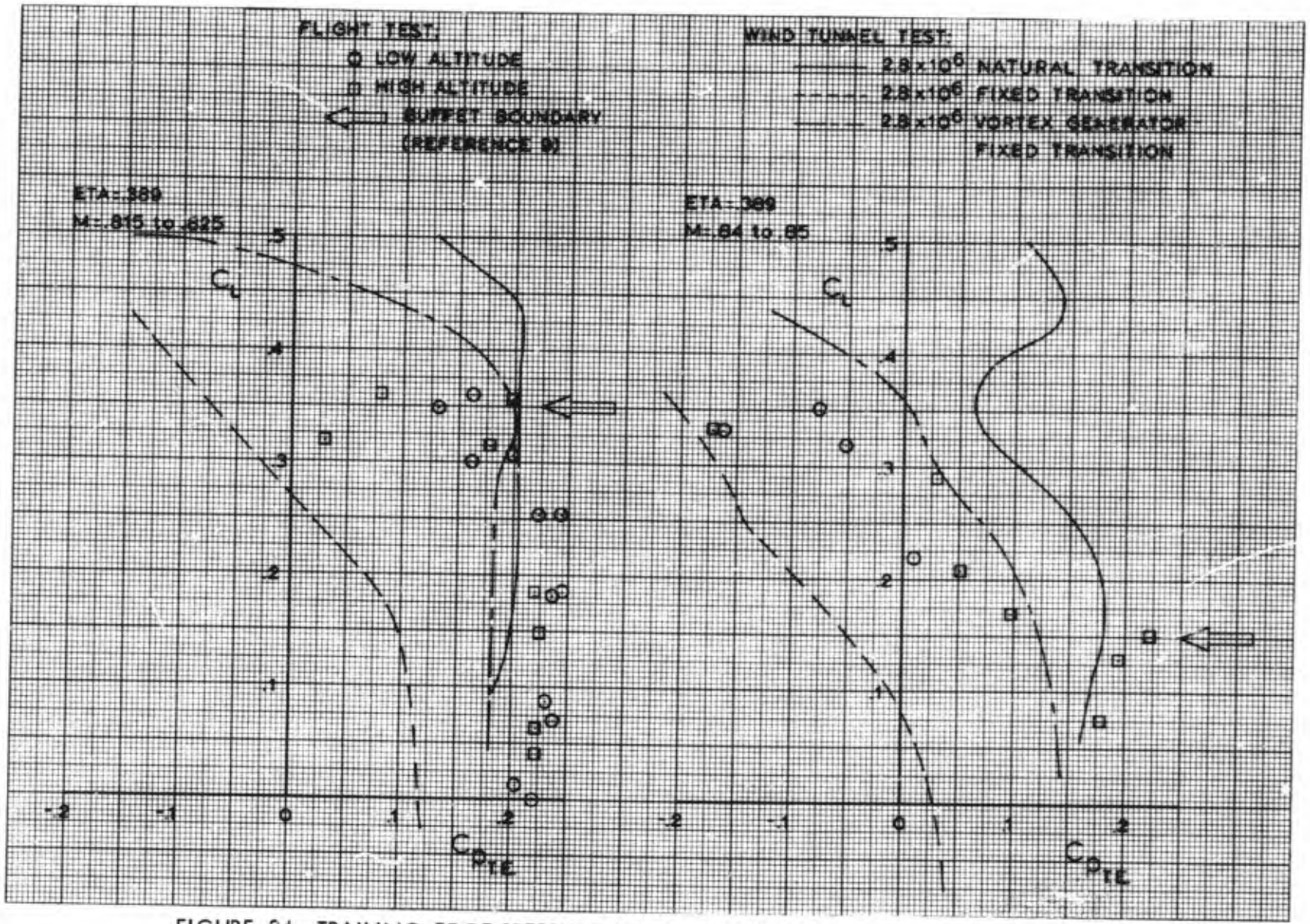

FIGURE 24 TRAILING-EDGE PRESSURE COMPARISONS FOR INDICATION OF AIRPLANE BUFFET

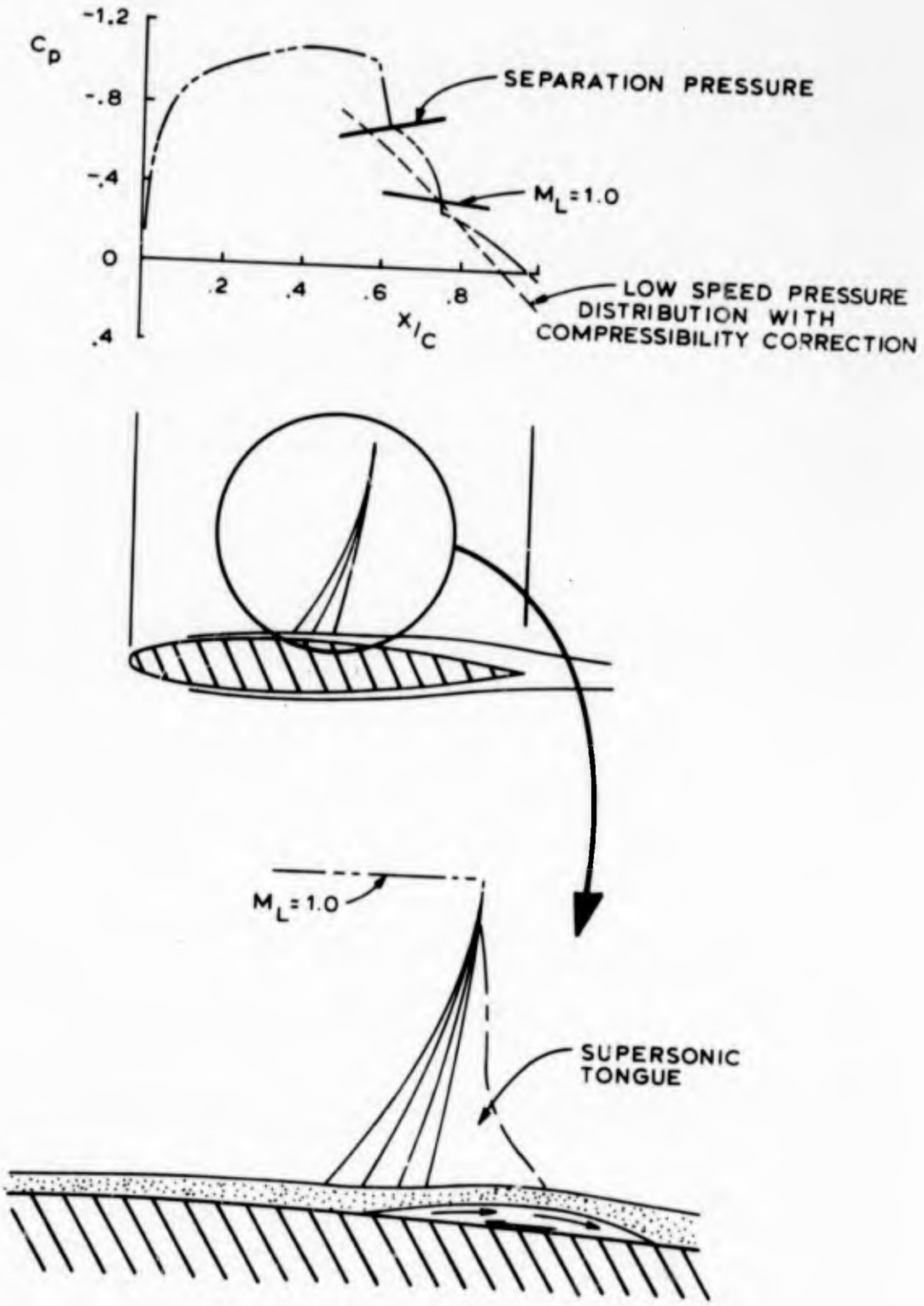

FIGURE 25 **PRINCIPLE** FEATURES OF TRANSONIC AIRFOIL SHOCK-BOUNDARY LAYER INTERACTION

than when the flow is attached. This fact results in the "bumps" in the pressure distribution behind the shocks shown in Figures 15 and 16. Figure 18 shows rather conclusively the presence of separation bubbles in the data obtained in this investigation and the eventual complete separation which occurs at the highest Mach numbers and angles-of-attack. It is interesting to note that, when reattachment occurs, the trailing-edge recovery can be as good as in totally unseparated cases, and there is even reason to suspect that flow conditions at the trailing-edge may be improved by the presence of a bubble, since the energy loss due to mixing at the edge of the bubble can be less than the loss due to skin friction.

Whether reattachment occurs or not, the eventual return to ambient pressure occurs in the wake aft of the trailing-edge. It is in this wake that the final reconciliation of the widely different flows from the upper and lower surface boundary layers and the undisturbed outer flow takes place. As indicated in the discussion of shock location, it is clear that the change in shock location is one of the outstanding factors in accomplishing this reconciliation for various test conditions. The fact that large shock location changes occur with flat Mach number gradients and small changes occur with steep gradients adds weight to this conclusion. As pointed out by Pearcey, there is a strong analogy between the function of the shock movement in this case and that observed in supersonic diffusers.

Figure 26 presents a comparison of interaction region pressure distributions and boundary layer profiles for several conditions. Data for two almost identical flight conditions (except for Reynolds number) are compared with similar data from the wind tunnel tests of Reference 3. These data show that for wind tunnel cases for which the shock moves forward, the velocity defect in the boundary layer at 80% chord shows corresponding increases, although at each extreme of this variation, the shock change is appreciable while the boundary layer change is almost imperceptible. This may be due to the fact that the definition of the wind tunnel boundary layer is rather sparse. The boundary layer heights shown are all scaled up to the dimensions of the full scale airplane. The relationship between shock location and the upper part of the boundary layer profile for the flight data is roughly compatible with that shown by the wind tunnel data. Near the airfoil surface, however, the flight data for 75 million Reynolds number indicate a separated flow; the total pressure for all of the pitot tubes in the rake below one inch is less than the local static pressure. The data obtained at the lower Reynolds number (42 million), however, show a positive dynamic pressure for all tubes of the rake. Differences in the shape of the surface pressure distribution would also indicate that the separation bubble extends farther aft for the higher Reynolds number case. An excellent trailing-edge pressure recovery (to $C_p = +0.23$) is shown in both cases. The sensitivity of the extent of the bubble shown by these data is rather remarkable in view of the very close agreement shown by the boundary layer profiles at 30% and 55% chord for these two flight conditions. The single comparable case for which a wind tunnel profile at 30% chord was available is also in agreement with the flight data.

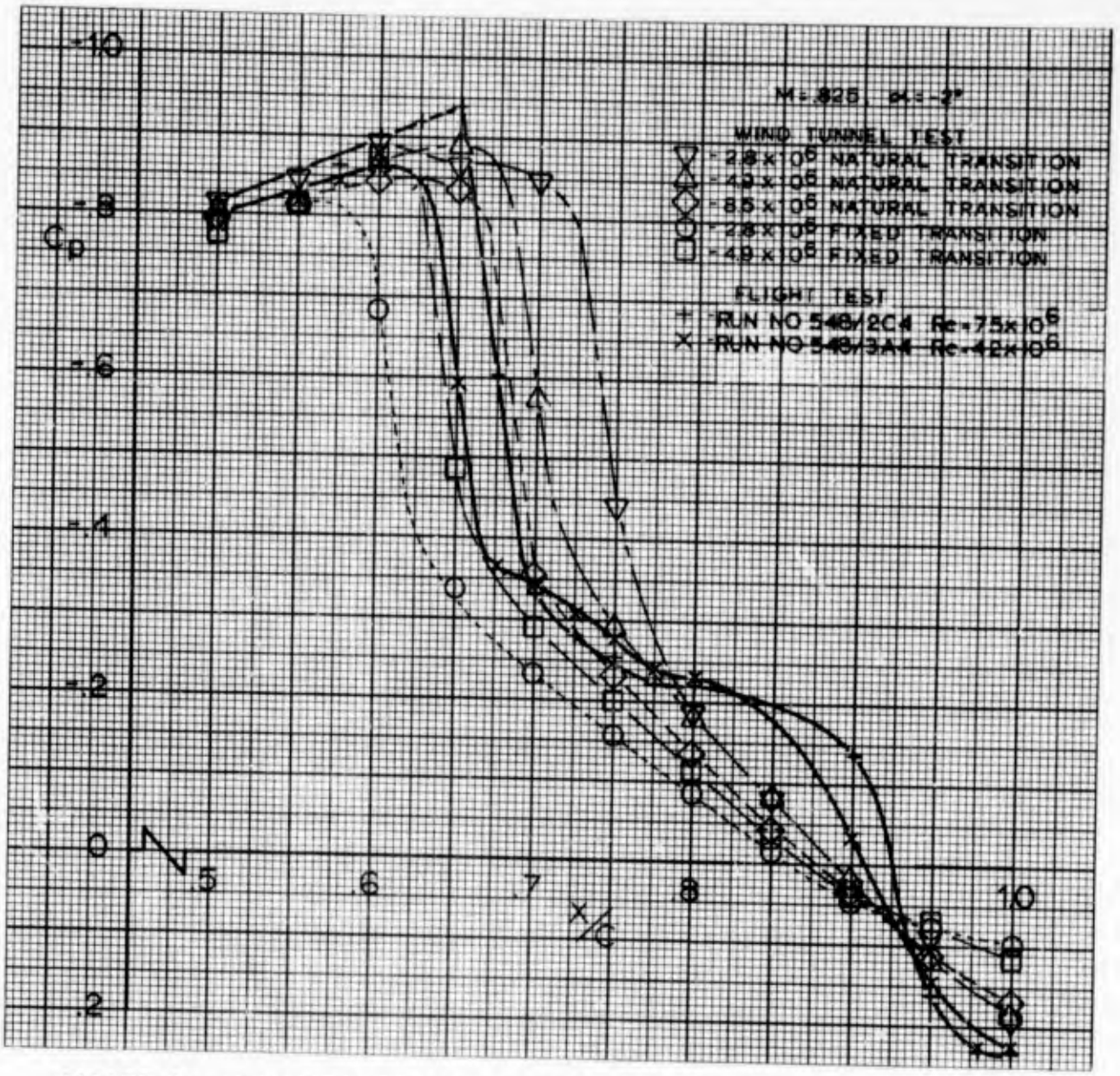

FIGURE 26 VARIATION OF INTERACTION REGION FLOW PROPERTIES
(a) PRESSURE D STRIBUTIONS

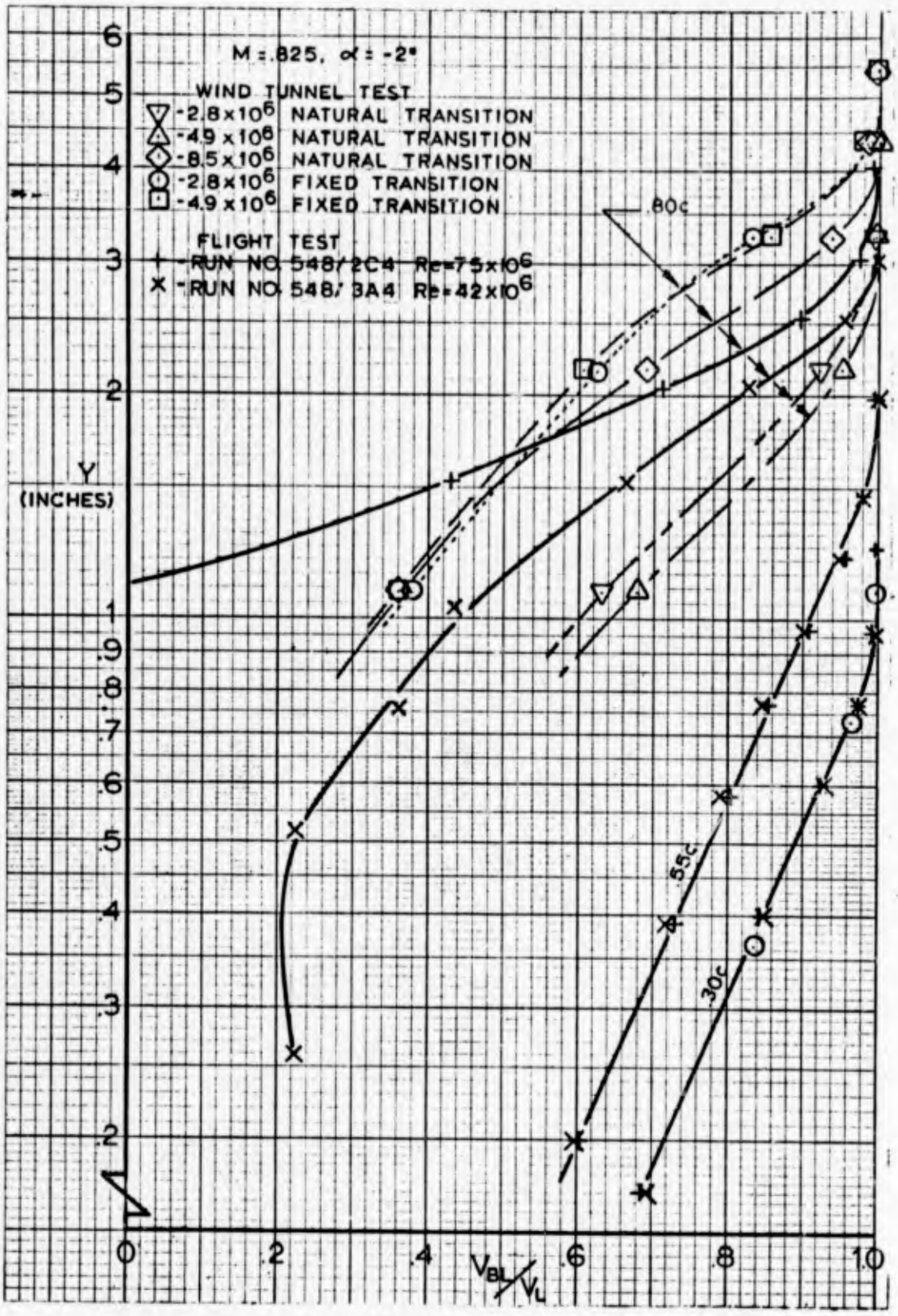

FIGURE 26 VARIATION OF INTERACTION REGION FLOW PROPERTIES
(b) BOUNDARY LAYER PROFILES

The velocity variation in the lower part of the 80% chord boundary layer for the low Reynolds number flight case in Figure 26 is rather unusual. The same velocity is indicated for the lower two probes of the boundary layer rake. This variation is, in fact, characteristic of the data for a large portion of the low Reynolds number flight cases tested. Data presented in Reference 14 show that velocity profiles tend to have this shape immediately behind a separation bubble. It is therefore possible that the predominance of this unusual shape in the low Reynolds number (approximately 40 million) flight cases indicates that a longer distance is required to rehabilitate the reattached boundary layer at the lower Reynolds number. There were insufficient tubes in the lower part of the boundary layer in the wind tunnel tests to show whether this condition exists in those cases.

Wind tunnel tests, in which conditions can be very closely controlled, with a large model which would enable detailed measurements in the boundary layer and in the separation bubble could provide data leading to a better understanding of the extremely complex flow processes taking place in these cases. Proper definition of these processes might inspire analytical work which could eventually enable a quantitative treatment of the interaction phenomenon.

SECTION IV

CONCLUSIONS

This report has considered the scale effects on the shock-boundary layer interaction phenomena for swept wings at transonic speeds. Comparisons have been made between wind tunnel data and flight data. Consideration has been given to analysis of pressure distribution, shock upstream Mach number, pressure recovery, shock location, trailing-edge pressure recovery, and boundary layer parameters.

The investigation has lead to the following conclusions:

1. Severe scale effects on shock-induced separation, resulting in changes in shock location, can occur with either natural or artificially produced turbulent boundary layers.

2. A comparison of these results on the wing of the C-141 airplane with results of previous studies on other airfoils would indicate that Mach number gradient forward of the shock has a large influence on the magnitude of the shock movement.

3. The characteristic nature of the separation appears to be that the separation begins just aft of the shock in the form of a small separation bubble and grows toward the trailing-edge as either Mach number or section angle-of-attack is increased.

4. Trailing-edge pressure recovery is excellent, even in the presence of a separation bubble.

5. Since wing buffet results from unsteady separated flows, prediction of buffet from wind tunnel tests is subject to the same kind of scale effect as shock location.

6. No single wind tunnel test configuration (e.g., natural transition, fixed transition, or vortex generators) will produce agreement with flight data over the full range of Mach numbers and angles-of-attack at all spanwise wing locations. Considerable three-dimensional effects do exist.

7. The most fruitful area for future study will probably be in better understanding of the scale effects on reattachment following separation aft of the shock.

BLANK PAGE

REFERENCES

1. Haines, A.G., Holder, D.W., and Pearcey, H.H., "Scale Effects at High Subsonic and Transonic Speeds, and Methods of Fixing Boundary Layer Transition in Model Experiments," ARC Technical Report R&M No. 3012.

2. Whittel, W.T., and Cooper, B.L., "Re-Defined Aerodynamic Data for Structural Design Based on In-Flight Measurements," Lockheed-Georgia Company ER-8211, February 1966.

3. Wright, J.M., "Development of Testing Technique Required to Duplicate Full Scale Wing Shock Location on a Wind Tunnel Model," Lockheed-Georgia Company LG1T6-1-16, May 1966.

4. Loving, D.L., "Wind-Tunnel-Flight Correlation of Shock-Induced Separated Flow," NASA TND-3580, September 1966.

5. B. H. Little, "Effects of Initial Turbulent Boundary Layer on Shock-Induced Separation in Transonic Flow," Lockheed-Georgia Company ER-9593, November 1967.

6. Stanewsky, E., and Hicks, G., "Scaling Effects on Shock-Boundary Layer Interaction in Transonic Flow," Technical Report AFFDL-TR-68-11, March 1968.

7. Maddox, B.W., and Honrath, J.F., "C-141 - High Speed Wind Tunnel Investigation of a 0.0275 Scale Pressure Model, Phase II," Lockheed-Georgia Company ER-5075, April 1963.

8. Bennett, J.A., and Goradia, S.H., "Methods for Analysis of Two-Dimensional Airfoils," Lockheed-Georgia Company ER-8591, July 1966.

9. McCabe, J.M., and Benefield, T.D., "C-141A Category II Stability and Control Test," AFFTC Technical Report 66-5, June 1965.

10. Pearcey, H.H., "Shock-Induced Separation and Its Prevention By Design and Boundary Layer Control," Boundary Layer and Flow Control, Volume 2, edited by G. V. Lachmann, Pergamon Press, New York, 1961.

11. Ward, K.E., "Contour Plotting for the Transonic Flight Test Drag Polar," Journal of Aircraft, Volume 5, No. 2, March-April 1968.

12. Chapman, D.R., Kuehn, D.M., and Larson, H.K., "Investigation of Separated Flows in Supersonic and Subsonic Streams with Emphasis on the Effect of Transition," NACA Report 1356, 1959.

13. Gadd, G.E., Holder, D.W., and Regan, J.D., "An Experimental Investigation of the Interaction Between Shock Waves and Boundary Layers," Proceedings of the Royal Aeronautical Society, Series A226, 1954.

14. Seddon, J., "The Flow Produced By Interaction of a Turbulent Boundary Layer With a Normal Shock Wave of Strength Sufficient to Cause Separation," Royal Aircraft Establishment ARC Technical Report R&M 3502, 1967.

Unclassified
Security Classification

DOCUMENT CONTROL DATA - R & D

(Security classification of title, body of abstract and indexing annotation must be entered when the overall report is classified)

1. ORIGINATING ACTIVITY *(Corporate author)*
Lockheed-Georgia Company
A Division of Lockheed Aircraft Corporation
Marietta, Georgia

2a. REPORT SECURITY CLASSIFICATION
Unclassified

2b. GROUP

3. REPORT TITLE

FLIGHT TEST INVESTIGATION OF TRANSONIC SHOCK-BOUNDARY LAYER PHENOMENA
VOLUME I

4. DESCRIPTIVE NOTES *(Type of report and inclusive dates)*
Final Technical Report - 5 October 1967 through 15 July 1968

5. AUTHOR(S) *(First name, middle initial, last name)*
Jones F. Cahill
Bill L. Cooper

6. REPORT DATE	7a. TOTAL NO. OF PAGES	7b. NO. OF REFS
July 1968	66	14

8a. CONTRACT OR GRANT NO.
F33 615-67-C-1777
b. PROJECT NO.
1366
c. Task No. 136612
d. Work Unit No. 136612009

9a. ORIGINATOR'S REPORT NUMBER(S)
AFFDL-TR-68-84 - Volume I

9b. OTHER REPORT NO(S) *(Any other numbers that may be assigned this report)*

10. DISTRIBUTION STATEMENT
This document is subject to special export controls and each transmittal to foreign governments or foreign nationals may be made only with prior approval of the Flight Dynamics Laboratory (FDMM), Wright-Patterson Air Force Base, Ohio 45433.

11. SUPPLEMENTARY NOTES
Vol. I - Data Analysis and Discussion
Vol. II - Presentation of Basic Data

12. SPONSORING MILITARY ACTIVITY
Air Force Flight Dynamics Laboratory
Air Force Systems Command
Wright-Patterson Air Force Base, Ohio 45433

13. ABSTRACT

A flight test investigation was made using a Lockheed C-141 airplane to obtain data related to scale effects on transonic shock-boundary layer interactions. The primary measurements consisted of wing surface chordwise pressure distributions at three spanwise stations, and boundary layer profiles for three chordwise positions at one spanwise station.

Volume I contains the data analysis and discussions of the test results. Volume II contains a detailed discussion of the data acquisition and reduction procedures plus a complete presentation of the basic data.

Results obtained, when compared with previously available wind tunnel data, showed that large scale effects on chordwise pressure distribution can occur with turbulent boundary layers on a wing having small Mach number gradients forward of the shock. A shock-induced separation, followed by flow reattachment, was shown to occur when the shock pressure rise reached a value approximately equal to that indicated in NACA Report 1356. For wing sections of the type used on the C-141, scale effects on buffet phenomena should be anticipated also.

Distribution of this abstract is unlimited.

DD FORM 1 NOV 65 1473

Unclassified
Security Classification

14. KEY WORDS	LINK A		LINK B		LINK C	
	ROLE	WT	ROLE	WT	ROLE	WT
Transonic Flow						
Shock Waves						
Boundary Layer Parameters						
Scaling Effects						
Shock Boundary Layer Interaction						
Flight Investigation						
Buffet Analysis						
Wing Static Pressure Distribution						
Shock Induced Separation						
C-141 Airplane						

AFFDL-TR-68-84 - N/A

JULY 1968

AD 835 774 = VOL 1
836 289 = VOL 2

ERRATA

FLIGHT TEST INVESTIGATION OF TRANSONIC SHOCK-BOUNDARY LAYER PHENOMENA

As an unfortunate and unforeseen side effect of the use of a computer-coupled automatic plotting system, the reproduction of some basic data figures in this report is rather poor. The enclosed pages list the section lift and pitching moment coefficients obtained from integration of the surface pressure distributions measured in this program. Section pitching moments are referenced to the section leading edge point.

AIR FORCE FLIGHT DYNAMICS LABORATORY

AIR FORCE SYSTEMS COMMAND

WRIGHT-PATTERSON AIR FORCE BASE, OHIO

FIG. NO.	MACH NO.	ETA .193		ETA .389		ETA .637	
		C_l	C_m	C_l	C_m	C_l	C_m
8a	.704	.130	-.045	.075	-.082	.034	-.067
8b	.706	.185	-.060	.182	-.106	.136	-.090
8c	.700	.318	-.090	.382	-.141	.291	-.127
8d	.700	.399	-.109	.437	-.169	.394	-.154
8e	.700	.440	-.117	.477	-.177	.447	-.165
8f	.700	.506	-.133	.567	-.200	.525	-.181
9a	.750	.062	-.031	.060	-.082	-.009	-.061
9b	.750	.165	-.056	.172	-.106	.119	-.089
9c	.752	.279	-.080	.302	-.138	.253	-.121
9d	.742	.266	-.077	.268	-.129	.231	-.116
9e	.742	.267	-.079	.271	-.128	.236	-.116
9f	.750	.339	-.096	.371	-.152	.318	-.140
9g	.750	.391	-.107	.415	-.166	.368	-.152
9h	.752	.451	-.120	.480	-.181	.455	-.172
10a	.762	0.0	0.0	0.59	-.085	-.004	-.042
10b	.770	.197	-.062	.149	-.120	.024	-.078
10c	.770	0.0	0.0	.140	-.098	.093	-.082
10d	.770	.172	-.058	.165	-.116	.115	-.091
10e	.770	0.0	0.0	.268	-.129	.220	-.113
10f	.770	.266	-.080	.280	-.140	.239	-.121
10g	.780	0.0	0.0	.366	-.157	.342	-.143
10h	.778	.329	-.094	.347	-.158	.337	-.146
10k	.770	0.0	0.0	.421	-.171	.389	-.155
10l	.772	.359	-.102	.434	-.181	.401	-.162
10m	.772	0.0	0.0	.455	-.177	.421	-.164
10n	.775	.394	-.111	.449	-.181	.420	-.170
11a	.795	0.0	0.0	.081	-.094	.041	-.081
11b	.794	.099	-.033	.193	-.127	-.007	-.069
11c	.794	0.0	0.0	.174	-.114	.133	-.100
11d	.802	.178	-.056	.195	-.134	.126	-.099
11e	.800	.253	-.078	.284	-.150	.228	-.120

FIG. NO.	MACH NO.	ETA .193		ETA .389		ETA .637	
		C_l	C_m	C_l	C_m	C_l	C_m
11f	.802	0.0	0.0	.268	-.136	.221	-.114
11g	.798	.246	-.077	.263	-.139	.198	-.115
11h	.800	.251	-.078	.265	-.135	.232	-.122
11k	.802	0.0	0.0	.351	-.161	.318	-.146
11l	.800	.327	-.098	.366	-.173	.326	-.147
11m	.795	0.0	0.0	.396	-.171	.335	-.141
11n	.800	.343	-.102	.386	-.178	.324	-.149
11o	.800	.374	-.111	.428	-.191	.405	-.172
11p	.802	0.0	0.0	.456	-.196	.403	-.166
12a	.820	.151	-.050	.288	-.151	.034	-.084
12b	.817	0.0	0.0	.089	-.095	-.011	-.072
12c	.820	0.0	0.0	.189	-.126	.086	-.096
12d	.820	.224	-.068	.275	-.163	.119	-.108
12e	.820	0.0	0.0	.258	-.141	.210	-.122
12f	.822	.258	-.083	.284	-.166	.216	-.127
12g	.820	0.0	0.0	.299	-.153	.245	-.130
12h	.822	.294	-.090	.353	-.183	.296	-.154
12k	.822	0.0	0.0	.341	-.170	.338	-.164
12l	.820	.316	-.095	.384	-.191	.341	-.169
12m	.820	.375	-.110	.436	-.195	.348	-.162
12n	.820	0.0	0.0	.413	-.182	.350	-.170
13a	.860	.157	-.045	.070	-.093	-.002	-.097
13b	.855	.222	-.067	.116	-.091	.108	-.124
13c	.845	.273	-.067	.248	-.114	.301	-.167
13d	.840	.332	-.077	.331	-.127	.397	-.185
13e	.844	.348	-.076	.344	-.117	.387	-.171
13f	.840	.363	-.084	.370	-.134	.442	-.194
14a	.690	.212	-.058	.133	-.082	.080	-.070
14b	.695	.254	-.070	.151	-.095	.120	-.079
14c	.700	.352	-.091	.269	-.117	.348	-.130
14d	.700	.537	-.133	.494	-.169	.500	-.169

FIG. NO.	MACH NO.	ETA .193		ETA .389		ETA .637	
		C_l	C_m	C_l	C_m	C_l	C_m
14e	.702	.469	-.122	.486	-.175	.453	-.166
14f	.700	.526	-.134	.559	-.192	.526	-.175
14g	.700	.576	-.144	.651	-.209	.626	-.204
15a	.751	.177	-.053	.101	-.092	.053	-.073
15b	.750	.297	-.086	.149	-.097	.125	-.088
15c	.748	.295	-.088	.255	-.130	.201	-.107
15d	.754	.367	-.105	.267	-.131	.221	-.116
15e	.754	.443	-.125	.423	-.166	.302	-.130
15f	.748	.457	-.126	.521	-.189	.449	-.167
15g	.750	.511	-.136	.586	-.204	.561	-.189
16a	.780	.346	-.102	.237	-.131	.221	-.108
16b	.765	.343	-.099	.366	-.157	.293	-.130
16c	.770	.502	-.146	.426	-.171	.377	-.155
16d	.770	.485	-.135	.531	-.193	.509	-.179
16e	.780	.448	-.127	.513	-.197	.488	-.177
17a	.790	.335	-.099	.115	-.099	.104	-.090
17b	.800	.219	-.068	.229	-.126	.139	-.097
17c	.796	.350	-.107	.320	-.150	.245	-.125
17d	.810	.253	-.079	.286	-.143	.264	-.131
17e	.810	.378	-.113	.379	-.186	.328	-.153
17f	.800	.382	-.111	.359	-.164	.343	-.149
17g	.792	.255	-.078	.216	-.122	.093	-.090
17h	.800	.412	-.121	.497	-.205	.467	-.181
17k	.800	.423	-.125	.494	-.201	.439	-.156
18a	.826	.302	-.087	.427	-.199	.124	-.107
18b	.822	.229	-.071	.285	-.160	.126	-.108
18c	.820	.377	-.112	.324	-.170	.248	-.134
18d	.822	.402	-.114	.440	-.198	.341	-.154
18e	.824	.346	-.102	.442	-.193	.389	-.177
18f	.825	.401	-.109	.456	-.179	.453	-.192
18g	.820	.381	-.113	.464	-.199	.445	-.187
18h	.830	.344	-.088	.390	-.166	.410	-.183

FIG. NO.	MACH NO.	ETA .193		ETA .389		ETA .637	
		C_l	C_m	C_l	C_m	C_l	C_m
19a	.850	.309	-.087	.428	-.193	.246	-.153
19b	.850	.364	-.082	.366	-.171	.388	-.190
19c	.840	.263	-.080	.271	-.166	.200	-.135
19d	.840	.302	-.086	.302	-.180	.262	-.148
19e	.848	.301	-.069	.314	-.155	.279	-.158
19f	.840	.348	-.083	.388	-.157	.413	-.187
19g	.850	.312	-.057	.320	-.104	.377	-.159

AIR FORCE FLIGHT DYNAMICS LABORATORY
AIR FORCE SYSTEMS COMMAND
WRIGHT-PATTERSON AIR FORCE BASE, OHIO